PRESSURIZED FUSELAGE STRESS ANALYSIS

Thesis by

Robert A. Chase

In Partial Fulfillment of the Requirements

for the Degree of

Doctor of Philosophy

California Institute of Technology

Pasadena, California

1955

ACKNOWLEDGEMENT

The author would like to express his appreciation to Dr. Max L. Williams, Jr. for his help in carrying out the theoretical development and to Dr. Ernest E. Sechler for his help and encouragement in carrying out the experimental investigation.

In addition he would like to extend his thanks to Mrs. Betty Wood for her assistance in producing the figures to to Mrs. Elizabeth Fox for typing the manuscript.

ABSTRACT

Theoretical methods for obtaining the complete stress analysis of a pressurized, stiffened circular cylinder of special geometry are presented. In certain limiting cases, the exact solutions are tractable, but in general the solutions lead to approximate results. There are practical cases for which none of the solutions is applicable. Accompanying the theoretical analysis is a short experimental program consisting of the strain gage instrumentation and testing of a Lucite and cellulose acetate model of typical aircraft structural geometry. The results compare favorably with the theoretical analysis.

TABLE OF CONTENTS

I. INTRODUCTION AND SUMMARY

The problem of estimating the weight penalty resulting from the internal pressurization of a conventional type all metal fuselage is frequently encountered by the structural engineer during the stress analysis of modern high altitude aircraft. This structure which consists primarily of frames, longerons, and external skin is basically designed to resist, in an efficient manner, the shears and bending moments resulting from air loads and inertial loads. Upon internal pressurization, however, this type of structure becomes an inefficient pressure vessel due primarily to longeron and frame bending. It is, then, the intention of the author to present in this thesis methods for evaluating some of the harmful effects of fuselage pressurization upon the load carrying capacity of that structure.

The principal structural implications of fuselage pressurization can be classified in the following manner. The primary structural effect of pressurization is the inducement of longitudinal and circumferential stresses in the skin panels bounded by adjacent longerons and frames. Since the longerons are adjacent to the outer skin panels and are supported internally by the frames, a portion of the pressure loading is carried by these members into the frames. The second important effect is, therefore, the stresses induced in the longerons by the outer skin panels. Because the frames can be non-circular and with variable cross-sectional structural properties, shears are transmitted to these members resulting in frame warpage and outward deflections. The third

important effect is, therefore, the stresses induced in the frames. Another important effect is the influence of cut outs, floors, and splices, i.e. any of the smaller component effects, upon the stresses induced in the primary load carrying components (frames, longerons and outer skin). The final effect concerns the stresses induced by a closing bulkhead, or the nose or tail section of the airplane. All of these principal effects when combined with the stresses induced by air loads result in the overall fuselage stress system.

Since, in general, the pressure loading on a panel is held in equilibrium by a non-linear interaction of the deflections and the stresses, the combined structural effects of fuselage pressurization and the inertial and air loads are not a simple superposition of the individual effects. It is unfortunate that no theory is available to the stress analyst to express this interaction in a satisfactory manner. Some portions of the structure may be stabilized by internal pressurization while others may be destabilized. At best, the stress analyst is only in a position at present to check his design for some over-pressure condition and speculate that the stress state due to the combined influence of pressurization, and air and inertial loads will not exceed the computed results. Or, he may choose to go ahead and superpose these individual effects and speculate that the result has not strayed too far from the true stress system.

The intention of the present analysis is to improve the methods by which the stress state due only to pressurization is obtained. When the frames are non-circular and/or the frame

cross-sectional structural properties vary considerably around the circumference, the bending of the frame is usually a critical condition. A non-circular fuselage cross-section is therefore an inefficient type of pressure vessel. Methods for evaluating this effect have been discussed in detail in reference 6. When the cross-section of the fuselage is circular and is, for most of its length, cylindrical, the critical component is usually the longeron due to excessive bending. The evaluation of the bending stresses induced in a longeron due to internal pressurization of circular fuselages is therefore important. A knowledge of the magnitude of load which is transmitted from longeron to frame when the skin is attached to the frames or when the frame is floating (skin attached only to the longerons) is important when the fatigue life of this attachment is to be investigated. New methods for obtaining answers to these questions are discussed in this paper.

The mathematical model which is highly idealized, scarcely resembles a fuselage in all of its detail. The complexity of extracting the solution in a more general sense forbids at present a model which is more complicated. This model is, before loading, a closed-ended circular cylinder of infinite length with uniform, evenly spaced frames and longerons, and constant skin thickness. Such a cylinder is illustrated in Fig. 1. The pressure difference, p, between the inside and the outside is constant. The longerons may be either continuous or pinned to the frames and the skin may be either attached to both frames and longerons or attached only to the longerons.

Physically, then, the following situation exists. The panel bounded by two adjacent longerons and frames if the skin is attached to the frames is, before loading, an initially curved rectangular plate in which the skin thickness is small compared to the panel width or length. The uniform pressure acting normally outward from the surface of the panel is held in equilibrium by the membrane stresses, curvatures, and the bending moments induced in the panel by the loading. The membrane stresses and lateral shears induced in the panel together with the deflection of the panel transmit a component of radial loading to the longeron, resulting in longeron bending. Similarly, load is transmitted to a frame by the outer skin; and since the longerons are attached to the frames, the longeron loading is ultimately taken out by the frames. These frame loadings cause the frames to deflect radially outward. One of the basic difficulties of solving this problem arises from the fact that all of these deflections, the deflection of the outer skin panel, the longerons and the frames must be compatible at the attachments. A second difficulty arises from the non-linear behavior with respect to pressure of the outer skin panel.

From the mathematical formulation of the idealized model, it is evident that the exact solution cannot be obtained in practice. However, due to the physical dimensions often encountered in typical fuselage designs, some important and useful solutions based on limiting conditions can be extracted. Such solutions will henceforth be designated "limiting solutions". Flügge[2] has suggested two of these limiting solutions in his discussion of pressurized

cabins. The first of these will be reviewed together with a discussion of the second and the derivation and application of several new limiting solutions will be presented.

Each of these limiting solutions must necessarily be restricted to a specific type of problem. In some cases, two limiting solutions overlap and comparisons can be made in order to gain confidence in the solutions. As must be expected, there are structural geometries for which no limiting solutions are applicable. A table illustrating the structural geometries for which there exist good solutions and the regions where the solutions fail is shown in Fig. 35.

Finally, an experimental program was carried out using a Lucite and cellulose acetate cylinder of geometry typical, though necessarily simplified, of a conventional all metal fuselage structure where in one phase of the test the frames were floating and in the other, the skin was attached to both frames and longerons. The experimental results are compared to the theoretical in Figs. 32 to 34. The complete program is discussed under the section entitled "Experimental Investigation".

II. NOTATION

p	Internal Pressure Difference
$q(x)$	Longeron Radial Loading
P	Panel Reduced Lateral Loading
q_n	Fourier Loading Coefficients
Q	Panel Loading Parameter
$4K^4, C$	Longeron Loading Constants
Q_n	Fourier Series Loading Parameters
$\bar{P}$	Loan Transmitted Between Longeron and Frame
σ_x	Panel Longitudinal Middle-Surface Stress
σ_θ	Panel Circumferential Middle-Surface Stress
$\bar{K}^2$	Panel Reduced Circumferential Unit Load
$\tau_{x\theta}$	Panel Middle-Surface Shear Stress
σ_L	Longeron Axial Stress
σ_F	Frame Axial Stress
σ_x'	Panel Longitudinal Bending Stress
σ_θ'	Panel Circumferential Bending Stress
σ_L'	Longeron Bending Stress
M_x	Panel Longitudinal Unit Bending Moment
M_θ	Panel Circumferential Unit Bending Moment
$M_{x\theta}$	Panel Unit Warping Moment
M	Longeron Bending Moment
Q_x	Panel Unit Lateral Shear
Q_θ	Panel Unit Lateral Shear
T	Stress Ratio
λ_n, τ_n	Fourier Series Stress Ratio Parameters

ϵ_x	Panel Longitudinal Middle-Surface Strain
ϵ_θ	Panel Circumferential Middle-Surface Strain
$\gamma_{x\theta}$	Panel Middle-Surface Shearing Strain
ϵ_L	Longeron Axial Strain
ϵ_F	Frame Axial Strain
E	Young's Modulus of Elasticity
D	Panel Bending Rigidity
ν	Poisson's Ratio
r, x, θ	Cylindrical Coordinates
X, Y, Z	Cartesian Coordinates
u, v	Displacements in the Surface of the Panel
w	Deflection of the Panel
$f(x)$	Longeron Radial Deflection
ΔR	Frame Radial Displacement
$\Delta R'$	Assumed Frame Radial Displacement
$\delta(x)$	Midpanel Deflections, $\delta(x) = w_1(x,0)$
R	Radius of the Fuselage (Cylinder)
a	Panel Semi-Length
b	Panel Semi-Width
α	Longeron Semi-Angular Spacing
t	Skin Thickness
A_F	Frame Cross-Sectional Area
A_L	Longeron Cross-Sectional Area
γ	Frame Geometric Parameter, $\gamma \equiv \frac{A_f}{2at}$
λ	Longeron Geometric Parameter, $\lambda \equiv \frac{A_L}{2bt}$
$\rho(x)$	Panel Circumferential Radius of Curvature

$K_x, K_\theta, K_{x\theta}$ Panel Curvatures

$\bar{c}$ Distance to Longeron Outer Fiber

I_L Longeron Moment of Inertia

A_n, B_n Fourier Coefficients

C_n Constants

$\mathcal{F}_n, \mathcal{E}_n$ Infinite Series Coefficients

ABBREVIATIONS

F.C.M.S.	Frames Close, Membrane Solution
F.C.P.S.	Frames Close, Plate Solution
F.C.S.S.	Frames Close, Shell Solution
F.N.C.-M.S.	Frames Not Close - Membrane Solution
F.N.C.-S.S.	Frames Not Close - Shell Solution
P.M.S.	Perturbation Membrane Solution

III. MATHEMATICAL FORMULATION

In view of the structural geometry common to most pressurized cabins, certain simplifying assumptions can be stated without significant loss in the accuracy of the mathematical representation.

The first assumption is that the frame, circular before loading, remains circular after loading which means that the frame deflection is uniform radially. This condition can prevail only if the loading on the frame is radial and uniform, which is generally not the case. However, since a frame section between two adjacent longerons is quite resistant to radial bending and the frame loading is periodic circumferentially, the bending of the frame is negligible compared to its extension.

The second assumption is that that portion of the longeron radial loading which is supported by the longeron axial load is small compared to the portion supported by longeron bending. Sample calculations of longeron bending involving conservative estimates of longeron radial and axial loads due to pressurization show that the longeron deflections with axial loading and without axial loading are virtually identical.

The last assumption is that the deflection of the outer skin panel bounded by two adjacent longerons and frames can be represented with sufficient accuracy by the theory of the large deflection of plates formulated by Theodore von Karman[3]. Large deflection theory is required here since the membrane stresses which are induced by the pressure loading and are affected by the panel radial deflection are significant in supporting the pressure loading. It

will be shown later that, in many cases, the panel can be considered as being a membrane, i. e. the bending stiffness can be neglected.

When these assumptions are considered in formulating the problem, some important conclusions can be drawn which will lead to useful limit solutions. This mathematical formulation of the problem will now be presented.

When dealing with the deflection of the panel bounded by two adjacent longerons and frames, it is convenient to describe the deflected surface by using the cylindrical coordinate system shown in Fig. 2. The reason for this is that the undeflected panel is part of a circular cylinder and the deflections of the longerons and frames, due to symmetry, are radial. The radius vector is denoted by r and its position is fixed by the angle θ and the x coordinate. The width of the panel is $2b$, its length, $2a$. Thus, the longeron spacing is $2b$ and the frame spacing is $2a$.

Panel Strain - Displacement Relations

If the displacement of a point on the middle surface of the panel is denoted by u in the x direction, and by v in the tangential direction, certain relationships between these displacements and the corresponding middle surface strains can be derived. Consider an infinitesimal element of width $R\,d\theta$ and length dx in the undeflected middle surface and of width, S, and length, T, in the deflected surface. From Fig. 3, it is evident that:

$$\epsilon_\theta = \frac{S}{R\,d\theta} - 1$$

But $$S^2 = \left(\frac{\partial r}{\partial \theta}\,d\theta\right)^2 + \left(\frac{\partial v}{\partial \theta}\,d\theta + r\,d\theta\right)^2$$

or neglecting $\left(\frac{\partial v}{r\partial\theta}\right)^2$ compared to $2\frac{\partial v}{r\partial\theta}$,

$$\left(\frac{s}{R\,d\theta}\right)^2 = \left(\frac{1}{R}\frac{\partial r}{\partial\theta}\right)^2 + \left(\frac{r}{R}\right)^2\left[1 + 2\frac{\partial v}{r\partial\theta}\right]$$

So $$\left(\frac{s}{R\,d\theta}\right)^2 = \left(\frac{r}{R}\right)^2\left[1 + 2\frac{\partial v}{r\partial\theta} + \left(\frac{\partial r}{r\partial\theta}\right)^2\right],$$

but since $$\frac{2}{r}\frac{\partial v}{\partial\theta} + \left(\frac{\partial r}{r\partial\theta}\right)^2 << 1,$$

then $$\frac{s}{R\,d\theta} \doteq \frac{r}{R}\left[1 + \frac{\partial v}{r\partial\theta} + \frac{1}{2}\left(\frac{\partial r}{r\partial\theta}\right)^2\right].$$

Therefore,

$$\epsilon_\theta = \frac{1}{R}\frac{\partial v}{\partial\theta} + \frac{r-R}{R} + \frac{1}{2Rr}\left(\frac{\partial r}{\partial\theta}\right)^2 \qquad (3.1)$$

From Fig. 4, it is easy to see that:

$$\epsilon_x = \frac{T}{dx} - 1 \quad ,$$

but $$\left(\frac{T}{dx}\right)^2 = \left(\frac{\partial r}{\partial x}\right)^2 + \left[1 + \frac{\partial u}{\partial x}\right]^2$$

$$\doteq \left(\frac{\partial r}{\partial x}\right)^2 + 1 + 2\frac{\partial u}{\partial x}$$

when $\left(\frac{\partial u}{\partial x}\right)^2$ is neglected compared to $2\frac{\partial u}{\partial x}$.

And since $$\left(\frac{\partial r}{\partial x}\right)^2 + 2\frac{\partial u}{\partial x} << 1,$$

then

$$\frac{I}{dx} \doteq 1 + \frac{\partial u}{\partial x} + \frac{1}{2}\left(\frac{\partial r}{\partial x}\right)^2$$

Therefore

$$\epsilon_x = \frac{\partial u}{\partial x} + \frac{1}{2}\left(\frac{\partial r}{\partial x}\right)^2 . \qquad (3.2)$$

Figs. 5 and 6 show how the shearing strain is related to u, v and r. In Fig. 5, the contribution to the shearing strain, $\gamma_{x\theta}$, due to displacements u and v is illustrated. Let this contribution be $\gamma_{x\theta_1}$; then it is evident that:

$$\gamma_{x\theta_1} = \frac{\frac{\partial u}{\partial \theta}\, d\theta}{r\, d\theta} + \frac{\partial v}{\partial x}\frac{dx}{dx}$$

$$= \frac{1}{r}\frac{\partial u}{\partial \theta} + \frac{\partial v}{\partial x}$$

Since the element deflects in the radial direction, in addition to the displacements u and v, there is a contribution to the shearing strain, $\gamma_{x\theta_2}$, due to this deflection. This is illustrated in Fig. 6, from which it follows that:

$$\gamma_{x\theta_2} = \frac{\partial r}{\partial x}\frac{dx}{dx}\frac{\partial r}{r\partial \theta}\frac{d\theta}{d\theta}$$

$$= \frac{1}{r}\frac{\partial r}{\partial x}\frac{\partial r}{\partial \theta}$$

Therefore, the total shearing strain is:

$$\gamma_{x\theta} = \frac{1}{r}\frac{\partial u}{\partial \theta} + \frac{\partial v}{\partial x} + \frac{1}{r}\left(\frac{\partial r}{\partial x}\right)\left(\frac{\partial r}{\partial \theta}\right) \qquad (3.3)$$

Equations (3.1), (3.2) and (3.3) are the large deflection strain-displacement relations for the cylindrical panel in cylindrical coordinates.

Panel Stress - Strain Relations

The stress is related to the strain by Hooke's law and since the panel membrane or middle surface stresses are a plane stress system, the stress-strain relations are:

$$\epsilon_x = \frac{1}{E}\left[\sigma_x - \nu\,\sigma_\theta\right] \tag{3.4}$$

$$\epsilon_\theta = \frac{1}{E}\left[\sigma_\theta - \nu\,\sigma_x\right] \tag{3.5}$$

$$\gamma_{x\theta} = \frac{2(1+\nu)}{E}\,\tau_{x\theta} \tag{3.6}$$

Panel Equations of Equilibrium

On an infinitesimal rectangular element in the middle surface of the panel there act certain forces and moments which must satisfy equilibrium in three mutually perpendicular directions - the longitudinal direction, the tangential direction and the radial direction. In Fig. 7 is shown the stresses acting in the longitudinal and tangential directions. Summing first the forces in the X direction, it is evident that:

$$\left(\sigma_x + \frac{\partial \sigma_x}{\partial x}dx\right)r\,d\theta - \sigma_x\, r\, d\theta + \left(\tau_{x\theta} + \frac{\partial \tau_{x\theta}}{\partial \theta}d\theta\right)dx - \tau_{x\theta}\,dx = 0$$

And neglecting the higher order terms, the result is:

$$\frac{\partial \sigma_x}{\partial x} + \frac{\partial \tau_{x\theta}}{r\,\partial \theta} = 0 \tag{3.7}$$

In a similar manner, summation of forces in the tangential direction implies:

$$\frac{\partial \sigma_\theta}{r\,\partial \theta} + \frac{\partial \tau_{x\theta}}{\partial x} = 0 \tag{3.8}$$

To deal with equilibrium of forces in the radial direction, it is convenient to separate the summation of forces into two parts - membrane forces and bending. First, the components of the membrane forces acting in the radial direction will be summed individually. These are shown in Figs. 9, 10 and 11. Then the lateral shear due to bending will be summed. This is shown in Fig. 8. Beginning with Fig. 9, the sum of the components of tangential membrane forces acting in the radial direction is:

$$\left(\sigma_\theta + \frac{\partial \sigma_\theta}{\partial \theta} d\theta\right)\left[\frac{\partial r}{r\,\partial \theta} + \frac{\partial}{\partial \theta}\left(\frac{1}{r}\frac{\partial r}{\partial \theta}\right)d\theta - d\theta\right] t\,dx - \sigma_\theta \frac{\partial r}{r\,\partial \theta}\, t\,dx$$

Simplifying and neglecting higher order terms, this becomes:

$$\left[\frac{\partial}{\partial \theta}\left(\frac{\sigma_\theta}{r}\frac{\partial r}{\partial \theta}\right) - \sigma_\theta\right] t\,d\theta\,dx \tag{3.9a}$$

The sum of the components of longitudinal (x direction) membrane forces acting in the radial direction is, from Fig. 10:

$$\left(\sigma_x + \frac{\partial \sigma_x}{\partial x} dx\right)\left(\frac{\partial r}{\partial x} + \frac{\partial^2 r}{\partial x^2} dx\right) t\,r\,d\theta - \sigma_x \frac{\partial r}{\partial x}\, t\,r\,d\theta$$

Simplifying and neglecting higher order terms, this becomes:

$$\left[\frac{\partial \sigma_x}{\partial x} \frac{\partial r}{\partial x} + \sigma_x \frac{\partial^2 r}{\partial x^2} \right] t\, r\, d\theta\, dx \qquad (3.9b)$$

The contribution due to the shear stress can easily be seen from Fig. 11. Summing components in the radial direction, the following is obtained:

$$\left(\tau_{x\theta} + \frac{\partial \tau_{x\theta}}{\partial \theta} d\theta \right)\left(\frac{\partial r}{\partial x} + \frac{\partial^2 r}{\partial x \partial \theta} d\theta \right) dx + \left(\tau_{x\theta} + \frac{\partial \tau_{x\theta}}{\partial x} dx \right\}$$

$$\left(\frac{\partial r}{r \partial \theta} + \frac{\partial}{\partial x} \frac{\partial r}{r \partial \theta} dx \right) r\, d\theta - \tau_{x\theta} \frac{\partial r}{\partial x} dx - \tau_{x\theta} \frac{\partial r}{\partial \theta} d\theta$$

Simplifying and neglecting higher order terms, this becomes:

$$\left[\frac{\partial}{\partial x} \left(\tau_{x\theta} \frac{\partial r}{r \partial \theta} \right) + \frac{1}{r} \frac{\partial}{\partial \theta} \left(\tau_{x\theta} \frac{\partial r}{\partial x} \right) \right] t\, r\, d\theta\, dx \qquad (3.9c)$$

The sum of equations (3.9abc) is the total component of the membrane forces acting on the element $r\,d\theta, dx$, in the radial direction.

From Fig. 8, it is seen that the component of lateral shear acting in the radial direction is:

$$\left(Q_\theta + \frac{\partial Q_\theta}{\partial \theta} d\theta \right) dx - Q_\theta dx + \left(Q_x + \frac{\partial Q_x}{\partial x} dx \right) r\, d\theta - Q_x\, r\, d\theta$$

Upon simplifying, this becomes:

$$\left[\frac{\partial Q_\theta}{r \partial \theta} + \frac{\partial Q_x}{\partial x} \right] r\, d\theta\, dx \qquad (3.9d)$$

When moments are summed with respect to the X axis and the tangential direction, two equations can be written by means of which the lateral shears, Q_x and Q_θ can be eliminated in the above expression. These equations are, neglecting higher order terms:

$$\frac{\partial M_\theta}{\partial \theta} d\theta dx + \frac{\partial M_{x\theta}}{\partial x} r d\theta dx - Q_\theta r d\theta dx = 0$$

$$\frac{\partial M_x}{\partial x} r d\theta dx + \frac{\partial M_{x\theta}}{\partial \theta} d\theta dx - Q_x r d\theta dx = 0$$

Simplifying:

$$\frac{\partial M_\theta}{r \partial \theta} + \frac{\partial M_{x\theta}}{\partial x} - Q_\theta = 0$$

$$\frac{\partial M_x}{\partial x} + \frac{\partial M_{x\theta}}{r \partial \theta} - Q_x = 0$$

When these equations are solved for Q_θ and Q_x and substituted into equation (3.9d), the following expression for the component of lateral shear in the radial direction results:

$$\left[\frac{1}{r}\frac{\partial}{\partial \theta}\left(\frac{\partial M_\theta}{r \partial \theta}\right) + \frac{2}{\sqrt{r}}\frac{\partial}{\partial x}\left(\frac{1}{\sqrt{r}}\frac{\partial M_{x\theta}}{\partial \theta}\right) + \frac{\partial^2 M_x}{\partial x^2}\right] r d\theta dx \qquad (3.9e)$$

Using the expressions relating the bending moments to the change in curvature of the deflected plate:

$$M_n = D(\Delta K_n + \nu \Delta K_t)$$

$$M_{nt} = D(1-\nu)\Delta K_{nt}$$

where ΔK is the change in curvature due to the deflection of the plate and n denotes the normal direction, t the tangential direction, the bending moments can be related to r .

In cylindrical coordinates, the curvature in the x direction is, assuming that $\frac{\partial r}{\partial x} << 1$:

$$K_x = - \frac{\partial^2 r}{\partial x^2}$$

The curvature in the tangential direction is, assuming that $\frac{1}{r}\frac{\partial r}{\partial \theta} << 1$,

$$K_\theta = \frac{1}{R} - \frac{1}{r^2}\frac{\partial^2 r}{\partial \theta^2}$$

And the cross curvature is, in view of the same assumptions:

$$K_{x\theta} = - \frac{1}{r}\frac{\partial^2 r}{\partial x \partial \theta}$$

Then, for the pressurized cylindrical fuselage problem, the expressions for the bending moments become:

$$M_x = -D\left[\frac{\partial^2 r}{\partial x^2} + \frac{\nu}{r^2}\frac{\partial^2 r}{\partial \theta^2} \right]$$

$$M_\theta = -D\left[\frac{1}{r^2}\frac{\partial^2 r}{\partial \theta^2} + \nu \frac{\partial^2 r}{\partial x^2} \right]$$

$$M_{x\theta} = -D(1-\nu)\frac{1}{r}\frac{\partial^2 r}{\partial x \partial \theta}$$

When these are substituted into equation (3.9e), the following expression for the component of lateral shear in the radial direction is obtained, assuming $\frac{\partial r}{\partial x} << 1$ and $\frac{\partial r}{r\partial \theta} << 1$:

$$-D\left[\frac{1}{r^4}\frac{\partial^4 r}{\partial \theta^4} + \frac{2}{r^2}\frac{\partial^4 r}{\partial x^2 \partial \theta^2} + \frac{\partial^4 r}{\partial x^4} \right] r\, d\theta\, dx \qquad (3.9f)$$

Equilibrium of all forces in the radial direction implies from equations (3.9abcf) that:

$$\left[-\sigma_\theta + \frac{\partial}{\partial\theta}\left(\frac{\sigma_\theta}{r}\frac{\partial r}{\partial\theta}\right)\right] t\,d\theta dx + \left[\frac{\partial\sigma_x}{\partial x}\frac{\partial r}{\partial x} + \sigma_x\frac{\partial^2 r}{\partial x^2}\right] t\,r\,d\theta dx$$

$$+ \left[\frac{\partial}{\partial x}\left(\frac{\tau_{x\theta}}{r}\frac{\partial r}{\partial\theta}\right) + \frac{1}{r}\frac{\partial}{\partial\theta}\left(\tau_{x\theta}\frac{\partial r}{\partial x}\right)\right] t\,r\,d\theta dx$$

$$- D\left[\frac{1}{r^4}\frac{\partial^4 r}{\partial\theta^4} + \frac{2}{r^2}\frac{\partial^4 r}{\partial x^2\partial\theta^2} + \frac{\partial^4 r}{\partial x^4}\right] r\,d\theta dx + p\,r\,d\theta dx = 0$$

Using equations (3.7) and (3.8), and simplifying, this becomes:

$$\frac{\sigma_\theta}{r}\left[\frac{\partial}{\partial\theta}\left(\frac{1}{r}\frac{\partial r}{\partial\theta}\right) - 1\right] + \sigma_x\frac{\partial^2 r}{\partial x^2} + \frac{2\tau_{x\theta}}{\sqrt{r}}\left[\frac{\partial}{\partial x}\left(\frac{1}{\sqrt{r}}\frac{\partial r}{\partial\theta}\right)\right] + \frac{p}{t} =$$

$$\frac{D}{t}\left[\frac{1}{r^4}\frac{\partial^4 r}{\partial\theta^4} + \frac{2}{r^2}\frac{\partial^4 r}{\partial x^2\partial\theta^2} + \frac{\partial^4 r}{\partial x^4}\right] \qquad (3.9)$$

Equations (3.7), (3.8) and (3.9) are the three required equations of panel equilibrium.

Longeron Equation of Equilibrium

In view of the second basic assumption stated at the beginning of this section, longeron bending can be determined by simple beam theory where the longeron axial load, $\sigma_L A_L$, is neglected compared to the lateral load, $q(x)$ (see Fig. 15b). If $f(x)$ is the deflection of the longeron with respect to its ends, then the equation of equilibrium is simply:

$$E I_L \frac{d^4 f(x)}{dx^4} = q(x)$$

However, the longeron load, $q(x)$, depends on the circumferential stress, $\sigma_\theta(x, \pm\kappa)$, which can be seen by referring to Fig. 16. If a

strip of width dx is considered, equilibrium of forces in the direction of $r(x,0)$, assuming that α is a small angle, implies:

$$q(x) = 2\alpha t\left[\frac{pR}{t} - \sigma_\theta(x,\alpha)\right] + 2t\int_0^\alpha \left\{\sigma_x \frac{\partial^2 r}{\partial x^2} + \frac{\partial}{\partial x}\left(\tau_{x\theta}\frac{\partial r}{r\partial\theta}\right)\right.$$

$$\left. -\frac{1}{r}\frac{\partial r}{\partial x}\left[\frac{1}{r}\frac{\partial}{\partial\theta}(r\tau_{x\theta})\right] - \frac{D}{t}\left[\frac{\partial^4 r}{\partial x^4} + \frac{1}{r^2}\frac{\partial^4 r}{\partial x^2\partial\theta^2}\right]\right\} r\,d\theta$$

From which the longeron equation of equilibrium becomes:

$$EI_L\frac{d^4 f(x)}{dx^4} = 2\alpha t\left[\frac{pR}{t} - \sigma_\theta(x,\alpha)\right] + 2t\int_0^\alpha \left\{\sigma_x \frac{\partial^2 r}{\partial x^2} + \frac{\partial}{\partial x}\left(\tau_{x\theta}\frac{\partial r}{r\partial\theta}\right)\right.$$

$$\left. -\frac{1}{r}\frac{\partial r}{\partial x}\left[\frac{1}{r}\frac{\partial}{\partial\theta}(r\tau_{x\theta})\right] - \frac{D}{t}\left[\frac{\partial^4 r}{\partial x^4} + \frac{1}{r^2}\frac{\partial^4 r}{\partial x^2\partial\theta^2}\right]\right\} r\,d\theta \qquad (3.10)$$

Longeron Stress - Strain Relation

Since the longeron is in a uniaxial state of stress, the relation between the longeron axial strain and stress is simply:

$$\epsilon_L = \frac{\sigma_L}{E} \qquad (3.11)$$

Frame Equation of Equilibrium

In view of the first assumption stated at the beginning of this section, namely, that the frame remains circular after loading, the mean of the periodic radial frame loading determines the uniform axial frame stress, σ_F. Bending of the frame will be assumed negligible, i.e. the inside radius of curvature of the frame is approximately equal to the outside radius of curvature. Then from Fig. 17, it is evident that the frame equilibrium equation is:

$$\sigma_F = \frac{1}{A_F\,\alpha}\left[\int_0^a q(x)\,dx - 2\int_0^\alpha Q_x(a,\theta)\,r\,d\theta\right]$$

or

$$\sigma_F = \frac{1}{A_F \alpha}\left[\int_0^a q(x)\,dx + 2D\int_0^{\alpha}\left(\frac{\partial^3 r}{\partial x^3} + \frac{1}{r^2}\frac{\partial^3 r}{\partial x \partial \theta^2}\right)_{x=a} r\,d\theta\right] \tag{3.12}$$

Frame Strain-Displacement Relation

If ΔR is the frame radial displacement, then:

$$\epsilon_F = \frac{\Delta R}{R} \tag{3.13}$$

Frame Stress-Strain Relation

In view of the assumption that the frame is stressed uniaxially, the stress-strain relation is:

$$\epsilon_F = \frac{\sigma_F}{E} \tag{3.14}$$

Longitudinal Equilibrium

If the pressurized cylinder is open ended, then the integration of the longitudinal forces around the circumference must vanish. Since pressurized fuselages contain air under pressure statically, a closed ended cylinder must be considered. In this case, in order to satisfy equilibrium the integration of the longitudinal forces around the circumference must equal the force due to the pressure acting on the cross-sectional area. Hence:

$$p = \frac{1}{Rb}\left[\sigma_L A_L + 2t\int_0^{\alpha}\sigma_x r\,d\theta\right] \tag{3.15}$$

Summary

Equations (3.1) through (3.15), when satisfied simultaneously together with certain boundary conditions which will be discussed

later, yield the solution to the idealized pressurized fuselage problem. One further simplifying assumption can be made without loss in generality; namely, that the ratio, $\frac{r}{R}$, varies only slightly from unity. This must be so since any strain is much less than unity. Furthermore, since equation (3.9), the equilibrium of panel forces in the radial direction, was determined by assuming that the slopes $\frac{1}{r}\frac{\partial r}{\partial \theta}$ and $\frac{\partial r}{\partial x}$ are much less than unity, this simplifying assumption should be extended to the other equations where applicable. This assumption, by the way, is necessary for the formulation of the large deflection plate theory in Cartesian coordinates[3]. Therefore, by replacing r by R in the first order terms and neglecting $\frac{1}{r}\frac{\partial r}{\partial \theta}$ and $\frac{\partial r}{\partial x}$ in the second order terms, equations (3.1) through (3.15) can be greatly simplified.

It may be mentioned at this point that an alternate presentation of these results can be obtained by specializing the general treatment given by Love in reference 7 to the case of a right circular cylinder. Timoshenko[3] also discusses the general equations to some extent. When the usual assumptions of large deflection analysis are used, as implied in Karman's treatment of the initially flat plate and relating to orders of magnitude of slopes and products of small forces and deformations, the resulting equations are the same as those obtained by the foregoing more direct physical derivation.

The following summary of these equations together with the boundary conditions to be discussed next represent the mathematical formulation of the problem.

Panel

Strain-Displacement Relations

$$\epsilon_\theta = \frac{1}{R}\frac{\partial v}{\partial \theta} + \frac{r-R}{R} + \frac{1}{2}\left(\frac{1}{R}\frac{\partial r}{\partial \theta}\right)^2 \tag{3.16}$$

$$\epsilon_x = \frac{\partial u}{\partial x} + \frac{1}{2}\left(\frac{\partial r}{\partial x}\right)^2 \tag{3.17}$$

$$\gamma_{x\theta} = \frac{1}{R}\frac{\partial u}{\partial \theta} + \frac{\partial v}{\partial x} + \frac{1}{R}\left(\frac{\partial r}{\partial x}\right)\left(\frac{\partial r}{\partial \theta}\right) \tag{3.18}$$

Stress-Strain Relations

$$\epsilon_x = \frac{1}{E}\left[\sigma_x - \nu\,\sigma_\theta\right] \tag{3.19}$$

$$\epsilon_\theta = \frac{1}{E}\left[\sigma_\theta - \nu\,\sigma_x\right] \tag{3.20}$$

$$\gamma_{x\theta} = \frac{2(1+\nu)}{E}\tau_{x\theta} \tag{3.21}$$

Equations of Equilibrium

$$\frac{\partial \sigma_x}{\partial x} + \frac{1}{R}\frac{\partial \tau_{x\theta}}{\partial \theta} = 0 \tag{3.22}$$

$$\frac{\partial \sigma_\theta}{R\,\partial \theta} + \frac{\partial \tau_{x\theta}}{\partial x} = 0 \tag{3.23}$$

$$\frac{\sigma_\theta}{R}\left[\frac{1}{R}\frac{\partial^2 r}{\partial \theta^2} - 1\right] + \sigma_x\frac{\partial^2 r}{\partial x^2} + \frac{2\tau_{x\theta}}{R}\frac{\partial^2 r}{\partial x\,\partial \theta} + \frac{p}{t} = \frac{D}{t}\left[\frac{1}{R^4}\frac{\partial^4 r}{\partial \theta^4} + \frac{2}{R^2}\frac{\partial^4 r}{\partial x^2\partial \theta^2} + \frac{\partial^4 r}{\partial x^4}\right] \tag{3.24}$$

Longeron

Equation of Equilibrium

$$E I_L \frac{d^4 f(x)}{dx^4} = 2\alpha t\left[\frac{pR}{t} - \sigma_\theta(x,\alpha)\right] + 2tR\int_0^\alpha \left\{\sigma_x \frac{\partial^2 r}{\partial x^2} + \frac{1}{R}\left[\frac{\partial \tau_{x\theta}}{\partial x}\frac{\partial r}{\partial \theta} - \frac{\partial \tau_{x\theta}}{\partial \theta}\frac{\partial r}{\partial x} + \tau_{x\theta}\frac{\partial^2 r}{\partial x \partial \theta}\right] - \frac{D}{t}\left[\frac{\partial^4 r}{\partial x^4} + \frac{1}{R^2}\frac{\partial^4 r}{\partial \theta^2 \partial x^2}\right]\right\} d\theta \tag{3.25}$$

Stress-Strain Relation

$$\epsilon_L = \frac{\sigma_L}{E} \tag{3.26}$$

Frame

Equation of Equilibrium

$$\sigma_F = \frac{1}{A_F k}\left[\int_0^a q(x)\,dx + 2DR\int_a^\alpha \left(\frac{\partial^3 r}{\partial x^3} + \frac{1}{R^2}\frac{\partial^3 r}{\partial x \partial \theta^2}\right)_{x=a} d\theta\right] \tag{3.27}$$

Strain-Displacement Relation

$$\epsilon_F = \frac{\Delta R}{R} \tag{3.28}$$

Stress-Strain Relation

$$\epsilon_F = \frac{\sigma_F}{E} \tag{3.29}$$

Longitudinal Equilibrium

$$p = \frac{\sigma_L A_L}{Rb} + \frac{2t}{b}\int_0^\alpha \sigma_x\, d\theta \tag{3.30}$$

The Boundary Conditions

Due to the choice of the coordinate system, the deflected surface, $r(x,\theta)$, becomes a doubly symmetric function of the independent variables, X and θ. That is:

$$r(X,\theta) = r(-X,\theta) = r(X,-\theta) = r(-X,-\theta)$$

Therefore, in order to discuss the boundary conditions of the problem, it is necessary to consider only that part of the deflected surface bounded by:

$$X = 0, a \qquad \theta = 0, \alpha$$

Panel Boundary Conditions

There are two variations of boundary conditions for the panel. Either the panel is attached to the frames together with the longerons or the panel is attached only to the longerons and the frames are floating. In the first case, the normal slopes must vanish along $X = a$ and $\theta = \alpha$ and the deflection of the panel along these edges must be compatible respectively with the deflections of the frame and the longeron. Hence:

Skin Attached to Frame

$$r(a,\theta) = R + \Delta R$$

$$r(X,\alpha) = R + \Delta R + f(x)$$

$$\frac{\partial r(a,\theta)}{\partial X} = 0$$

$$\frac{\partial r(X,\alpha)}{R\,\partial\theta} = 0$$

In the latter case, the normal slopes must vanish along $X = a$ and $\theta = \alpha$, and the deflection of the panel along the edge where $\theta = \alpha$ must be compatible with the longeron deflection. Since the panel is not attached to the frame, the shear, Q_X, is continuous for all values of X. Furthermore, the shear is an odd periodic function of X with period $2a$. Hence, the shear, $Q_X(a,\theta)$ must vanish.

The boundary conditions are, therefore:

Floating Frame

$$\left[\frac{\partial^3 r}{\partial x^3} + \frac{1}{R^2} \frac{\partial^3 r}{\partial x \partial \theta^2} \right]_{x=a} = 0$$

$$r(x, \alpha) = R + \Delta R + f(x)$$

$$\frac{\partial r(a, \theta)}{\partial x} = 0$$

$$\frac{\partial r(x, \alpha)}{R \partial \theta} = 0$$

Longeron Deflection Boundary Conditions

Either the longerons are simply supported by the frames or clamped to the frames. In the first case, the longeron deflection, with respect to the frame, $f(x)$, and bending moment must vanish at the frames. The latter case implies that the slope and deflection must vanish at the frames. Therefore, since $f(x) = f(-x)$, the longeron deflection boundary conditions become:

Simply Supported Longeron

$$f(a) = 0$$

$$\frac{d^2 f(a)}{dx^2} = 0$$

Clamped Longeron

$$f(a) = 0$$

$$\frac{df(a)}{dx} = 0$$

IV. LIMITING SOLUTIONS

Often the structural geometry of a pressurized fuselage is such that certain simplifying assumptions peculiar to a specific design can be made with little loss in accuracy. Therefore, even though the exact solution to the formulated problem presented in the previous section can not be obtained, four tractable limiting solutions, when applied properly to the physical situation, yield some useful results. It is important to realize that these solutions can never apply exactly to the physical situation, though checks can be made in order to obtain some measure of the resulting accuracy. Some of these checks will be discussed along with the development of the four limiting solutions.

A. Frames Close Together - Skin Attached to Frames

The simplest limiting solution was first obtained by Flügge[2]. This solution is applicable to the structure where the number of longerons is large, the frames are close together, and the skin is attached to the frames. In this case, the following additional assumptions can be made: 1) the longerons remain straight after loading, 2) the panel deflection in the radial direction is uniform, 3) the panel longitudinal and circumferential stresses, σ_x and σ_θ, are uniform, and 4) the longeron axial stress σ_L, is uniform. The longeron bending stress, $\sigma_L'(x)$, can not be evaluated by the solution. The assumption that the panel deflection is uniform radially implies that this solution is only applicable to those geometries where the panels can be considered as thick, initially curved plates. The development is

outlined below.

When these assumptions are introduced into the governing equations, (3.16) through (3.30), the following simplified set is obtained:

Panel

Strain-Displacement Relations

$$\epsilon_\theta = \frac{\Delta R}{R} \tag{4.1}$$

$$\epsilon_x = \text{constant} \tag{4.2}$$

$$\gamma_{x\theta} = 0 \tag{4.3}$$

Stress-Strain Relations

$$\epsilon_\theta = \frac{1}{E}\left[\sigma_\theta - \nu \sigma_x\right] \tag{4.4}$$

$$\epsilon_x = \frac{1}{E}\left[\sigma_x - \nu \sigma_\theta\right] \tag{4.5}$$

$$\gamma_{x\theta} = \frac{2(1+\nu)}{E} \tau_{x\theta} \tag{4.6}$$

Equations of Equilibrium

Equations (3.22) and (3.23) vanish.

$$\sigma_\theta = \frac{pR}{t} \tag{4.7}$$

Longeron

Equation of Equilibrium

$$EI_L \frac{d^4 f(x)}{dx^4} = 2\alpha t\left[\frac{pR}{t} - \sigma_\theta\right] \tag{4.8}$$

Stress-Strain Relation

$$\epsilon_L = \frac{\sigma_L}{E} \tag{4.9}$$

Frame

Equation of Equilibrium

$$\sigma_F = \frac{1}{A_F \kappa} \int_0^a q(x)\, dx \tag{4.10}$$

Strain-Displacement Relation:

$$\epsilon_F = \frac{\Delta R}{R} \tag{4.11}$$

Stress-Strain Relation:

$$\epsilon_F = \frac{\sigma_F}{E} \tag{4.12}$$

Longitudinal Equilibrium

$$p = \frac{\sigma_L A_L}{Rb} + \frac{2t\sigma_x}{R} \tag{4.13}$$

Since the panel radial deflection, $r-R$, has been prescribed as being a constant, and the stresses, σ_θ and σ_x, have been prescribed as being uniform, all of the equations, (4.1) through (4.13), can not be satisfied simultaneously. The solution which results in compatible displacements between panel, longeron and frames (assuming the longerons remain straight), and satisfies equilibrium of the section cut out by the planes $x=0$ and $x=2a$, is Flügge's limiting solution for frames close together. The longitudinal equilibrium equation (4.13) implies that:

$$\sigma_x = \frac{pR}{2t} - \frac{\sigma_L A_L}{2\kappa R t} \tag{4.14}$$

Equilibrium is satisfied in the tangential direction by the relation:

$$\sigma_\theta = \frac{PR}{t} - \frac{\sigma_F A_F}{2at} \tag{4.15}$$

Since the stresses are uniform, the compatibility conditions become (neglecting the small influence of the eccentricities of the centroids of the components):

$$\epsilon_x = \epsilon_L \tag{4.16}$$

$$\epsilon_\theta = \epsilon_F \tag{4.17}$$

Which from equations (4.4), (4.5), (4.9) and (4.12), it follows that:

$$\sigma_L = \sigma_x - \nu \sigma_\theta \tag{4.18}$$

$$\sigma_F = \sigma_\theta - \nu \sigma_x \tag{4.19}$$

Equations (4.14), (4.15), (4.18) and (4.19) completely define the stress state. Solving for each stress independently yields:

$$\sigma_\theta = \frac{PR}{t} \frac{1 + \lambda + \frac{\gamma \nu}{2}}{(1+\gamma)(1+\lambda) - \gamma\lambda\nu^2} \tag{4.20}$$

$$\sigma_x = \frac{PR}{2t} \frac{1 + \gamma + 2\lambda\nu}{(1+\lambda)(1+\gamma) - \lambda\gamma\nu^2} \tag{4.21}$$

$$\sigma_F = \frac{PR}{t} \frac{1 + \lambda(1-\nu^2) - \frac{\nu}{2}}{(1+\gamma)(1+\lambda) - \gamma\lambda\nu^2} \tag{4.22}$$

$$\sigma_L = \frac{PR}{2t} \frac{1 + \gamma(1-\nu^2) - 2\nu}{(1+\gamma)(1+\lambda) - \gamma\lambda\nu^2} \tag{4.23}$$

where it is convenient to define the two area ratios:

$$\lambda \equiv \frac{A_L}{2bt}$$

$$\gamma \equiv \frac{A_F}{2at}$$

One interesting conclusion which can be drawn from this solution and which is typical of all solutions is the strong dependence on Poisson's ratio. This is due to the biaxial stress state in the panels and the uniaxial stress state in the longerons and frames.

A check to obtain a measure of the resulting accuracy of the solution can easily be made by computing the longeron maximum deflection, $f(o)$, and comparing this to the panel radial deflection for the fictitious case where the frame area is zero, $\Delta R_{A_F=0}$. Since it was assumed that the longerons remain straight after loading, for a valid solution it is essential that:

$$\frac{f(o)}{\Delta R_{A_F=0}} << 1$$

The longeron loading which is necessarily uniform by assumption is given by:

$$q(x) = q_o = \frac{\sigma_F A_F b}{Ra} \tag{4.24}$$

Whereupon simple beam theory gives for the central longeron deflection:

$$f(o) = \frac{q_o a^4}{24 E I_L} = \frac{\sigma_F A_F b a^3}{24 E I_L R} \tag{4.25}$$

The deflection of the panel for $A_F = 0$ $(\gamma = 0)$ is:

$$\Delta R_{A_F=0} = \frac{PR^2}{Et} \frac{1 + \lambda(1-\nu^2) - \frac{\nu}{2}}{(1+\lambda)} \tag{4.26}$$

So that:

$$\frac{f(o)}{\Delta R_{A_F=0}} = \frac{A_F R b}{24 I_L}\left(\frac{a}{R}\right)^3 \frac{1}{1+\gamma-\frac{\gamma\lambda\nu^2}{1+\lambda}} << 1 \qquad (4.27)$$

Note the strong dependence of the ratio of half the frame spacing to the fuselage radius, $\frac{a}{R}$. The validity of the other assumptions can not be checked easily.

Flügge's second limiting solution is applicable to the case where the longerons are spaced closely enough so that the skin panel can be considered as behaving like a thick plate in the circumferential direction, but the frames are too far apart to satisfy this condition in the longitudinal direction. In this case, the problem can be satisfactorily formulated by considering an anisotropic shell stiffened by evenly spaced frames. The solution given in reference 3, page 404, has been extended by Flügge[2] to include an anisotropic shell. The anisotropy in this case as opposed to the first solution is due to stiffening of the shell by the closely spaced longerons only. The frames result in discontinuity shearing forces. Few fuselage structural geometries presently in existence satisfy the requirements of this limiting solution.

B. 1 Frames Close Together - Floating Frames

When the skin is not attached to the frames and the frames are close together, the only requirement for an exact solution of the formulated problem is that the longerons remain straight after loading. An exact solution is tractable in this case because the

skin behaves like an initially curved infinite strip plate bounded by the longerons under uniform lateral loading. As before, a check can easily be performed to show the validity of this assumption. Cross-sections of this strip are shown in Figs. 12a and 12b. Introducing the fact that r and v are functions of θ only, and u is a function of x only, the equations representing the mathematical formulation of the problem become:

Panel

Strain-Displacement Relations

$$\epsilon_\theta = \frac{1}{R}\frac{dv}{d\theta} + \frac{r-R}{R} + \frac{1}{2}\left(\frac{1}{R}\frac{dr}{d\theta}\right)^2 \tag{4.28}$$

$$\epsilon_x = \frac{du}{dx} \tag{4.29}$$

$$\gamma_{x\theta} = 0 \tag{4.30}$$

Stress-Strain Relations

$$\epsilon_x = \frac{1}{E}\left[\sigma_x - \nu\sigma_\theta\right] \tag{4.31}$$

$$\epsilon_\theta = \frac{1}{E}\left[\sigma_\theta - \nu\sigma_x\right] \tag{4.32}$$

$$\gamma_{x\theta} = \frac{2(1+\nu)}{E}\tau_{x\theta} \tag{4.33}$$

Equations of Equilibrium

$$\sigma_x = F_1(\theta) \tag{4.34}$$

$$\sigma_\theta = F_2(x) \tag{4.35}$$

$$\frac{\sigma_\theta}{R}\left[\frac{1}{R}\frac{d^2r}{d\theta^2} - 1\right] + \frac{P}{t} = \frac{D}{t}\frac{1}{R^4}\frac{d^4r}{d\theta^4} \tag{4.36}$$

Longeron

Equation of Equilibrium

$$\sigma_\theta = \frac{pR}{t} \tag{4.37}$$

Equation (4.37) is invalid by assumption that $f(x) = 0$

Stress-Strain Relation

$$\epsilon_L = \frac{\sigma_L}{E} \tag{4.38}$$

Frame

Equation of Equilibrium

$$\sigma_F = \frac{2at}{A_F}\left[\frac{pR}{t} - \sigma_\theta\right] \tag{4.39}$$

Strain-Displacement Relation

$$\epsilon_F = \frac{\Delta R}{R} \tag{4.40}$$

Stress-Strain Relation

$$\epsilon_F = \frac{\sigma_F}{E} \tag{4.41}$$

Longitudinal Equilibrium

$$p = \frac{\sigma_L A_L}{Rb} + \frac{2t}{b}\int_0^\alpha \sigma_x \, d\theta \tag{4.42}$$

From equations (4.28), (4.29), (4.31), (4.32), (4.34) and (4.35), it follows that σ_x and σ_θ are constants. In that case, equation (4.42) becomes:

$$\sigma_x = \frac{1}{2t}\left[pR - \frac{\sigma_L A_L}{b}\right] \tag{4.43}$$

The strains ϵ_x and ϵ_L must be equal for compatible displacements.

Hence:

$$\sigma_L = \sigma_x - \nu \sigma_\theta \tag{4.44}$$

Putting this fact into equation (4.43), the following equation for longitudinal equilibrium is obtained:

$$\sigma_x = \frac{1}{1+\lambda}\left(\frac{pR}{2t} + \lambda \nu \sigma_\theta\right) \tag{4.45}$$

Where, as before:

$$\lambda \equiv \frac{A_L}{2bt}$$

In this case, in order to describe the deflection of the panel it becomes more convenient to use the Cartesian coordinate system shown in Fig. 12b. If α is a small angle (large number of longerons), then the frame displacement, ΔR, shown in Fig. 12a can be represented as a boundary displacement, $\alpha \Delta R$, shown in Fig. 12b. If $\omega_0(y)$ is the initial deflection of the strip and $\omega_1(y)$ is the change in deflection after loading, then the equation of equilibrium of forces in the ω direction can be written in the usual manner[3]:

$$\frac{d^4\omega_1}{dy^4} - K^2\left[\frac{d^2\omega_0}{dy^2} + \frac{d^2\omega_1}{dy^2}\right] = Q \tag{4.46}$$

where

$$D \equiv \frac{Et^3}{12(1-\nu^2)}$$

$$K^2 \equiv \frac{\sigma_\theta t}{D}$$

$$Q \equiv \frac{p}{D}$$

The boundary conditions for the unknown deflection, ω_1,

are:

$$\omega_1(b) = \frac{d\omega_1(b)}{dY} = 0$$

and the initial deflection, ω_o , can be approximated for sufficiently small α by:

$$\omega_o(Y) = \frac{1}{2R}(b^2 - Y^2)$$

The differential equation (4.46) can easily be solved. The general even solution is:

$$\omega_1(Y) = A\,\cosh KY - \frac{1}{K^2}\left[\frac{\Phi}{K^2} + B\right] - \frac{\Phi Y^2}{2K^2}$$

where $$\Phi \equiv Q - \frac{K^2}{R^2}$$

and A, B, are arbitrary constants.

Applying the required boundary conditions,

$$\omega_1(Y) = \frac{\Phi}{K^2}\left\{\frac{b}{K}\,\frac{\cosh KY - \cosh Kb}{\sinh Kb} + \frac{1}{2}(b^2 - Y^2)\right\} \qquad (4.47)$$

K is still unknown since σ_θ has not been determined. Equation (4.47), therefore, satisfies equilibrium for any value of σ_θ . That value of σ_θ which satisfies compatibility results in the proper solution.

The strain-displacement relation in Cartesian coordinates[3] is:

$$\epsilon_\theta = \frac{du}{dY} + \frac{1}{2}\left[\left(\frac{d\omega}{dY}\right)^2 - \left(\frac{d\omega_o}{dY}\right)^2\right] \qquad (4.48)$$

where $\omega = \omega_o + \omega_1$ ≡ total deflection.

From the stress-strain relations, it is evident that ϵ_θ is constant.

Integrating equation (4.48) from $Y=0$ to $Y=b$ implies that:

$$\epsilon_\theta b = u(b) + \frac{1}{2}\int_0^b \left[\left(\frac{dw}{dY}\right)^2 - \left(\frac{dw_0}{dY}\right)^2\right] dY ,$$

but

$$u(b) = \alpha \Delta R = \frac{b \Delta R}{R} .$$

Therefore, it follows that compatibility requires:

$$\epsilon_\theta = \frac{\Delta R}{R} + \frac{1}{2b}\int_0^b \left[\left(\frac{d(w_0+w_1)}{dY}\right)^2 - \left(\frac{dw_0}{dY}\right)^2\right] dY \qquad (4.49)$$

Substituting equation (4.47) into (4.49) after differentiating and integrating, the compatibility condition becomes:

$$\epsilon_\theta = \frac{\Delta R}{R} + \frac{1}{2b}\left(\frac{Q}{K^2} - \frac{1}{R}\right)\left\{\frac{Qb^3}{2K^2}\left[2 - \left(\coth Kb - \frac{1}{Kb}\right)\left(\coth Kb + \frac{4}{Kb}\right)\right] + \frac{b^3}{2R}\coth Kb\left[\coth Kb - \frac{1}{Kb}\right]\right\} \qquad (4.50)$$

Finally, substituting equations (4.32), (4.40), (4.41), (4.39) and (4.45) into (4.50), the compatibility condition which satisfies equilibrium in the radial direction becomes:

$$\frac{K^2 D}{t}\left\{\frac{1+\lambda(1-\nu^2)}{1+\lambda} + \frac{1}{\gamma}\right\} - \frac{pR}{t}\left\{\frac{\nu}{2(1+\lambda)} + \frac{1}{\gamma}\right\} = \frac{E}{2b}\left(\frac{Q}{K^2} - \frac{1}{R}\right)\left\{\frac{Qb^3}{2K^2}\left[\frac{5}{3} - \left(\coth Kb - \frac{1}{Kb}\right)\left(\coth Kb + \frac{4}{Kb}\right)\right] - \frac{b^3}{2R}\left[\frac{1}{3} - \coth Kb\left(\coth Kb - \frac{1}{Kb}\right)\right]\right\} \qquad (4.51)$$

where

$$K^2 \equiv \frac{\sigma_\theta t}{D}$$

$$\lambda \equiv \frac{A_L}{2bt}$$

$$\gamma \equiv \frac{A_F}{2at}$$

$$Q \equiv \frac{p}{D}$$

K can be determined from equation (4.51) by trial and error or other means. Hence, σ_θ is known. Then it is a simple matter to determine the other stress components from:

$$\sigma_x = \frac{1}{1+\lambda}\left(\frac{pR}{2t} + \lambda \nu \sigma_\theta\right)$$

$$\sigma_F = \frac{1}{\gamma}\left(\frac{pR}{t} - \sigma_\theta\right)$$

$$\sigma_L = \sigma_x - \nu \sigma_\theta$$

The validity of the assumption that the longerons remain straight can be checked as before by computing the ratio of the maximum deflection of the longeron, $f(o)$, to the radial skin deflection without frames, $\Delta R_{A_F=0}$. In this case, the longeron loading is given by:

$$q(x) = q_o = \frac{2b}{R}(pR - \sigma_\theta t)$$

And for continuous longerons, the maximum deflection is:

$$f(o) = \frac{q_o a^4}{24 E I_L} = \frac{a^4 b}{12 E I_L}\left(p - \frac{\sigma_\theta t}{R}\right)$$

The radial deflection of the panel for $A_F = o$ is the same as before so that:

$$\frac{f(0)}{\Delta R_{A_F=0}} = \frac{a^4 b t (1+\lambda)\left(1 - \frac{\sigma_\theta t}{pR}\right)}{12 I_L R^2 \left[1+\lambda(1-\nu^2) - \frac{\nu}{2}\right]} \tag{4.52}$$

For the solution to be valid, it is required that:

$$\frac{f(0)}{\Delta R_{A_F=0}} << 1$$

B2. Frames Close Together - Floating Frames - Membrane Solution

In the previous solution, the bending of the skin panel was included in the equation of equilibrium. When the panel thickness is very small compared to the width and the pressure is sufficiently high, the contribution of the membrane forces in supporting the pressure loading is much greater than that of the plate bending. The bending rigidity, D, in the plate equation of equilibrium may therefore be neglected, resulting in the equation of equilibrium of a membrane:

$$\sigma_\theta t \left[\frac{d^2 w_0}{dy^2} + \frac{d^2 w_1}{dy^2} \right] = -p \tag{4.53}$$

The compatibility condition, assuming that the panel behaves like a membrane, is, upon setting $D=0$ in the previous solution:

$$\sigma_\theta \left\{ \frac{1+\lambda(1-\nu^2)}{1+\lambda} + \frac{1}{\gamma} \right\} - \frac{pR}{t} \left\{ \frac{\nu}{2(1+\lambda)} + \frac{1}{\gamma} \right\} = \frac{Eb^2}{6} \left[\left(\frac{p}{\sigma_\theta t} \right)^2 - \frac{1}{R^2} \right], \tag{4.54}$$

from which σ_θ may be determined by trial and error or other means, and:

$$\sigma_x = \frac{1}{1+\lambda}\left(\frac{pR}{2t} + \lambda\nu\sigma_\theta\right) \tag{4.55}$$

$$\sigma_F = \frac{1}{\gamma}\left(\frac{pR}{t} - \sigma_\theta\right) \tag{4.56}$$

$$\sigma_L = \sigma_x - \nu\sigma_\theta \tag{4.57}$$

The check on the validity of the assumption that the longerons remain straight after loading is identical with the previous plate analysis:

$$\frac{f(o)}{\Delta R_{A_F=0}} = \frac{a^4 b t\left(1 - \frac{\sigma_\theta t}{pR}\right)(1+\lambda)}{12\, I_L R^2\left[1+\lambda(1-\nu^2) - \frac{\gamma}{2}\right]} << 1 \tag{4.58}$$

These two previous solutions offer a good means for obtaining, in more complicated cases, some insight concerning the validity of the assumption that the skin panel behaves essentially like a membrane. This matter, the validity of the membrane assumption, will be discussed in detail in a later part.

C. Frames Not Close Together - Floating Frames - Membrane Solution

When the frames are not sufficiently close together, the deflection of the longerons must be taken into account. An approximate solution can be obtained for the case of floating frames, if the following assumptions are set forth: 1) The skin panel behaves essentially like a membrane, 2) The skin panel curvature in the longitudinal direction and the cross curvature are much smaller than the curvature in the circumferential direction, 3) The panel shear stress,

$\tau_{x\theta}$, is small compared to the normal stresses, σ_x and σ_θ , and 4) The longitudinal stress, σ_x , is constant. The first assumption is valid when the panel skin thickness is small compared to its width, and the second and third assumptions imply that the ratio of the radius, R , of the cylinder to the longeron radius of curvature, $\frac{1}{f''(x)}$, must be much smaller than unity. In view of these conditions then, the more exact equations reduce to the following set:

Panel

Strain-Displacement Relations

$$\epsilon_\theta = \frac{1}{R}\frac{\partial v}{\partial \theta} + \frac{r-R}{R} + \frac{1}{2}\left(\frac{1}{R}\frac{\partial r}{\partial \theta}\right)^2 \tag{4.59}$$

$$\epsilon_x = \frac{\partial u}{\partial x} + \frac{1}{2}\left(\frac{\partial r}{\partial x}\right)^2 \tag{4.60}$$

$$\gamma_{x\theta} = 0 \tag{4.61}$$

Stress-Strain Relations

$$\epsilon_x = \frac{1}{E}\left[\sigma_x - \nu\sigma_\theta\right] \tag{4.62}$$

$$\epsilon_\theta = \frac{1}{E}\left[\sigma_\theta - \nu\sigma_x\right] \tag{4.63}$$

$$\gamma_{x\theta} = \frac{2(1+\nu)}{E}\tau_{x\theta} \tag{4.64}$$

Equations of Equilibrium

$$\sigma_x = \text{CONSTANT} \tag{4.65}$$

$$\sigma_\theta = \sigma_\theta(x) \tag{4.66}$$

$$\frac{\sigma_\theta}{R}\left[\frac{1}{R}\frac{\partial^2 r}{\partial\theta^2} - 1\right] = -\frac{p}{t} \tag{4.67}$$

Longeron

Equation of Equilibrium

$$EI_L \frac{d^4 f(x)}{dx^4} = 2\alpha t\left[\frac{pR}{t} - \sigma_\theta(x)\right] \tag{4.68}$$

Stress-Strain Relation

$$\epsilon_L = \frac{\sigma_L}{E} \tag{4.69}$$

Frame

Equation of Equilibrium

$$\sigma_F = \frac{1}{A_F \alpha}\int_0^a q(x)\,dx \tag{4.70}$$

Strain-Displacement Relation

$$\epsilon_F = \frac{\Delta R}{R} \tag{4.71}$$

Stress-Strain Relation

$$\epsilon_F = \frac{\sigma_F}{E} \tag{4.72}$$

Longitudinal Equilibrium

$$p = \frac{\sigma_L A_L}{Rb} + \frac{2t}{b}\int_0^\alpha \sigma_x\,d\theta \tag{4.73}$$

Substituting equations (4.65) and (4.66) into equations (4.62) and (4.63), it is clear that ϵ_θ and ϵ_x are functions of x alone. These strains will in general result in the panel edge displacement, $V(x,\alpha)$, which should vanish. For this reason, it is essential that the longeron deflection be small in order to insure a reasonably accurate solution.

From equation (4.67), the circumferential curvature must depend on x alone, since σ_θ is a function of x alone. Therefore, the cross-section of the skin panel for a given x must remain circular after loading. This is illustrated in Fig. 13, from which it follows that equation (4.67) can be written:

$$\sigma_\theta(x) = \frac{p\rho(x)}{t} \tag{4.74}$$

The remaining problem is essentially one of geometry. The radius, $\rho(x)$, can be expressed in terms of $\sigma_\theta(x)$ and the sum of the longeron and frame displacements in the following manner. Assuming that α is a small angle, i.e. many longerons, the radius vector, r, can be written:

$$r(x,\theta) = R + \Delta R + f(x) + \delta(x)\left[1 - \left(\frac{\theta}{\alpha}\right)^2\right] \tag{4.75}$$

and the angle, β:

$$\beta = \alpha - \frac{1}{R + f(x) + \Delta R} \left.\frac{\partial r}{\partial \theta}\right|_{\theta=\alpha} \tag{4.76}$$

Substituting equation (4.75) after differentiation into (4.76) and neglecting $f(x) + \Delta R$ compared to R, β may be written:

$$\beta = \alpha\left[1 + \frac{2\delta(x)}{R\alpha^2}\right] \tag{4.77}$$

The circumferential strain, ϵ_θ, is by definition:

$$\epsilon_\theta = \frac{\rho(x)\beta}{R\alpha} - 1 \tag{4.78}$$

The slope, $\frac{1}{R}\frac{\partial r}{\partial \theta}$, is small compared to unity, so that:

$$\rho(x)\beta \doteq \int_0^\alpha r\, d\theta \tag{4.79}$$

Upon substituting equation (4.75) into the above and integrating, it follows that:

$$\rho\beta = \alpha\left[R + \Delta R + f(x) + \tfrac{2}{3}\delta(x)\right] \tag{4.80}$$

The circumferential strain then becomes:

$$\epsilon_\theta = \frac{1}{R}\left[f(x) + \Delta R + \tfrac{2}{3}\delta(x)\right] \tag{4.81}$$

If equations (4.80) and (4.81) are substituted into equation (4.74), the equilibrium equation, and $\Delta R + f(x) + \frac{2}{3}\delta(x)$ is neglected compared to R, then:

$$\sigma_\theta = \frac{pR}{t}\left[\frac{1}{1 + \frac{2\delta(x)}{R\alpha^2}}\right] \tag{4.82}$$

The procedure for the approximate solution of these equations will be discussed now. One means of solution is obtained if equations (4.81) and (4.82) are substituted into equation (4.68) such that σ_θ and $\delta(x)$ are eliminated. Then, in principle, the only unknown other than $f(x)$ is ΔR, a constant. Hence, from this resulting equation, the longeron deflection can be determined as a function of x and ΔR.

From equation (4.73), it follows that:

$$\sigma_x = \frac{1}{2\alpha t}\left[pb - \frac{\sigma_L A_L}{R}\right] \tag{4.83}$$

since σ_x is constant. If the longitudinal panel displacement at the longeron is to be compatible with the longeron displacement, then, since $\tau_{x\theta}$ is assumed zero:

$$\epsilon_x = \epsilon_L$$

From the stress-strain relations, this implies that:

$$\sigma_L = \sigma_x - \nu \sigma_\theta$$

and from equation (4.83), σ_x is not constant but a function of θ. This paradox arises from the assumption that $\tau_{x\theta}$ is everywhere zero. Since the role of σ_x in the determination of $\sigma_\theta(x)$ is relatively insignificant (due to Poisson's ratio) it will be determined as an approximation from the previous case where the frames are close together and the skin is attached to the frames. Hence, from equation (4.21):

$$\sigma_x = \frac{PR}{2t} \frac{1 + \gamma + 2\lambda\nu}{(1+\lambda)(1+\gamma) - \lambda\gamma\nu^2}$$

By eliminating $\delta(x)$ from equation (4.81) by substituting equation (4.82) into it, the circumferential stress, σ_θ, can be determined as a function of x and ΔR. The longeron loading, $q(x)$, is determined from the relation:

$$q(x) = 2\alpha t \left[\frac{PR}{t} - \sigma_\theta(x) \right]$$

which is also dependent upon ΔR. The frame stress, σ_F, is determined from equation (4.70) and the resulting ΔR from equations (4.71) and (4.72).

A second and more practical means of solution which will be adopted here is to estimate a particular ΔR which, of course, is less than the panel deflection when there are no frames. Then $\sigma_F A_F$ is computed from equation (4.70). That frame area which is obtained as a result of the assumed value of ΔR will be different, in general, from the actual frame area. This process is repeated

by estimating different frame deflections, ΔR , until the proper frame area is obtained. Solving for $\delta(x)$ in equation (4.81) after substituting σ_θ obtained from equation (4.82), it follows that:

$$\delta(x) = \frac{3}{4} b \left\{ -\left[K_1 + \frac{f(x)}{b} \right] + \sqrt{K_2 + K_3 \frac{f(x)}{b} + \left[\frac{f(x)}{b} \right]^2} \right\} \quad (4.84)$$

where

$$K_1 \equiv \frac{b}{3R} + \frac{\Delta R}{b} + \frac{\nu \sigma_x R}{Eb}$$

$$K_2 \equiv \frac{1}{9}\left(\frac{b}{R}\right)^2 + \left(\frac{\nu \sigma_x R}{Eb}\right)^2 + \frac{4pR}{3Et} - \frac{2}{3}\left[\frac{\Delta R}{R} + \frac{\nu \sigma_x}{E}\right]\left[1 - \frac{3\Delta R R}{b^2}\right]$$

$$K_3 \equiv 2\left[\frac{\Delta R}{b} + \frac{\nu \sigma_x R}{Eb} - \frac{b}{3R} \right]$$

Note that for a given pressure, p , and assumed value of the frame displacement, ΔR , the quantities, K_1 , K_2 and K_3 are determined. When equation (4.63) is substituted into equation (4.81), it follows that:

$$\sigma_\theta = \frac{E}{R}\left[f(x) + \Delta R + \frac{2}{3}\delta(x) \right] + \nu \sigma_x \quad (4.85)$$

When this equation, together with the previous expression for $\delta(x)$, is substituted into the expression for the longeron loading, $q(x)$, this becomes:

$$q(x) = \kappa t \left\{ 2\left[\frac{pR}{t} - \frac{E\Delta R}{R} + \frac{E}{6}\left(\frac{b}{R}\right)^2 - \frac{\nu}{2}\sigma_x \right] - \frac{Eb}{R}\left[f(x) + \sqrt{K_2}\sqrt{1 + \frac{K_3}{K_2}\frac{f(x)}{b} + \frac{1}{K_2}\left[\frac{f(x)}{b}\right]^2} \right] \right\} \quad (4.86)$$

Note that if certain conditions are satisfied, the longeron loading, $q(x)$, becomes approximately a linear function of the longeron deflection, $f(x)$. These conditions are:

$$\frac{K_3}{K_2}\frac{f(x)}{b} << 1$$

and

$$\frac{f(x)}{b} << K_3$$

Under these circumstances, the longeron loading is given by:

$$q(x) = \frac{1}{EI_L}\left[C - 4K^4 f(x)\right] \tag{4.87}$$

where

$$\frac{C}{EI_L} \equiv \frac{2bt}{R}\left[\frac{pR}{t} - \frac{\nu}{2}\sigma_x + \frac{E}{R}\left(\frac{b^2}{6R} - \frac{\Delta R}{2} - \frac{b}{2}\sqrt{K_2}\right)\right]$$

$$\frac{4K^4}{EI_L} \equiv \frac{Ebt}{R^2}\left[1 + \frac{K_3}{2\sqrt{K_2}}\right]$$

From the definition of K_1, K_2, and K_3, for sufficiently small pressures,

$$K_1 = O\left(\frac{b}{R}\right)$$

$$K_2 = O\left(\frac{b^2}{R^2}\right)$$

$$K_3 = O\left(\frac{b}{R}\right)$$

In this case the linearization conditions become the single restriction that:

$$\frac{f(x)}{b} << \frac{b}{R}$$

This condition is usually satisfied in conventional structural design. The validity of this linearization is dependent, therefore, upon the magnitude of the pressure loading, p, and the above restriction.

The pressure must be such that:

$$\frac{pR}{Et} << \left(\frac{b}{R}\right)^2$$

This restriction limits the solution to small pressure for some structural geometries. In order to alleviate this difficulty should it arise, another means for linearization will be discussed.

The longeron loading is almost always positive (outward) for positive internal pressurization. Hence, a linear approximation in the positive range of $q(x)$ is sufficient. When the structural geometry and pressure are such that the above restrictions are not satisfied, then the exact variation can be plotted in the positive range of $q(x)$ and a suitable linearization made. This has the added advantage of limiting the linearization by visual inspection to the cases where good results can be obtained. An example of such a linearization is illustrated in Fig. 19. It is clear in this case that the linear approximation is quite representative of the actual behavior. The longeron loading can therefore be expressed by:

$$q(x) = \frac{1}{EI_L}\left[C - 4K^4 f(x)\right]$$

where $\frac{C}{EI_L}$ is the $q(x)$ axis intercept and $\frac{4K^4}{EI_L}$ is the negative slope of the linear variation. When this expression is substituted into the longeron equilibrium equation (4.68), an ordinary linear differential equation expressing the longeron deflection, $f(x)$, is obtained:

$$\frac{d^4 f(x)}{dx^4} = C - 4K^4 f(x) \qquad (4.88)$$

The general solution to this differential equation is:

$$f(x) = C_1 \sinh Kx \sin Kx + C_2 \cosh Kx \cos Kx + C_3 \sinh Kx \cos Kx + C_4 \cosh Kx \sin Kx + \frac{C}{4K^4} \quad (4.89)$$

and since the even solution is required, $C_3 = C_4 = 0$. The coefficients will be determined from the boundary conditions:

Case a - Continuous Longerons

$$f(a) = 0$$
$$\frac{df(a)}{dx} = 0$$

Case b - Simply Supported Longerons

$$f(a) = 0$$
$$\frac{d^2 f(a)}{dx^2} = 0$$

In either case, $f(a) = 0$, which implies:

$$C_2 = -\frac{1}{\cosh Ka \cos Ka}\left[C_1 \sinh Ka \sin Ka + \frac{C}{4K^4}\right] \quad (4.90)$$

Case a - Continuous Longerons

$\frac{df(a)}{dx} = 0$ implies:

$$C_2 = -C_1 \frac{\cosh Ka \sin Ka + \sinh Ka \cos Ka}{\sinh Ka \cos Ka - \cosh Ka \sin Ka} \quad (4.91)$$

Solving for C_1 and C_2 from equations (4.90) and (4.91), it follows that:

$$f(x) = \frac{C}{4K^4}\left\{1 - \frac{(\cosh Ka \sin Ka + \sinh Ka \cos Ka)\cosh Kx \cos Kx}{\sin Ka \cos Ka + \sinh Ka \cosh Ka} + \frac{(\cosh Ka \sin Ka - \sinh Ka \cos Ka)\sinh Kx \sin Kx}{\sin Ka \cos Ka + \sinh Ka \cosh Ka}\right\} \quad (4.92)$$

The longeron maximum bending moment is obtained from the relation:

$$M_{MAX.} = EI_L \frac{d^2 f(a)}{dx^2} \tag{4.93}$$

Differentiating equation (4.92) twice, setting $x = a$ and substituting into equation (4.93) results in:

$$M_{MAX.} = \frac{CEI_L}{2K^2} \frac{\sinh Ka \cosh Ka - \sin Ka \cos Ka}{\sinh Ka \cosh Ka + \sin Ka \cos Ka} \tag{4.94}$$

from which the longeron maximum bending stress can be obtained by the expression:

$$\sigma'_{L_{MAX}} = \frac{M_{MAX}\, \bar{c}}{I_L} \tag{4.95}$$

When the expression for the longeron loading, equation (4.87), is substituted into equation (4.70), the frame stress is given by:

$$\sigma_F = \frac{1}{A_F K E I_L} \int_0^a \left[C - 4K^4 f(x) \right] dx \tag{4.96}$$

Performing the required integration by using equation (4.92), the expression for the frame stress becomes:

$$\sigma_F = \frac{RC}{EI_L A_F b K} \frac{\cosh^2 Ka \sin^2 Ka + \sinh^2 Ka \cos^2 Ka}{\sin Ka \cos Ka + \sinh Ka \cosh Ka} \tag{4.97}$$

Case b - Simply Supported Longerons

When the longerons are simply supported, the bending moment must vanish at the frames. Therefore,

$$\frac{d^2 f(a)}{dx^2} = 0$$

which implies that:

$$C_2 = C_1 \frac{\cosh ka \cos ka}{\sinh ka \sin ka} \tag{4.98}$$

Solving for C_1 and C_2 from equations (4.90) and (4.98), it follows that:

$$f(x) = \frac{C}{4K^4}\left[1 - \frac{\sinh ka \sin ka \sinh kx \sin kx}{\cosh^2 ka \cos^2 ka + \sinh^2 ka \sin ka} - \frac{\cosh ka \cos ka \cosh kx \cos kx}{\cosh^2 ka \cos^2 ka + \sinh^2 ka \sin ka}\right] \tag{4.99}$$

In this case the maximum longeron bending moment is given by:

$$M_{MAX} = EI_L \frac{d^2 f(0)}{dx^2} \tag{4.100}$$

and by using equation (4.99):

$$M_{MAX.} = -\frac{CEI_L}{2K^2}\left[\frac{\sinh ka \sin ka}{\cosh^2 ka \cos^2 ka + \sinh^2 ka \sin^2 ka}\right], \tag{4.101}$$

from which the longeron maximum bending stress can be obtained by the expression:

$$\sigma'_{L\,MAX} = \frac{M_{MAX}\,\bar{c}}{I_L} \tag{4.102}$$

Performing the required integration by using equation (4.99), the expression for the frame stress, equation (4.96), becomes:

$$\sigma_F = \frac{RC}{2EI_L A_F b K} \frac{\sinh ka \cosh ka + \sin ka \cos ka}{\cosh^2 ka \cos^2 ka + \sinh^2 ka \sin^2 ka} \tag{4.103}$$

Computational Procedure

A review of the computational procedure will now be presented. The following steps are required to obtain the solution:

1) The longitudinal stress, σ_x , is computed from equation (4.21).

2) A value of the frame displacement, $\Delta R'$, is chosen (prime indicates estimated frame deflection). Note that:

$$0 \leq \Delta R' \leq \frac{pR^2}{Et} \frac{1+\lambda(1-\nu^2)-\frac{\nu^2}{}}{(1+\lambda)}$$

which is the skin radial deflection when the frame area is zero.

3) The quantities C and K are computed.

4) The frame axial force, $\sigma_F A_F$, is computed from equation (4.97) for continuous longerons and (4.103) for simply supported longerons by multiplying by A_F , the true frame area.

5) The frame area which is compatible with the chosen frame displacement, $\Delta R'$, is obtained from equation (4.71) and equation (4.72), or:

$$A_F' = \frac{(\sigma_F A_F) R}{\Delta R E}$$

6) If the above obtained frame area is less than the actual frame area, then the chosen $\Delta R'$ was too large, and for the next estimate a smaller $\Delta R'$ is required. If the frame area is too large then $\Delta R'$ must be reduced. Then steps 2) through 5) are repeated until the computed frame area, A_F' , consistent with $\Delta R'$, is equal to the

actual frame area. The actual frame deflection is then known.

7) The longeron central deflection, $f(o)$, is computed from equation (4.92) or equation (4.99) depending on the longeron boundary conditions and $\frac{f(o)}{b}$ is compared with $\frac{b}{R}$ in order to check the validity of the first method of linearization if it is utilized. Otherwise, of course, step 7) may be omitted.

8) $\delta(o)$ is computed from equation (4.84).

9) The maximum circumferential skin stress is computed from equation (4.82), namely:

$$\sigma_{\theta_{MAX}} = \sigma_\theta(o) = \frac{pR}{t}\left[\frac{1}{1 + \frac{2\delta(o)}{R\alpha^2}}\right] \qquad (4.73)$$

10) The longeron axial stress, σ_L, is obtained from equation (4.73):

$$\sigma_L = \frac{Rb}{A_L}\left[p - 2t\frac{\sigma_x}{R}\right]$$ since σ_x is constant.

11) The maximum longeron stress is obtained by adding to the maximum bending stress given by equation (4.95) or (4.102) the axial stress obtained in the previous step, or:

$$\sigma_{L_{MAX}} = \sigma_L + \sigma'_{L_{MAX}}$$

12) The frame axial stress is easily obtained from:

$$\sigma_F = \frac{E\Delta R}{R}$$

13) Often the load transmitted between the longeron and frame, $\bar{P}$, is required. This is simply given in this case by:

$$\bar{P} = \frac{2b}{R}\sigma_F A_F$$

This completes the procedure for the desired quantities for the stress analysis of this configuration.

When the skin is attached to the frames and the longeron deflection is significant, the solution is not obtainable by other than numerical means. However, when the additional restriction is made that the actual frame deflection is nearly equal to the fictitious skin deflection when the frame area is zero, a useful solution is obtainable by energy considerations. This solution, the perturbation membrane solution, will be discussed next.

D. Perturbation Membrane Theory

For the fourth and last of the limiting solutions treated, consider the pressurized cylinder without frames but with longerons. In this case, the skin middle surface stresses are uniform. When the frames are added, radial forces are required at the frame attachment points in order to have compatible deflections of the frames and the cylinder. If these radial forces are small so that the inward deflection of the cylinder is small compared to the outward deflection of the frames, then the skin middle surface stresses will be altered or perturbed only slightly. Therefore, it is expected that the variation of the skin middle surface stresses, σ_x and σ_θ is small over the entire panel surface. This being the case, the assumption that these stresses are uniform can be made and, therefore, the shear stress, $\tau_{x\theta}$, can be taken as zero. With this in mind, the mathematical formulation of the problem can be considerably simplified. Suppose it is further assumed that the skin panel behaves like a membrane. Then these equations reduce to the following set:

Panel

Strain-Displacement Relations

$$\epsilon_\theta = \frac{1}{R}\frac{\partial v}{\partial \theta} + \frac{r-R}{R} + \frac{1}{2}\left(\frac{1}{R}\frac{\partial r}{\partial \theta}\right)^2 \tag{4.104}$$

$$\epsilon_x = \frac{\partial u}{\partial x} + \frac{1}{2}\left(\frac{\partial r}{\partial x}\right)^2 \tag{4.105}$$

$$\gamma_{x\theta} = \frac{1}{R}\frac{\partial u}{\partial \theta} + \frac{\partial v}{\partial x} + \frac{1}{R}\left(\frac{\partial r}{\partial x}\right)\left(\frac{\partial r}{\partial \theta}\right) \tag{4.106}$$

Stress-Strain Relations

$$\epsilon_x = \frac{1}{E}\left(\sigma_x - \nu\sigma_\theta\right) \tag{4.107}$$

$$\epsilon_\theta = \frac{1}{E}\left(\sigma_\theta - \nu\sigma_x\right) \tag{4.108}$$

$$\gamma_{x\theta} = \frac{2(1+\nu)}{E}\tau_{x\theta} \tag{4.109}$$

Equations of Equilibrium

$$\sigma_x = \text{constant} \tag{4.110}$$

$$\sigma_\theta = \text{constant} \tag{4.111}$$

$$\frac{\sigma_\theta}{R}\left[\frac{1}{R}\frac{\partial^2 r}{\partial \theta^2} - 1\right] + \sigma_x\frac{\partial^2 r}{\partial x^2} = -\frac{p}{t} \tag{4.112}$$

Longeron

Equation of Equilibrium:

Since the panel lateral shear must vanish for a membrane, and since the circumferential stress, σ_θ, is uniform, it follows that (see Fig. 15a):

$$EI_L \frac{d^4 f(x)}{dx^4} = -2t\sigma_\theta \frac{\partial r}{R\partial\theta}\Big|_{\theta=\alpha} \tag{4.113}$$

Stress-Strain Relation:

$$\epsilon_L = \frac{\sigma_L}{E} \tag{4.114}$$

Frame

Equation of Equilibrium:

(a) Frames attached to the skin:

$$\sigma_F = \frac{1}{A_F R}\left[\int_0^a q(x)\,dx - 2\sigma_x t R \int_0^\alpha \frac{\partial r}{\partial x}\Big|_{x=a} d\theta\right] \tag{4.115a}$$

(b) Floating frames:

$$\sigma_F = \frac{1}{A_F R}\left[\int_0^a q(x)\,dx\right] \tag{4.115b}$$

Strain-Displacement Relation:

$$\epsilon_F = \frac{\Delta R}{R} \tag{4.116}$$

Stress-Strain Relation:

$$\epsilon_F = \frac{\sigma_F}{E} \tag{4.117}$$

Longitudinal Equilibrium

$$p = \frac{\sigma_L A_L}{Rb} + \frac{2t}{b}\int_0^\alpha \sigma_x\,d\theta \tag{4.118}$$

The equation of panel equilibrium in the normal direction, equation (4.112), has been simplified to such an extent that it can be integrated directly since σ_x and σ_θ are now constants for a given pressure.

In order that the longeron displacement is compatible with the panel displacement, it is required that:

$$\epsilon_\theta = \epsilon_L$$

since σ_θ , σ_x and σ_L are uniform. By using equations (4.107), (4.108) and (4.114), this condition is satisfied if:

$$\sigma_L = \sigma_x - \nu \sigma_\theta$$

When this is substituted into equation (4.118), σ_x can be written as a function of σ_θ , or:

$$\sigma_x = \frac{1}{1+\lambda}\left[\frac{pR}{2t} + \lambda \nu \sigma_\theta\right] \qquad (4.119)$$

The panel boundary conditions for the two panel conditions - frames attached to skin and floating frames, are:

D1. Frames Attached to Skin:

$$r(a,\theta) = R + \Delta R$$
$$r(x,\alpha) = R + \Delta R + f(x)$$

D2. Floating Frames:

$$\frac{\partial r(a,\theta)}{\partial x} = 0$$
$$r(x,\alpha) = R + \Delta R + f(x)$$

An important conclusion results from defining a new dependent variable and a new independent variable. Let

$$Y = R\theta$$

and $$\omega = r - (R + \Delta R)$$

Then equation (4.112), the skin panel equilibrium equation, becomes:

$$\sigma_\theta \frac{\partial^2 \omega}{\partial Y^2} + \sigma_x \frac{\partial^2 \omega}{\partial x^2} = -\left[\frac{p}{t} - \frac{\sigma_\theta}{R}\right], \qquad (4.120)$$

together with the boundary conditions:

D. 1. Frames Attached to Skin:

$$\omega(a, y) = 0$$

$$\omega(x, b) = f(x)$$

D. 2. Floating Frames:

$$\frac{\partial \omega(a, y)}{\partial x} = 0$$

$$\omega(x, b) = f(x)$$

Note that this equation together with the boundary conditions is identical with that for the deflection of a rectangular membrane with uniform membrane forces, $\sigma_\theta t$ and $\sigma_x t$, under a reduced uniform pressure, $p - \frac{\sigma_\theta t}{R}$. The boundary condition, $\omega(x, b) = f(x)$, is obtained from the integrated equation for the deflection of the longeron, or:

$$EI_L \frac{d^4 f(x)}{dx^4} = -2\sigma_\theta t \left.\frac{\partial \omega}{\partial y}\right|_{y=b}, \qquad (4.121)$$

where the boundary conditions are:

Case a. - Continuous Longerons

$$f(a) = 0$$

$$\frac{df(a)}{dx} = 0$$

Case b. - Simply Supported Longerons

$$f(a) = 0$$

$$\frac{d^2 f(a)}{dx^2} = 0$$

Hence, the simultaneous solution of equations (4. 120) and (4. 121) together with the appropriate boundary conditions, 1 or 2, and a or b, will yield the deflection of the skin panel, $\omega(x, y)$, containing the unknown quantity, σ_θ. Mathematically, this is equivalent to the deflection of a rectangular pure membrane under uniform lateral pressure, supported on two opposite edges by elastic beams, and either fixed on the other two edges or having zero slopes normal

to those edges. This is illustrated in Fig. 14. The loading on the elastic supports is shown in Fig. 15a and 15b. The solution to this problem will now be discussed, followed by the method for determining the unknown circumferential stress, σ_θ .

The Deflection of a Rectangular Membrane with Uniform Pressure Loading - Two Opposite Edges Fixed - The Other Two Supported by Uniform Beams

Rewriting equation (4.120) in the form:

$$\frac{\partial^2 w}{\partial x^2} + T \frac{\partial^2 w}{\partial y^2} = -P , \qquad (4.122)$$

where

$$T \equiv \frac{\sigma_\theta}{\sigma_x} = \frac{1+\lambda}{\frac{pR}{2t\sigma_\theta} + \lambda \nu}$$

$$P \equiv \frac{1}{\sigma_x}\left[\frac{p}{t} - \frac{\sigma_\theta}{R}\right] = \frac{1+\lambda\left(\frac{p}{t} - \frac{\sigma_\theta}{R}\right)}{\frac{pR}{2t} + \lambda \nu \sigma_\theta} ,$$

the solution can be obtained by the use of Fourier series. Let

$$w(x,y) = \sum_{n=0}^{\infty} B_n(y) \cos\frac{(2n+1)\pi x}{2a}$$

Then the boundary condition, $w(a,y) = 0$, is satisfied and the condition of symmetry with respect to the x axis is satisfied. The uniform loading can also be expanded in a similar Fourier cosine series of the form:

$$P = \sum_{n=0}^{\infty} q_n \cos\frac{(2n+1)\pi x}{2a}$$

where

$$q_n = \frac{2P}{a}\int_0^a \cos\frac{(2n+1)\pi x}{2a}\,dx = \frac{4P}{\pi}\frac{(-1)^n}{(2n+1)}$$

Substituting these expansions for $w(x,y)$ and P in equation (4.122) by appropriate differentiation, and cancelling $\cos\frac{(2n+1)\pi x}{2a}$ term by

term, results in the ordinary differential equation:

$$B_n''(Y) - \lambda_n^2 B_n(Y) = -Q_n$$

where

$$\lambda_n^2 = \frac{1}{T}\left[\frac{(2n+1)\pi}{2a}\right]^2$$

$$Q_n = \frac{4P}{\pi T}\frac{(-1)^n}{(2n+1)}$$

The solution of this equation which satisfies symmetry with respect to the Y axis is:

$$B_n(Y) = A_n \cosh \lambda_n Y + \frac{Q_n}{\lambda_n^2}$$

The boundary condition, $w(x,b) = f(x)$, implies that:

$$f(x) = \sum_{n=0}^{\infty}\left[A_n \cosh \lambda_n b + \frac{Q_n}{\lambda_n^2}\right]\cos\frac{(2n+1)\pi x}{2a}$$

Therefore, the membrane deflection takes on the form:

$$w(x,Y) = \sum_{n=0}^{\infty}\left[A_n \cosh \lambda_n Y + \frac{Q_n}{\lambda_n^2}\right]\cos\frac{(2n+1)\pi x}{2a} \qquad (4.123)$$

where the A_n's are determined from the beam deflection, $f(x)$.

The loading on the beam is, from equation (4.121):

$$q(x) = -2\sigma t \left.\frac{\partial w}{\partial Y}\right|_{Y=b}$$

From equation (4.123), it is evident that:

$$\left.\frac{\partial w}{\partial Y}\right|_{Y=b} = \sum_{n=0}^{\infty} A_n \lambda_n \sinh \lambda_n b \cos\frac{(2n+1)\pi x}{2a}$$

Substituting this into the differential equation for the beam deflection, $f(x)$, it follows that:

$$\frac{d^4 f(x)}{dx^4} = - \frac{2\sigma_\theta t}{EI_L} \sum_{n=0}^{\infty} A_n \lambda_n \sinh \lambda_n b \cos \frac{(2n+1)\pi x}{2a}$$

The even solution to this differential equation is:

$$f(x) = - \frac{2\sigma_\theta t}{EI_L} \sum_{n=0}^{\infty} A_n \lambda_n \sinh \lambda_n b \left[\frac{2a}{(2n+1)\pi}\right]^2 \cos \frac{(2n+1)\pi x}{2a} + C_0 + C_2 x^2$$

Case a. Continuous Longerons

Since $f'(a)$ must vanish for continuous longerons, it follows that:

$$f'(a) = \frac{2\sigma_\theta t}{EI_L T^2} \sum_{n=0}^{\infty} \frac{A_n}{\lambda_n^3} \frac{(2n+1)\pi}{2a} \sinh \lambda_n b (-1)^n + 2C_2 a = 0$$

Therefore:

$$C_2 = - \frac{\sigma_\theta t}{EI_L T^2} \sum_{n=0}^{\infty} \frac{A_n}{\lambda_n^3} \frac{(2n+1)\pi}{2a} \sinh \lambda_n b (-1)^n$$

The second boundary condition, $f(a)=0$, implies that:

$$C_0 = - C_2 a^2$$

Solving for C_0 and C_2 and substituting into the expression for $f(x)$, the resulting longeron deflection is given by:

$$f(x) = - \frac{2\sigma_\theta t}{EI_L T^2} \left\{ \sum_{n=0}^{\infty} \frac{A_n}{\lambda_n^3} \sinh \lambda_n b \cos \frac{(2n+1)\pi x}{2a} + \frac{1}{2a}(x^2 - a^2) \sum_{m=0}^{\infty} \frac{A_m}{\lambda_m^3} \frac{(2m+1)\pi (-1)^m}{2a} \sinh \lambda_m b \right.$$

Expanding $(x^2 - a^2)$ in a Fourier cosine series with period $4a$, it follows that:

$$(x^2 - a^2) = - \frac{32a^2}{\pi^3} \sum_{n=0}^{\infty} \frac{(-1)^n}{(2n+1)^3} \cos \frac{(2n+1)\pi x}{2a}$$

Let

$$K \equiv \frac{16a}{\pi^3} \sum_{m=0}^{\infty} \frac{A_m}{\lambda_m^3} \frac{(2m+1)\pi (-1)^m}{2a} \sinh \lambda_m b = \text{CONSTANT}$$

Then, the longeron deflection becomes:

$$f(x) = -\frac{2\sigma_\theta t}{EI_L T^2}\sum_{n=0}^{\infty}\left[\frac{A_n}{\lambda_n^3}\sinh\lambda_n b - \frac{K(-1)^n}{(2n+1)^3}\right]\cos\frac{(2n+1)\pi x}{2a} \qquad (4.124)$$

Equating this to the previous requirement that:

$$f(x) = \sum_{n=0}^{\infty}\left[A_n \cosh\lambda_n b + \frac{Q_n}{\lambda_n^2}\right]\cos\frac{(2n+1)\pi x}{2a}$$

and solving for A_n, one obtains:

$$A_n = -\frac{\frac{Q_n}{\lambda_n^2} - \frac{2\sigma_\theta t\, K(-1)^n}{EI_L T^2 (2n+1)^3}}{\frac{2\sigma_\theta t}{EI_L K^2}\frac{\sinh\lambda_n b}{\lambda_n^3} - \cosh\lambda_n b}$$

This can be written in the form:

$$A_n = \alpha_n K - \beta_n \qquad (4.125)$$

where

$$\alpha_n = \frac{(-1)^n}{(2n+1)^3}\frac{1}{\left[\frac{\sinh\lambda_n b}{\lambda_n^3} + \frac{EI_L T^2}{2\sigma_\theta t}\cosh\lambda_n b\right]}$$

$$\beta_n = \frac{Q_n}{\lambda_n^2}\frac{1}{\left[\frac{2\sigma_\theta t}{EI_L T^2}\frac{\sinh\lambda_n b}{\lambda_n^3} + \cosh\lambda_n b\right]}$$

And K can be written:

$$K = \sum_{m=0}^{\infty}\gamma_m A_m \qquad (4.126)$$

where

$$\gamma_m = \frac{8}{\pi^2}\frac{(2m+1)(-1)^m}{\lambda_m^3}\sinh\lambda_m b$$

Substituting equation (4.125) into (4.126), the following results:

$$K = \sum_{m=0}^{\infty}\gamma_m\left[\alpha_m K + \beta_m\right]$$

Now since K is a constant, independent of m, then it follows that:

$$K = \frac{\sum_{m=0}^{\infty} \gamma_m \beta_m}{1 - \sum_{m=0}^{\infty} \alpha_m \gamma_m}$$

Therefore, the coefficients, A_n, are:

$$A_n = \frac{\alpha_n \sum_{m=0}^{\infty} \gamma_m \beta_m}{1 - \sum_{m=0}^{\infty} \alpha_m \gamma_m} + \beta_n$$

which, when simplified, can be written:

$$A_n = -\frac{16}{\pi^3} Pa^2 \left[\frac{1}{1 - \frac{128 a^3 t \sigma_x^{1/2} \sigma_\theta^{1/2}}{\pi^5 E I_L} \sum_{m=0}^{\infty} \frac{\beta_m}{(2m+1)^2}} \right] \frac{(-1)^n \beta_n}{\sinh \lambda_n b} \tag{4.127}$$

where

$$\beta_n = \frac{1}{(2n+1)^3 \coth \lambda_n b + \frac{16 a^3 t \sigma_x^{1/2} \sigma_\theta^{1/2}}{\pi^3 E I_L}}$$

Substituting this into equation (4.123) and simplifying, the deflection of the membrane becomes:

$$\omega(x,y) = \frac{16}{\pi^3} Pa^2 \sum_{n=0}^{\infty} \frac{(-1)^n}{(2n+1)^3} \left\{ 1 - \left[\frac{(2n+1)^3 \beta_n}{1 - \frac{128 a^3 t \sigma_x^{1/2} \sigma_\theta^{1/2}}{\pi^5 E I_L} \sum_{m=0}^{\infty} \frac{\beta_m}{(2m+1)^2}} \right] \frac{\cosh \lambda_n y}{\sinh \lambda_n b} \right\} \cos \frac{(2n+1)\pi x}{2a} \tag{4.128}$$

The beam maximum bending moment is obtained from the relation:

$$M_{MAX.} = \frac{E I_L}{2} f''(a) = \frac{E I_L}{2} \frac{\partial^2 \omega(a,b)}{\partial x^2}$$

Differentiating and simplifying, this results in:

$$M_{MAX.} = \frac{64}{\pi^5} \frac{P a^3 t \sigma_x^{1/2} \sigma_\theta^{1/2}}{\left[\sum_{n=0}^{\infty} \frac{1}{(2n+1)^2 \beta_n} - \frac{128 a^3 t \sigma_x^{1/2} \sigma_\theta^{1/2}}{\pi^5 E I_L} \right]} \qquad (4.129)$$

Case b. Simply Supported Longerons

Since $f''(a)$ must vanish for continuous longerons, it follows that:

$$C_2 = 0$$

The second boundary condition, $f(a)=0$, implies that:

$$C_0 = 0$$

Hence, the longeron deflection is simply:

$$f(x) = - \frac{2\sigma_\theta t}{E I_L} \sum_{n=0}^{\infty} A_n \lambda_n \sin \lambda_n b \left[\frac{2a}{(2n+1)\pi} \right]^4 \cos \frac{(2n+1)\pi x}{2a}$$

Equating this to the previous requirement that:

$$f(x) = \sum_{n=0}^{\infty} \left[A_n \cosh \lambda_n b + \frac{Q_n}{\lambda_n^2} \right] \cos \frac{(2n+1)\pi x}{2a}$$

and solving for A_n, it follows that:

$$A_n = - \frac{16}{\pi^3} P a^2 \frac{(-1)^n \beta_n}{\sinh \lambda_n b} \qquad (4.130)$$

Substituting this into equation (4.123) and simplifying, the deflection of the membrane becomes:

$$\omega(x,y) = \frac{16}{\pi^3} P a^2 \sum_{n=0}^{\infty} \frac{(-1)^n}{(2n+1)^3} \left[1 - (2n+1)^3 \beta_n \frac{\cosh \lambda_n y}{\sinh \lambda_n b} \right] \cos \frac{(2n+1)\pi x}{2a} \qquad (4.131)$$

The beam maximum bending moment is obtained from the relation:

$$M_{MAX.} = \frac{EI_L}{2} f''(0) = \frac{EI_L}{2} \frac{\partial^2 w(0,6)}{\partial x^2}$$

Differentiating and simplifying, this becomes:

$$M_{MAX.} = \frac{32}{\pi^4} P a^3 t \sigma_x^{1/2} \sigma_\theta^{1/2} \sum_{n=0}^{\infty} \frac{(-1)^n \beta_n}{(2n+1)} \qquad (4.132)$$

The Deflection of a Rectangular Membrane with Uniform Pressure Loading - Two Opposite Edges with Zero Normal Slope - The Other Two Supported by Uniform Beams

In this case, the solution of equation (4.122) must be represented by a Fourier cosine series satisfying the boundary condition that:

$$\frac{\partial w(a,Y)}{\partial x} = 0$$

This slope boundary condition is satisfied if:

$$w(x,Y) = \frac{1}{2} B_0(Y) + \sum_{n=1}^{\infty} B_n(Y) \cos \frac{n\pi x}{a}$$

When this is substituted into equation (4.122), the following equation obtained:

$$-\sum_{n=1}^{\infty} B_n(Y) \left(\frac{n\pi}{a}\right)^2 \cos \frac{n\pi x}{a} + T \left\{ \frac{1}{2} B_0''(Y) + \sum_{n=1}^{\infty} B_n''(Y) \cos \frac{n\pi x}{a} \right\} = -P$$

If this equation is to be satisfied for all values of x, then it follows that:

$$B_0''(Y) = -\frac{2P}{T}$$

$$B_n''(Y) - \tau_n^2 B_n(Y) = 0$$

where

$$\tau_n^2 = \frac{1}{T} \left(\frac{n\pi}{a}\right)^2$$

The even solutions of these ordinary differential equations are, respectively:

$$B_0(y) = -\frac{py^2}{T} + C_2$$

$$B_n(y) = A_n \cosh \tau_n y$$

The boundary condition, $\omega(x,b) = f(x)$, implies that:

$$f(x) = \frac{1}{2} B_0(b) + \sum_{n=1}^{\infty} B_n(b) \cos \frac{n\pi x}{a}$$

Hence, $\frac{1}{2} B_0(b)$ and $B_n(b)$ are just the Fourier cosine coefficients of the unknown beam deflection, $f(x)$. Now:

$$B_0(b) = -\frac{pb^2}{T} + C_2$$

which implies that:

$$B_0(y) = \frac{p}{T}(b^2 - y^2) + B_0(b)$$

Also:

$$B_n(y) = A_n \cosh \tau_n b$$

which implies that:

$$B_n(y) = B_n(b) \frac{\cosh \tau_n y}{\cosh \tau_n b}$$

Hence, the deflection of the membrane becomes:

$$\omega(x,y) = \frac{p}{2T}(b^2 - y^2) + \frac{1}{2} B_0(b) + \sum_{n=1}^{\infty} B_n(b) \frac{\cosh \tau_n y}{\cosh \tau_n b} \cos \frac{n\pi x}{a} \qquad (4.133)$$

The loading on the beam is, from equation (4.121):

$$q(x) = -2\sigma_0 t \left.\frac{\partial \omega}{\partial y}\right|_{y=b}$$

From equation (4.133), it is evident that:

$$\left.\frac{\partial \omega}{\partial y}\right|_{y=b} = -\frac{pb}{T} + \sum_{n=1}^{\infty} B_n(b) \tau_n \tanh \tau_n b \cos \frac{n\pi x}{a}$$

Substituting this into the differential equation for the beam deflection, $f(x)$, it follows that:

$$\frac{d^4 f(x)}{dx^4} = \frac{2\sigma_\theta t}{EI_L}\left\{\frac{Pb}{T} - \sum_{n=1}^{\infty} B_n(b)\,\tau_n\,TANH\,\tau_n b\,\cos\frac{n\pi x}{a}\right\}$$

The even solution to this differential equation is:

$$f(x) = \frac{2\sigma_\theta t}{EI_L}\left\{\frac{Pbx^4}{24T} - \sum_{n=1}^{\infty} B_n(b)\,\tau_n\,TANH\,\tau_n b\left(\frac{a}{n\pi}\right)^4\cos\frac{n\pi x}{a} + C_0 + C_2 x^2\right\}$$

Case a. Continuous Longerons (clamped beams)

Since $f'(a)$ must vanish for continuous longerons, it follows that:

$$f'(a) = \frac{2\sigma_\theta t}{EI_L}\left\{\frac{Pba^3}{6T} + 2C_2 a\right\} = 0$$

Therefore:

$$C_2 = -\frac{Pba^2}{12T}$$

The second boundary condition, that $f(a)$ must vanish, implies that:

$$C_0 = \frac{Pba^4}{24T} + \sum_{n=1}^{\infty} B_n(b)\,\tau_n\,TANH\,\tau_n b\left(\frac{a}{n\pi}\right)^4(-1)^n$$

Substituting these constants into the expression for $f(x)$, the resulting longeron deflection is:

$$f(x) = \frac{2\sigma_\theta t}{EI_L}\left\{\frac{Pb}{24T}(x^2-a^2)^2 + \sum_{m=1}^{\infty} B_m(b)\,\tau_m\,TANH\,\tau_m b\left(\frac{a}{m\pi}\right)^4(-1)^m - \sum_{n=1}^{\infty} B_n(b)\,\tau_n\,TANH\,\tau_n b\left(\frac{a}{n\pi}\right)^4\cos\frac{n\pi x}{a}\right\}$$

Expanding $(x^2-a^2)^2$ in a Fourier cosine series with period $2a$, it follows that:

$$(x^2-a^2)^2 = \frac{8}{15}a^4 - 48\sum_{n=1}^{\infty}(-1)^n\left(\frac{a}{n\pi}\right)^4\cos\frac{n\pi x}{a}$$

Therefore,

$$f(x) = \frac{2\sigma_\theta t}{EI_L}\left\{\frac{Pba^4}{45T} + \sum_{m=1}^{\infty} B_m(b)\,\tau_m \,TANH\,\tau_m b\left(\frac{a}{m\pi}\right)^4(-1)^m \right.$$

$$\left. - \sum_{n=1}^{\infty}\left[B_n(b)\,\tau_n \,TANH\,\tau_n b\left(\frac{a}{n\pi}\right)^4 + \frac{2Pb}{T}(-1)^n\left(\frac{a}{n\pi}\right)^4\right\}\cos\frac{n\pi x}{a}\right.$$

Equating this to the previous requirement that:

$$f(x) = \tfrac{1}{2}B_o(b) + \sum_{n=1}^{\infty} B_n(b)\cos\frac{n\pi x}{a}$$

it follows that:

$$\tfrac{1}{2}B_o(b) = \frac{2\sigma_\theta t}{EI_L}\left\{\frac{Pba^4}{45T} + \sum_{m=1}^{\infty} B_m(b)\,\tau_m \,TANH\,\tau_m b\left(\frac{a}{m\pi}\right)^4(-1)^m\right\}$$

and

$$B_n(b) = -\frac{2\sigma_\theta t}{EI_L}\left\{B_n(b)\,\tau_n \,TANH\,\tau_n b\left(\frac{a}{n\pi}\right)^4 + \frac{2Pb}{T}(-1)^n\left(\frac{a}{n\pi}\right)^4\right\}$$

in order that the relation hold for all values of x . Solving for $B_n(b)$ from the second of the two relations, it follows that:

$$B_n(b) = \frac{\frac{2Pb}{T}(-1)^{n+1}}{\left(\frac{n\pi}{a}\right)^4\frac{EI_L}{2\sigma_\theta t} + \tau_n \,TANH\,\tau_n b}$$

Substituting this into the first of the two relations results in:

$$\tfrac{1}{2}B_o(b) = \frac{2\sigma_\theta t\,Pba^4}{45EI_L T}\left\{1 - \frac{90}{a^4}\sum_{m=1}^{\infty}\frac{\left(\frac{a}{m\pi}\right)^4}{1 + \left(\frac{m\pi}{a}\right)^4\frac{EI_L}{2\sigma_\theta t}\frac{COTH\,\tau_m b}{\tau_m}}\right\}$$

Hence, the Fourier coefficients are known and upon substitution into equation (4.133) :

$$\omega(x,y) = \frac{P}{2}\frac{\sigma_x}{\sigma_\theta}(b^2 - y^2) + \frac{4a^4}{\pi^4}\frac{Pbt\sigma_x}{EI_L}\left\{\frac{\pi^4}{90} - \frac{2a^3 t\sigma_x^{1/2}\sigma_\theta^{1/2}}{\pi^3 EI_L}\sum_{m=1}^{\infty}\right.$$

$$\left.\frac{\xi_m}{m^4\,TANH\,\tau_m b} - \sum_{n=1}^{\infty}\frac{\xi_n(-1)^n}{n}\frac{COSH\,\tau_n y}{SINH\,\tau_n b}\cos\frac{n\pi x}{a}\right\} \qquad (4.134)$$

where

$$\xi_n = \frac{1}{n^3 \coth \tau_n b + \frac{2a^3 t \sigma_x^{1/2} \sigma_\theta^{1/2}}{\pi^3 E I_L}}$$

The beam maximum bending moment is obtained from the relation:

$$M_{MAX.} = \frac{EI_L}{2} f''(a) = \frac{EI_L}{2} \frac{\partial^2 w(a,b)}{\partial x^2}$$

Differentiating and simplifying, this results in:

$$M_{MAX.} = \frac{1}{3} P b a^2 t \sigma_x \left[1 - \frac{12}{\pi^5} \frac{a^3 t \sigma_x^{1/2} \sigma_\theta^{1/2}}{E I_L} \sum_{n=1}^{\infty} \frac{\xi_n}{n^2} \right] \qquad (4.135)$$

Case b. Simply Supported Longerons

Since $f''(a)$ must vanish for continuous longerons, it follows that:

$$C_2 = -\frac{P b a^2}{4T} - \frac{1}{2} \sum_{m=1}^{\infty} B_m(b) \tau_m \tanh \tau_m b \left(\frac{a}{m\pi}\right)^2 (-1)^m$$

The second boundary condition, that $f(a)$ must vanish, implies that:

$$C_0 = \frac{5 P b a^4}{24 T} + \sum_{m=1}^{\infty} B_m(b) \tau_m \tanh \tau_m b \left[\frac{a^2}{2} + \left(\frac{a}{m\pi}\right)^2 \right] \left(\frac{a}{m\pi}\right)^2 (-1)^m$$

Hence, the longeron displacement is:

$$f(x) = \frac{2\sigma_\theta t}{E I_L} \left\{ \frac{P b}{24 T} (x^4 - 6a^2x^2 + 5a^4) - \sum_{n=1}^{\infty} B_n(b) \tau_n \tanh \tau_n b \left(\frac{a}{n\pi}\right)^4 \right.$$
$$\left. \cos \frac{n\pi x}{a} + (a^2 - x^2) \sum_{m=1}^{\infty} B_m(b) \mu_m + 2 \sum_{m=1}^{\infty} B_m(b) \mu_m \left(\frac{a}{m\pi}\right)^2 \right\}$$

where

$$\mu_m = \frac{1}{2} \tau_m \tanh \tau_m b \left(\frac{a}{m\pi}\right)^2 (-1)^m$$

Expanding $(x^4 - 6a^2x^2 + 5a^4)$ and $(a^2 - x^2)$ in a Fourier cosine series of period $2a$, it results that:

$$(x^4 - 6a^2x^2 + 5a^4) = \frac{16a^4}{5} - 16a^4 \sum_{n=1}^{\infty} \frac{(-1)^n}{(n\pi)^2} \left[1 + \frac{3}{(n\pi)^2} \right] \cos \frac{n\pi x}{a}$$

and

$$(a^2 - x^2) = \frac{2}{3} a^2 - 4a^2 \sum_{n=1}^{\infty} \frac{(-1)^n}{(n\pi)^2} \cos \frac{n\pi x}{a}$$

Therefore, $f(x)$ can be written

$$f(x) = \frac{2\sigma_\theta t}{EI_L}\left\{\frac{2\rho b a^4}{15T} + \frac{2}{3}a^2\sum_{m=1}^{\infty}\mu_m + 2\sum_{m=1}^{\infty}\mu_m\left(\frac{a}{m\pi}\right)^2 - \sum_{n=1}^{\infty}\left[\frac{2\rho b a^4(-1)^n}{3T(n\pi)^2}\left(1+\frac{3}{n^2\pi^2}\right) + B_n(b)\tau_n \tanh\tau_n b\left(\frac{a}{n\pi}\right)^4 + 4a^2\sum_{m=1}^{\infty}\mu_m\frac{(-1)^n}{n^2\pi^2}\right]\cos\frac{n\pi x}{a}\right\}$$

But from the previous result,

$$f(x) = \frac{1}{2}B_0(b) + \sum_{n=1}^{\infty}B_n(b)\cos\frac{n\pi x}{a}$$

In order that these relations hold for all values of x, then it follows that:

$$\frac{1}{2}B_0(b) = \frac{4\sigma_\theta t}{EI_L}\left\{\frac{\rho b a^4}{15T} + a^2\sum_{m=1}^{\infty}\left(\frac{1}{3}+\frac{1}{m^2\pi^2}\right)\mu_m\right\}$$

and

$$B_n(b) = \frac{2\sigma_\theta t}{EI_L}\left\{\frac{2}{3}\frac{\rho b a^4}{T}\frac{(-1)^{n+1}}{(n\pi)^2}\left[1+\frac{3}{(n\pi)^2}\right] - B_n(b)\tau_n\tanh\tau_n b\left(\frac{a}{n\pi}\right)^2 + 4a^2\sum_{m=1}^{\infty}\mu_m\frac{(-1)^n}{(n\pi)^2}\right\}$$

Solving for $B_n(b)$ from the second of the two relations:

$$B_n(b) = V_n + \eta_n N$$

Where:

$$V_n \equiv \frac{\frac{2}{3}\frac{\rho}{T}ba^4\frac{(-1)^{n+1}}{(n\pi)^2}\left[1+\frac{3}{(n\pi)^2}\right]}{\frac{EI_L}{2\sigma_\theta t} + \tau_n\tanh\tau_n b\left(\frac{a}{n\pi}\right)^4}$$

$$\eta_n \equiv \frac{4a^2\frac{(-1)^{n+1}}{(n\pi)^2}}{\frac{EI_L}{2\sigma_\theta t} + \tau_n\tanh\tau_n b\left(\frac{a}{n\pi}\right)^4}$$

$$N \equiv \sum_{m=1}^{\infty}B_m(b)\mu_m = \text{CONSTANT}$$

Now since N is a constant, it can be evaluated from the above relation, or:

$$N = \frac{\sum_{m=1}^{\infty} \nu_m \mu_m}{1 - \sum_{m=1}^{\infty} \eta_m \mu_m}$$

So that:

$$B_n(6) = \nu_n + \frac{\eta_n \sum_{m=1}^{\infty} \nu_m \mu_m}{1 - \sum_{m=1}^{\infty} \eta_m \mu_m} \tag{4.136}$$

Solving for $\frac{1}{2} B_0(6)$ from the first of the two relations, it follows that:

$$\frac{1}{2} B_0(6) = \frac{4\sigma_\theta t}{E I_L}\left\{ \frac{P 6 a^4}{15 T} + \sum_{m=1}^{\infty} \rho_m \left[\nu_m + \frac{\eta_m \sum_{k=1}^{\infty} \nu_k \mu_k}{1 - \sum_{k=1}^{\infty} \eta_k \mu_k} \right] \right\} \tag{4.137}$$

where: $\rho_m = \frac{a}{2}^2 \tau_m \, TANH \, \tau_m 6 \left(\frac{a}{m\pi}\right)^2 (-1)^m \left[\frac{1}{3} + \frac{1}{(m\pi)^2} \right]$

When equations (4.136) and (4.137) are substituted into equation (4.133) it follows after simplification that:

$$w(x,y) = \frac{P}{T}\left\{ \frac{1}{2}(b^2 - y^2) + \frac{4}{15}\frac{\sigma_\theta t 6 a^4}{E I_L}\left[1 - \frac{10}{3}\frac{a^3 t \sigma_x^{1/2} \sigma_\theta^{1/2}}{\pi^3 E I_L} \sum_{m=1}^{\infty} \left\{ \left[1 + \frac{3}{(m\pi)^2} \right] \right.\right.$$

$$\left. - \frac{\sum_{k=1}^{\infty} \left[1 + \frac{3}{(k\pi)^2} \right] \xi_k}{\frac{\pi^3 E I_L}{4 a^3 t \sigma_x^{1/2} \sigma_\theta^{1/2}} - \sum_{k=1}^{\infty} \xi_k} \right\} \left(1 + \frac{3}{m^2 \pi^2} \right) \xi_m - \frac{5}{\pi^2} \sum_{n=1}^{\infty} \left\{ \left[1 + \frac{3}{(n\pi)^2} \right] \right.$$

$$\left.\left. - \frac{\sum_{m=1}^{\infty} \left[1 + \frac{3}{(m\pi)^2} \right] \xi_m}{\frac{\pi^3 E I_L}{4 a^3 t \sigma_x^{1/2} \sigma_\theta^{1/2}} - \sum_{m=1}^{\infty} \xi_m} \right\} (-1)^n n \xi_n \frac{COSH \, \tau_n y}{SINH \, \tau_n b} \cos \frac{n\pi x}{a} \right] \tag{4.138}$$

The beam maximum bending stress is obtained from the relation:

$$M_{MAX.} = EI_L f''(a) = EI_L \frac{\partial^2 w(a,b)}{\partial x^2}$$

Differentiation and simplifying, this results in:

$$M_{MAX.} = \frac{1}{2} P \sigma_x t b a^2 \left[1 + \frac{16}{3\pi^3} \frac{a^3 t \sigma_x^{1/2} \sigma_\theta^{1/2}}{EI_L} \sum_{M=1,3,5}^{\infty} \left\{ \left[1 + \frac{3}{(n\pi)^2} \right] - \frac{\sum_{m=1}^{\infty} \left[1 + \frac{3}{(m\pi)^2} \right] \xi_m}{\frac{\pi^3 EI_L}{4a^3 t \sigma_x^{1/2} \sigma_\theta^{1/2}} - \sum_{m=1}^{\infty} \xi_m} \right\} (-1)^n \xi_n \right] \tag{4.139}$$

where

$$\xi_n = \frac{1}{n^3 \coth \tau_{nb} + \frac{2a^3 t \sigma_x^{1/2} \sigma_\theta^{1/2}}{\pi^3 EI_L}}$$

Now that the solutions to these problems have been obtained, their application to the perturbation solutions of the pressurized fuselage will now be discussed.

Application to the Perturbation Membrane Solution.

The only quantity remaining which must be evaluated in order to complete the perturbation membrane solution is the circumferential stress, σ_θ . This is readily accomplished by using energy methods in the following manner. Castigliano's second theorem[5], or the theorem of least work, states that if an elastic system is deformed by given forces on the boundaries and nowhere on the boundary are the displacements prescribed, then of all stress components satisfying the equations of equilibrium and the stress boundary conditions, the true stress components are those such that the total

strain energy of the system is a minimum. This principle is a degenerate case of the principle of minimum complementary energy since the work done by the forces over that part of the boundary where the displacements are prescribed is zero.

The approximate perturbation solution is obtained by choosing a reasonable variation of stress in the membrane panel, in this case uniform, and satisfying equilibrium for all values of the unknown uniform circumferential stress, σ_θ . Then the total strain energy of the elastic system - frames, longerons and skin - is determined as a function of the unknown stress, σ_θ . That value of σ_θ which makes the strain energy of the complete system a minimum should, by Castigliano's second theorem, result in the best approximation. The determination of σ_θ by the use of Castigliano's second theorem is valid in this case since nowhere on the boundary are the displacements prescribed and, therefore, all of the requirements have been satisfied. With this plan in mind, the total strain energy of the sufficient partial system will now be evaluated.

Skin Panel Strain Energy

The strain energy density of a membrane with uniform membrane stresses is given by:

$$d U_M = \frac{t}{2E}\left[\sigma_x^2 + \sigma_\theta^2 - 2\nu \sigma_x \sigma_\theta \right] dx\, dy$$

When this is integrated over the surface of one panel and when the equilibrium equation (4.55) is used, the following expression for the panel strain energy as a function of the circumferential stress is obtained:

$$U_M = \frac{2abt}{E}\left[\sigma_x^2 + \sigma_\theta^2 - 2\nu \sigma_x \sigma_\theta \right] \qquad (4.140)$$

Longeron Strain Energy

The strain energy of one longeron of length $2a$ consists of two parts. The axial stress in the longeron imparts strain energy to the longeron of amount:

$$U_{L_{\sigma_L}} = \frac{A_L a}{E} \sigma_L^2$$

The bending of the longeron produces strain energy of amount:

$$U_{L_{\sigma_L'}} = EI_L \int_0^a \left[\frac{\partial^2 w}{\partial x^2} \right]_{y=b}^2 dx = EI_L \int_0^a f''(x)^2 dx$$

Hence, the total longeron strain energy is:

$$U_L = \frac{A_L a}{E} \sigma_L^2 + EI_L \int_0^a \left[\frac{\partial^2 w}{\partial x^2} \right]_{y=b}^2 dx \qquad (4.141)$$

Strain Energy of the Frame Section Between Two Adjacent Longerons

The strain energy per unit length of the frame is:

$$\frac{dU_F}{R\,d\theta} = \frac{1}{2} A_F \frac{\sigma_F^2}{E}$$

Using the equilibrium equation (4.56), this becomes:

$$\frac{dU_F}{R\,d\theta} = \frac{A_F}{2E\gamma^2} \left(\frac{pR}{t} - \sigma_\theta \right)^2$$

The strain energy of the frame section between two adjacent longerons is, therefore:

$$U_F = \frac{1}{2} A_F \frac{\sigma_F^2}{E} R \int_{-\alpha}^{\alpha} d\theta = \frac{2abt}{E\gamma} \left(\frac{pR}{t} - \sigma_\theta \right)^2 \qquad (4.142)$$

Total Strain Energy

The sum of equation (4.140), (4.141), and (4.142) represents the total strain energy of the section of the structure shown in Fig. 18.

Since every such section behaves identically, it is only necessary to minimize the strain energy of one of these sections. Hence, let:

$$U_T = U_M + U_L + U_F$$

The Determination of the Circumferential Stress

The stresses, σ_x , σ_L and σ_F , can all be considered as being a function of the unknown stress, σ_θ . In addition, $f(x)$, the longeron displacement, can be considered as being a function of σ_θ as well as x . These relations occur as a result of having satisfied the equilibrium conditions previously obtained. Therefore, the total strain energy, U_T , is a function of σ_θ only. The requirement that the strain energy is a minimum, therefore, results in the additional condition:

$$\frac{dU_T}{d\sigma_\theta} = \frac{d}{d\sigma_\theta}\left[U_M + U_L + U_F\right] = 0 \qquad (4.143)$$

This resulting equation, the determining equation for the circumferential stress, is an implicit function of that variable, and, hence, must be determined by trial or by graphical methods. Equation (4.143) can be represented, therefore, by:

$$\varphi(\sigma_\theta) = 0$$

This equation is greatly complicated by the fact that the longeron strain energy is represented by an infinite series with the circumferential stress contained within the coefficients and as a multiplier outside of the summation. Therefore, a far more rapid (though not as accurate) method for determining the circumferential stress from the minimum strain energy condition is by plotting the

total strain energy, U_T , as a function of σ_θ . In this manner the circumferential stress which results in the minimum total strain energy can easily be obtained. An example of such a plot is shown in Fig. 20.

Determination of the Longeron Strain Energy for Each Boundary Condition

I. Skin Attached to Frames

From equation (4. 123), it is evident that upon differentiation:

$$f''(x) = -\sum_{n=0}^{\infty} B_n(b)\left[\frac{(2n+1)\pi}{2a}\right]^2 \cos\frac{(2n+1)\pi x}{2a}$$

When this is substituted into equation (4. 141), one obtains:

$$U_L = \frac{A_L a}{E}\sigma_L^2 + EI_L\int_0^a\left\{\sum_{n=0}^{\infty} B_n(b)\left[\frac{(2n+1)\pi}{2a}\right]^2 \cos\frac{(2n+1)\pi x}{2a}\right\}^2 dx$$

This expression may be integrated term by term and from the fact that:

$$\int_0^a \cos\frac{(2n+1)\pi x}{2a}\cos\frac{(2m+1)\pi x}{2a}\,dx = \begin{cases} 0 & n \neq m \\ \frac{a}{2} & n = m \end{cases}$$

it follows that:

$$U_L = \frac{A_L a}{E}\sigma_L^2 + \frac{EI_L a}{2}\sum_{n=0}^{\infty}\lambda_n^4 T^2 B_n(b)^2$$

The longeron stress expressed as a function of the circumferential stress, σ_θ , is:

$$\sigma_L = \frac{1}{1+\lambda}\left[\frac{PR}{2t} - \nu\sigma_\theta\right]$$

When this is introduced into the equation for the longeron strain energy, the result is:

$$U_L = \frac{A_L a}{E(1+\lambda)^2}\left[\frac{pR}{2t} - \nu\sigma_\theta\right]^2 + \frac{EI_L a}{2}\sum_{n=0}^{\infty} \lambda_n^4 T^2 B_n(b)^2 \qquad (4.144)$$

Case a. Continuous Longerons

From the previous result for the case of the skin attached to the frames,

$$B_n(b) = A_n \cosh \lambda_n b + \frac{Q_n}{\lambda_n^2}$$

When equation (4.127) is substituted into this relation, it follows that:

$$B_n(b) = \frac{16\,p a^2}{\pi^3}\sum_{n=0}^{\infty}\frac{(-1)^n}{(2n+1)^3}\left\{1 - \frac{(2n+1)^3 \delta_n}{1 - \frac{128 a^3 t \sigma_x^{1/2}\sigma_\theta^{1/2}}{\pi^5 EI_L}\sum_{m=0}^{\infty}\frac{\delta_m}{(2m+1)^2}}\right\}$$

and, therefore, from equation (4.144),

$$U_L = \frac{A_L a}{E(1+\lambda)^2}\left[\frac{pR}{2t} - \nu\sigma_\theta\right]^2 + \frac{8}{\pi^2}\left[p - \frac{\sigma_\theta t}{R}\right]^2 \frac{EI_L a}{\sigma_x^2 t^2}\sum_{n=0}^{\infty}$$

$$\left\{\frac{1}{(2n+1)} - \frac{(2n+1)^2 \delta_n \coth \lambda_n b}{1 - \frac{128 a^3 t \sigma_x^{1/2}\sigma_\theta^{1/2}}{\pi^5 EI_L}\sum_{m=0}^{\infty}\frac{\delta_m}{(2m+1)^2}}\right\}^2 \qquad (4.145)$$

Case b. Simply Supported Longerons

From equation (4.131), it is seen that:

$$B_n(b) = \frac{16Pa^2}{\pi^3}\sum_{n=0}^{\infty}\frac{(-1)^n}{(2n+1)^3}\left[1 - (2n+1)^3 S_n \coth \lambda_n b\right]$$

and therefore, from equation (4.144):

$$U_L = \frac{A_L a}{E(1+\lambda)^2}\left[\frac{pR}{2t} - \nu\sigma_\theta\right]^2 + \frac{8}{\pi^2}\left[p - \frac{\sigma_\theta t}{R}\right]^2 \frac{EI_L a}{\sigma_x^2 t^2}\sum_{n=0}^{\infty}$$
$$\left\{\frac{1}{(2n+1)} - S_n (2n+1)^2 \coth \lambda_n b\right\}^2 \qquad (4.146)$$

II. Floating Frames

From equation (4.133), one finds that upon differentiation,

$$f''(x) = -\sum_{n=1}^{\infty} B_n(b)\left(\frac{n\pi}{a}\right)^2 \cos\frac{n\pi x}{a}$$

When this is substituted into equation (4.141), it follows that:

$$U_L = \frac{A_L a}{E}\sigma_L^2 + EI_L\int_0^a\left\{\sum_{n=1}^{\infty} B_n(b)\left(\frac{n\pi}{a}\right)^2 \cos\frac{n\pi x}{a}\right\}^2 dx$$

This expression may be integrated term by term and from the fact that:

$$\int_0^a \cos\frac{n\pi x}{a}\cos\frac{m\pi x}{a}\,dx = \begin{cases} 0 & n \neq m \\ \frac{a}{2} & n = m \end{cases}$$

it follows that:

$$U_L = \frac{A_L a}{E(1+\lambda)^2}\left[\frac{pR}{2t} - \nu\sigma_\theta\right]^2 + \frac{\pi^4 EI_L}{2a^3}\sum_{n=1}^{\infty} n^4 B_n(b)^2 \qquad (4.147)$$

Case a. Continuous Longerons

From the previous result for the case of floating frames and

continuous longerons:

$$B_n(b) = -\frac{4}{\pi^4}\frac{Pbta^4\sigma_\theta}{EI_L}\frac{\xi_n(-1)^n}{n\,TANH\,\tau_n b}$$

and therefore, from equation (4.147):

$$U_L = \frac{A_L a}{E(1+\lambda)^2}\left[\frac{PR}{2t}-\nu\sigma_\theta\right]^2+\frac{8}{\pi^4}\left[p-\frac{\sigma_\theta t}{R}\right]^2\frac{b^2a^5}{EI_L}\sum_{n=1}^{\infty}\left[\frac{\xi_n n}{TANH\,\tau_n b}\right]^2 \qquad (4.148)$$

Case b. Simply Supported Longerons

From equation (4.138), it is evident that:

$$B_n(b) = -\frac{4}{3}\frac{Pba^4\sigma_\theta t}{\pi^2 EI_L T}\left\{\left[1+\frac{3}{(n\pi)^2}\right]-\frac{\sum_{m=1}^{\infty}\left[1+\frac{3}{(m\pi)^2}\right]\xi_m}{\frac{\pi^3 EI_L}{4a^3t\sigma_x^{1/2}\sigma_\theta^{1/2}}-\sum_{m=1}^{\infty}\xi_m}\right\}(-1)^n n\,\xi_n\,COTH\,\tau_n b$$

and therefore, from equation (4.147):

$$U_L = \frac{A_L a}{E(1+\lambda)^2}\left[\frac{PR}{2t}-\nu\sigma_\theta\right]^2+\frac{4}{9}\left[p-\frac{\sigma_\theta t}{R}\right]^2\frac{b^2a^5}{EI_L}\left\{1+\frac{18}{\pi^4}\sum_{n=1}^{\infty}\frac{1}{n^4}\left[1+\frac{2}{3}\frac{a^3t\sigma_x^{1/2}\sigma_\theta^{1/2}}{\pi EI_L}\left\{\left[1+\frac{3}{(n\pi)^2}\right]-\frac{\sum_{m=1}^{\infty}\left[1+\frac{3}{(m\pi)^2}\right]\xi_m}{\frac{\pi^3 EI_L}{4a^3t\sigma_x^{1/2}\sigma_\theta^{1/2}}-\sum_{m=1}^{\infty}\xi_m}\right\}n^2\xi_n\right]^2\right\} \qquad (4.149)$$

Evaluation of the Infinite Series

The longeron strain energy must be evaluated from equations (4.145), (4.146), (4.148) or (4.149), depending on the case, by the

partial summation of an infinite series. The rate of convergence of these series may be low in some cases or high in others. In each case, however, the resulting series becomes asymptotic rapidly to very elementary series where the sum is known. These asymptotic terms, together with their sums, are listed below for the four variations.

I:

Case a.

$$\left\{ \frac{1}{(2n+1)} - \frac{(2n+1)^2 \beta_n \coth \lambda_n b}{1 - \frac{128 a^3 t \sigma_x^{1/2} \sigma_\theta^{1/2}}{\pi^5 E I_L} \sum_{m=0}^{\infty} \frac{\beta_m}{(2m+1)^2}} \right\}^2 \longrightarrow$$

$$\left\{ 1 - \frac{1}{1 - \frac{128 a^3 t \sigma_x^{1/2} \sigma_\theta^{1/2}}{\pi^5 E I_L} \sum_{m=0}^{\infty} \frac{\beta_m}{(2m+1)^2}} \right\}^2 \frac{1}{(2n+1)^2}$$

where: $$\sum_{n=0}^{\infty} \frac{1}{(2n+1)^2} = \frac{\pi^2}{8}$$

$$\frac{\beta_m}{(2m+1)^2} \longrightarrow \frac{1}{(2m+1)^5} \quad ; \quad \sum_{m=0}^{\infty} \frac{1}{(2m+1)^5} = 1.00449$$

Case b.

$$\left\{ \frac{1}{2n+1} - \beta_n (2n+1)^2 \coth \lambda_n b \right\}^2 \longrightarrow 0$$

II:

Case a.

$$\left\{ \frac{\xi_n n}{\tanh \tau_n b} \right\}^2 \longrightarrow \frac{1}{n^4}$$

where: $$\sum_{n=1}^{\infty} \frac{1}{n^4} = \frac{\pi^4}{90}$$

Case b

$$\frac{1}{n^4}\left[1+\frac{2}{3}\frac{a^3 t \sigma_x^{1/2}\sigma_\theta^{1/2}}{\pi E I_L}\left\{\left[1+\frac{3}{(n\pi)^2}\right]-\frac{\sum_{m=1}^{\infty}\left[1+\frac{3}{(m\pi)^2}\right]\xi_m}{\frac{\pi^3 E I_L}{4a^3 t\sigma_x^{1/2}\sigma_\theta^{1/2}}-\sum_{m=1}^{\infty}\xi_m}\right\}n^2\xi_n\right]^2$$

$$\longrightarrow \quad \frac{1}{n^4}$$

where: $\sum_{n=1}^{\infty}\frac{1}{n^4}=\frac{\pi^4}{90}$; $\xi_n \longrightarrow \frac{1}{n^3}$, $\sum_{n=1}^{\infty}\frac{1}{n^3}=1.20206$

The procedure for the summation of the infinite series in the expressions for the longeron strain energies is, therefore:

1) evaluate the sum of the asymptotic series;
2) evaluate the partial sum of the exact series to as many terms as are required for agreement with the asymptotic terms;
3) evaluate the same partial sum of the asymptotic series;
4) subtract the partial sum of the asymptotic series from the exact sum of that series and add the result to the partial sum of the exact series, thus obtaining an approximate sum of the required series.

Computational Procedure

The following steps are required for the analysis by the perturbation membrane theory:

1) The total strain energy is evaluated for large increments of the circumferential stress, σ_θ . The range of σ_θ is:

$$0 \le \sigma_\theta \le \frac{pR}{t}$$

2) The value of the circumferential stress, σ_θ , which results in the minimum total strain energy of the system is approximated by plotting U_T versus σ_θ .

3) The total strain energy is evaluated for small increments of the circumferential stress about the approximate value obtained in step 2.

4) The more exact value of σ_θ is obtained by plotting again.

5) The longitudinal skin, frame, and longeron axial stresses are obtained from equations (4.55), (4.56) and (4.57) respectively.

6) The maximum longeron bending moment is obtained from equations (4.129), (4.132), (4.135) or (4.139) depending on the structural geometry, and the maximum longeron stress evaluated. The longeron axial stress is added to the maximum bending stress in order to obtain the maximum longeron stress.

7) The load transmitted between the longeron and the frame attachment is evaluated from the following relations for each case:

Ia: $$\bar{P} = \frac{64}{\pi^3}\left[\frac{\rho a^2 t \sigma_x^{1/2}\sigma_\theta^{1/2}}{1 - \frac{128 a^3 t \sigma_x^{1/2}\sigma_\theta^{1/2}}{\pi^5 E I_L}\sum_{m=0}^{\infty}\frac{\mathcal{J}_m}{(2m+1)^2}}\right]\sum_{n=0}^{\infty}\mathcal{J}_n$$

Ib: $$\bar{P} = \frac{64}{\pi^3}\rho a^2 t \sigma_x^{1/2}\sigma_\theta^{1/2}\sum_{n=0}^{\infty}\mathcal{J}_n$$

IIa and IIb: $$\bar{P} = \frac{2b}{R}\sigma_F A_F$$

V. EVALUATION OF THE VALIDITY OF THE MEMBRANE ASSUMPTION

Because the membrane assumption was required in several of the previous limiting solutions, the error introduced by neglecting the bending rigidity of the outer skin panel must be evaluated in order to gain confidence in the theory. A comparison of the results obtained for the simplified problem of rigid longerons and floating frames when in one case the bending rigidity of the skin panel was neglected and in the second case the exact solution was obtained, affords a means for evaluating this error.

Referring back to these two solutions, in both cases it was shown that the middle surface stress, σ_θ , is given by:

$$\sigma_\theta = \frac{1}{1+\lambda(1-\nu^2)} \left\{ E(1+\lambda)\left[\frac{\Delta R}{R} + \frac{1}{2b}\int_0^b \left[\left(\frac{d(\omega_0+\omega_1)}{dy} \right)^2 - \left(\frac{d\omega_0}{dy} \right)^2 \right] dy \right] - \nu \frac{pR}{2t} \right\} \tag{5.1}$$

Hence, given the deflection of the skin $\omega(y)$ and the frame deflection, ΔR , the middle surface circumferential stress, σ_θ , can be evaluated. The circumferential stress obtained when the plate equilibrium equations are used will always be less than that obtained by neglecting the bending rigidity of the plate resulting in the membrane analysis. If the results obtained by the membrane equation compare favorably with those obtained by the plate equation, then the membrane assumption is valid.

In order to describe the range of structural geometry and internal pressure for which the membrane assumption is valid, it is necessary to define a permissible error in the circumferential

stress. The following arbitrary criterion will be adopted:

$$0.95\sigma_\theta(\text{membrane}) \leq \sigma_\theta(\text{plate}) \leq \sigma_\theta(\text{membrane})$$

It is evident from equation (5.1) that the greatest differences in the two theories are likely to occur when the frame is rigid, i.e. $\Delta R=0$, and the geometric parameter λ is a maximum, i.e. $\lambda=1$. When this conservatism is introduced, the above criterion becomes dependent only upon the internal pressure, the material properties, the radius of the cylinder, the longeron spacing, and the panel width to thickness ratio. A curve of the transition point for aluminum structures based on the above criterion is shown in Fig. 21. Points to the right of the curve result in membrane stresses within the above criterion and therefore the membrane assumption is valid. Plate theory is required when the structure is such that the corresponding point lies to the left of the curve.

When the skin is attached to the frames or the longeron deflection is significant, the question of validity of the membrane assumption becomes more complicated. Unfortunately, a more exact theory which is not known is required in order to evaluate this error. One can only speculate that since the skin panels of most fuselage structures are much longer than wide, the mid-panel elements behave like elements of an infinite strip plate and the previous criterion is applicable.

Fig. 21 represents the most undesirable conditions for the applicability of the membrane theory. When the criterion represented by this figure is not met for a specific case, the membrane theory may still be applicable if the frame displacement and the parameter,

λ , are not zero and unity respectively. In this case, the middle surface stresses must be computed by the membrane theory and the plate theory previously described, taking the frame deflection and the value of λ into account. This more exact criterion may prove the validity of the membrane assumption for that case.

VI. SAMPLE ANALYSIS

As was stated previously, there exist structural geometries coupled with certain ranges of internal pressure such that none of the limiting solutions are applicable. These are illustrated in Fig. 35. Of course, the closer the structural geometries and pressures (if required) are to the limiting cases for which the limiting solutions are exact, the more accurate will be the resulting analysis. The following typical example will serve as a guide in working out other cases.

Example. Continuous Longerons - Floating Frames

$E = 10^7$ psi

$R = 82$ ins.

$t = 0.032$ ins.

$p = 13.4$ psi

$I_L = 0.0166$ in^4

$A_L = 0.129$ sq. ins.

$A_F = 0.300$ sq. ins.

$a = 17$ ins.

$b = 6$ ins.

$\nu = 1/3$

$\bar{c} = 0.5$ ins.

The analysis will be worked out for each of the limiting solutions and the results justified and compared.

Frames Close Together - Floating Frames

1. Plate Solution

The solution of equation (4.51) by trial and error yields:

$$K = 30.05$$

from which

$$\sigma_\theta = 28,800 \text{ psi}$$

which results in:

$$\sigma_X = 15,300 \text{ psi}$$

$$\sigma_F = 20,400 \text{ psi}$$

$$\sigma_L = 5,600 \text{ psi}$$

The condition for the validity of this limiting solution is that:

$$\frac{f(o)}{\Delta R_{A_F=0}} << 1$$

From equation (4.52), it follows that:

$$\frac{f(o)}{\Delta R_{A_F=0}} = 2.27$$

Hence this solution is not valid in this case.

2. Membrane Solution

Solving equation (4.54) for σ_θ by trial and error, it follows that:

$$\sigma_\theta = 28,800 \text{ psi}$$

which is identical with the previous result, illustrating the validity of the membrane solution. This results in:

$$\sigma_X = 15,300 \text{ psi}$$

$$\sigma_F = 20,400 \text{ psi}$$

$$\sigma_L = 5,600 \text{ psi}$$

The criterion for the validity of this limiting solution is the same as the previous solution:

$$\frac{f(o)}{\Delta R_{A_F=0}} << 1$$

Hence this solution is also invalid in this case, and the frames can not be considered close together.

Frames Not Close Together - Floating Frames - Membrane Solution

Plotting $q(x)$ versus $f(x)$ and obtaining the best linear fit,

the following results were obtained for three choices of $\Delta R'$:

$\Delta R'$	A_F
0.080	0.490
0.100	0.338
0.110	0.284

from which it is evident by plotting that:

$$\Delta R = 0.107 \text{ ins.}$$

$$C = 2.42 \times 10^{-4} \text{ in.}^{-3}$$

$$K^2 = 0.0208 \text{ in.}^{-2}$$

From equation (4.92), it follows that:

$$f(o) = 0.144 \text{ ins.}$$

and from equation (4.84),

$$\delta(o) = -00144 \text{ ins.}$$

The maximum circumferential stress is, from equation (4.82),

$$\sigma_{\theta MAX.} = 36,800 \text{ psi}$$

and

$$\sigma_X = 15,300 \text{ psi}$$

$$\sigma_F = 13,050 \text{ psi}$$

$$\sigma_L = 5,600 \text{ psi}$$

The maximum longeron bending stress obtained from equations (4.94) and (4.95) is:

$$\sigma'_{L MAX.} = 30,000 \text{ psi}$$

Hence, the maximum longeron stress is:

$$\sigma_{L MAX.} = 35,600 \text{ psi}$$

The load transmitted between the longeron and frame attachment is:

$$\bar{P} = 573 \text{ lbs.}$$

The membrane assumption has already been verified from a comparison of the results of the first two limiting solutions.

Perturbation Membrane Solution

Solving for the total strain energy in the system upon assuming various values for the circumferential stress, σ_θ , the graph in Fig. 20 is obtained. From this plot it is evident that for minimum strain energy in the system,

$$\sigma_\theta = 30,600 \text{ psi}$$

Hence,

$$\sigma_x = 15,400 \text{ psi}$$

$$\sigma_F = 13,800 \text{ psi}$$

$$\sigma_L = 5,200 \text{ psi}$$

The maximum longeron bending stress is obtained from equation (4.135), resulting in:

$$\sigma_{L'_{MAX.}} = 34,900 \text{ psi}$$

Hence, the maximum longeron stress is:

$$\sigma_{L_{MAX}} = \sigma_L + \sigma_{L'_{MAX.}} = 40,100 \text{ psi}$$

The load transmitted between the longeron and frame attachment is:

$$\bar{P} = 606 \text{ lbs.}$$

These results are in good agreement with those obtained from the previous solution.

The condition for the validity of this analysis, in addition to

the membrane condition which has already been verified, is:

$$\sigma(\Delta R) = \sigma(\Delta R_{A_F=0})$$

Now, the frame deflection when the frame area vanishes, as given by equation 4.26 is:

$$\Delta R_{A_F=0} = 0.238$$

The actual frame deflection is:

$$\Delta R = 0.113$$

VII. EXPERIMENTAL INVESTIGATION

In order to have some physical basis for gaining confidence in the theory, it was decided that an experimental program should be undertaken. The test would consist of adequate instrumentation for the measurement of critical stresses upon internal pressurization of two fuselage sections, one with floating frames and the other with the skin attached to the frames - both having continuous longerons.

For the test to be representative of the mathematical model, and still be economically feasible, certain compromises in the geometry of the structure were required. First of all, the test specimen necessarily had to be a reduced scale model for reasons quite obvious; and, secondly, safety precautions and ease of manufacture suggested the choice of material as a plastic with a low modulus of elasticity, bonded by suitable cements. This meant that the line contact between the outer skin, and the longerons and frames, as simulated by riveting, could not be met and, consequently, secondary stresses would be induced into the longerons and frames. Furthermore, for ease of assembly without resorting to complicated jigs, adequate attachment of the longerons to the frame would require notching the frames since the skin would be attached to both frames and longerons for the latter phase of the program. This would result in a three-dimensional stress state in the longerons and frames in the area of the notches.

Despite these difficulties in simulating the mathematical model, it was felt that the influence upon the desired experimental

results would be within the accuracy of the instrumentation and the program was initiated with the designing of a plastic model fuselage section of this type.

Structural Model Design

The choice of the type of plastic for the various structural components resulted from a consideration of: 1) the elastic properties of the material, 2) machinability and formability, and 3) brittleness.

The high handling stresses in the thin skin required a plastic which was not brittle but had good elastic properties within the entire stress range anticipated. For these reasons, cellulose acetate sheet, manufactured by the Eastman Kodak Co., was chosen. The tolerances held on the homogeneity of the material and the thickness of the sheet left little to be desired.

The material for the frame must necessarily have outstanding forming properties since it was realized that the circular frame could be manufactured to closer tolerances by first machining straight strips and then forming around a circular form. The thermal plastic, Lucite, (methyl methacrylate) has excellent formability at temperatures around 250°F. The elastic properties of the material are sufficient within the stress levels anticipated. Though the material is brittle, the handling loads were not expected to cause failure of the frames. Therefore, it was felt that the plastic, Lucite, would be ideal for this structural component.

Lucite was also chosen for the longeron material in order to restrict the variation in the elastic properties of the structural

components to two, thus facilitating the computation of the theoretical results. The handling loads on the longerons were insufficient to discard the material due to its brittleness.

The bonding agents, as it turned out, were arrived at by trial and error. It was decided early that, where possible, agents which did not attack or seriously alter the material properties of the mating components would be used.

Various acetate nitrate agents were tried. In all cases, upon drying without pressure, many bubbles were formed with a large loss in strength at the joint. However, one cement, Radio Service Cement, No. 30-2, manufactured by the General Cement Manufacturing Co., Rockford, Illinois, was far superior to the others in minimizing the formation of bubbles. The resulting strength was found adequate. This cement apparently does not attack Lucite at all and has very little effect on cellulose acetate. For these reasons, this bonding agent was used to unite without pressure frames with longerons and the skin to both longerons and frames where required.

Since the frames were manufactured by forming two halves around a circular form and then bonding these to complete the frame, it was felt that these parts must be fused together to resist the load. A mixture of Lucite chips dissolved in ethelene dichloride was used for this purpose. Though the material properties are highly altered in the region of the bond for as long as six months after bonding, it was felt that since the region of this influence is extremely small compared to the total volume of the frame, this effect could be neglected in order to expedite the test.

The overall dimensions of the plastic test model were chosen from a consideration of feasibility of manufacture and the stored energy for safety's sake should the model rupture during a test. A diameter of 13 inches could be manufactured with the machinery available. The energy associated with this diameter up to a length of around four diameters was considered safe enough.

Since the finite length test model was to simulate an infinitely long cylinder, the number of frames required was defined by the frame spacing and the influence of the end bulkheads upon the instrumented center section. It was hoped and later verified by testing that seven frames would be sufficient to eliminate end effect.

The longeron spacing was easily arrived at by taking the minimum number of longerons required to sufficiently satisfy the restriction on the theoretical analysis and to represent a realistic situation. Twenty degree longeron spacing or eighteen longerons was satisfactory; thus resulting in a panel width of around two inches.

To simulate reality, a panel aspect ratio of at least two is required for the case where the frames are attached to the skin. In view of this, the frame spacing was fixed as four inches.

The choice of skin thickness was made upon a compromise of: 1) the desired maximum b/t ratio so that the membrane assumption would be best satisfied, and 2) the maximum thickness to facilitate strain gage instrumentation and accuracy. The compromise resulted, of course, in the minimum b/t ratio for which the membrane assumption (see Fig. 21) was valid. This thickness turned

out to be nominally 0.010 inches.

The frame cross-sectional area was made larger than required for two reasons. First, the frame axial stress was kept low to prevent fracture of the bonded surfaces; and, secondly, it was decided to violate the conditions of the perturbation solutions as much as possible by having stiff frames so that this influence, if significant, would show up. A frame cross-section of one-eighth by three-eighths of an inch was therefore chosen.

The longeron cross-section was restricted by the minimum size for which standard SR-4 A-7 electrical resistance strain gages could be used without alteration. This turned out to be one-eighth by one-eighth of an inch.

A very troublesome design detail was the geometry of the end bulkheads. These members had to be removable so that the interior of the cylinder could be accessible for strain gage instrumentation. Furthermore, the end effects could be minimized by allowing the end frame to expand radially with little resistance and by preventing any bending moments induced in the end bulkheads from carrying over to the longerons. The design indicated in Fig. 22, detail A, resulted. The end frame, which is doubly thick to prevent rolling due to the slight eccentricity of the end load through the seal, is merely warped sufficiently to provide installation and removal of the circular end bulkhead. One end bulkhead was provided with a tap for pressurization and the other for the manometer for pressure measurement.

A single test specimen served for both phases of the test. After completion of the phase I test where the frames were floating, a cement gun was utilized to cement the skin to the frame without removing the skin from the internal structure. In this manner, the gages in the phase I test could be re-used for the phase II test.

In closing the discussion on the structural model design, a review of the region where the test model fails to simulate the mathematical model is: 1) the skin is attached over one complete face of the longeron, thus inducing cross strains or a three-dimensional stress state in the longerons, 2) the longerons are attached to the frames by notching the frames and bonding, resulting in an influence on both frames and longerons, and 3) the electrical resistance gages influence the stress states in the region of their attachments. (This is discussed in detail next).

Instrumentation

The data required from the test model are the following strains as a function of pressure: 1) the midpanel longitudinal strain, ϵ_x , 2) the midpanel circumferential strain, ϵ_θ , 3) the longeron axial strain, ϵ_L , 4) the maximum longeron strain, $\epsilon_{L_{MAX.}}$, and 5) the axial frame strain, ϵ_F . In addition to these measurements of strains, tensile stress-strain data and Poisson's ratio for Lucite and cellulose acetate are required for the reduction of the strain data to the desired stress data.

It was realized early that electrical resistance strain gages would be the only practical and convenient means of measuring the desired strains with the available equipment, even though, due to

the smallness of the structural components and the low moduli of elasticity of the model materials, the gages themselves would carry a portion of the load and, therefore, would influence the results. Research was undertaken to develop new gages which would be more suitable for this test. Since the paper backing upon which most SR-4 electrical resistance wire strain gages are supported is of the order of 0.003 of an inch thick and the modulus of elasticity of the paper is approximately one million pounds per square inch, some means had to be devised for laying the wire directly upon the plastic.

This was most conveniently accomplished for the 0.010 inch skin by winding the wire around the skin by drilling tiny holes. This is illustrated in detail in Fig. 24. Only six lengths of one mil Nichrome wire were used to prevent any appreciable load from being carried by the wires. Consequently the gage length had to be extended to three-quarters of an inch so that the resistance would be high enough to prevent excessive heating of the wires using a one and one-half volt system. The wire spacing was kept at a nominal one-thirty second of an inch in order to have as much skin associated with a single wire as possible without appreciable cross strain influence.

This integral wound strain gage cancels the bending strain in the skin, measuring directly the axial strain. In other words, it replaces two back to back gages which are normally required. The wire is bonded to the cellulose acetate skin by thinned Radio Service Cement which has previously been used by the GALCIT

structures group for SR-4 strain gage instrumentation with good success. The thickness of the layer of dried cement is estimated at five ten thousandths of an inch from micrometer measurements. The holes through which the strain gage wire are passed is adequately filled with cement so that the influence of the holes is negligible. In order to investigate the accuracy of this gage without correction or calibration of the gage factor to take into account the load carried by the gage, the following tests were conducted. One tensile strip of 0.010" cellulose acetate one inch wide was instrumented with a Huggenberger extensometer and the modulus of elasticity of the material obtained. A second tensile strip was instrumented with an integral wound gage and the stress-strain curve obtained. The results of this latter test are shown in Fig. 26, where the modulus of elasticity is given as

$$E = 4.07 \times 10^5 \text{ PSI}$$

The difference in moduli of elasticity obtained by the two methods is less than two percent, thus supporting the idea that the integral wound gage carries little load indeed. In view of these tests, no calibration of the skin gages was required. The gage factor of the one mil Nichrome wire is:

$$G.F. = 2.00 \pm 2\%$$

A tangential integral wound gage was mounted on the strip in order to determine Poisson's ratio for the cellulose acetate. The results of that test are shown in Fig. 27. The value of Poisson's ratio obtained for cellulose acetate was:

$$\nu = 0.316$$

No convenient methods for mounting integral gages on the longerons were devised due to the difficulty of mounting the interior gage. Therefore, it was decided that SR-4 A-7 strain gages would be used and that the gage factors for bending and axial loads would be obtained by separate calibration tests. The modulus of elasticity of the Lucite used for this test was obtained by a tensile test using a Huggenberger extensometer. The results of this test are shown in Fig. 28, from which it is evident that:

$$E = 3.72 \times 10^5 \text{ PSI}$$

When mounting the A-7 gages using Radio Service Cement as before, the paper backing on one side of the gage was removed in order to minimize as much as possible the load carried by the gage. A beam to simulate the longeron with attached skin was made as shown in Fig. 25. The two gages were mounted on the calibration beam exactly as they would be on the test model. The results of the two calibration tests for axial load and bending using the stated gage factor of the gages (G.F. = 1.93) are shown in Fig. 29 and Fig. 30. These tests show that the calibration factor for bending is:

$$K_B = 1.68$$

and for axial stress

$$K_A = 1.39$$

Therefore, for the data reduction, the gage factor for maximum

longeron bending strain is given by:

$$(G.F.)_B = \frac{1.93}{1.68} = 1.15$$

and for longeron axial strain:

$$(G.F.)_A = \frac{1.93}{1.39} = 1.39$$

It is assumed that superposition of strains is valid when separating the axial strain and the bending strain from the combined strain state.

The frame instrumentation for axial strain was for the first phase of the test realized unsuccessfully by stretching a single strain gage wire across the diameter of the frame. Due to slight irregularities in the roundness of the frame the indicated strain was highly in error. As a matter of fact, up to pressures of one pound per square inch, this gage was indicating compressive strains. Rather than repeat the test, the skin was attached to the frame for the second phase of the test. A single A-7 strain gage was used without calibration to measure the frame strain for this test with reliable results even though the strain level was very small.

The location of the electrical resistance strain gages is shown in Fig. 31.

The dummy gages during both phases of the test were exact replicas of the conditions which existed on the test model. A portion of skin upon which were mounted two integral wound gages served as dummy gages for the skin longitudinal and circumferential

gages. The calibration beam for the longeron gages previously mentioned served as the dummy gages for that member. An A-7 gage mounted on a Lucite strip served as the dummy gage for the frame gage during the phase two test.

The unit resistance change of the gages was measured by the usual Wheatstone bridge circuit and a balancing type Leeds and Northrup potentiometer. The readings for each gage were accomplished by switching the potentiometer circuit to each gage by use of a selector panel illustrated in Fig. 23. The voltage source was composed of two, one and one-half volt, type 4FH Burgess dry cells hooked up in parallel to result in the desired one and one-half volt source. The gage readings are measured in millivolts, and the conversion to strain is:

$$\epsilon = \frac{4\,\Delta MV \times 10^{-3}}{(G.F.)(B.V.)}$$

where ΔMV is the millivolt change, and $B.V.$ is the source battery voltage. Since no calibration of the skin gages was required, the formulas for conversion to strain for these gages are:

$$\epsilon_x = \frac{2(\Delta MV)_x \times 10^{-3}}{B.V.}$$

$$\epsilon_\theta = \frac{2(\Delta MV)_\theta \times 10^{-3}}{B.V.}$$

where $G.F. = 2.00$.

Since the skin stress system is essentially one of plane stress, the skin stress-strain relations are:

$$\sigma_x = \frac{E}{(1-\nu^2)}(\epsilon_x + \nu\epsilon_\theta)$$

$$\sigma_\theta = \frac{E}{(1-\nu^2)}(\epsilon_\theta + \nu\epsilon_x)$$

The longeron axial strain is related to the change in millivolt reading by:

$$\epsilon_L = \frac{4(\Delta MV)_L \times 10^{-3}}{(G.F.)_A (B.V.)} = \frac{2.88(\Delta MV)_L \times 10^{-3}}{(B.V.)}$$

and the longeron maximum bending strain by:

$$\epsilon'_{L_{MAX.}} = \frac{4(\Delta MV)_{L'_{MAX.}} \times 10^{-3}}{(G.F.)_B (B.V.)} = \frac{3.48(\Delta MV)_{L'_{MAX.}} \times 10^{-3}}{(B.V.)}$$

where $(\Delta MV)_L$ is the average millivolt change reading and $(\Delta MV)_{L'_{MAX}}$ is one half of the difference in millivolt change of the two gages. Conversion to stress is independent of Poisson's ratio since the longeron stress state is assumed uniaxial (though violated).

The internal pressure of the test model is controlled by the regulator indicated in Fig. 23. This is a throttling system where the pressure line is tapped from a cylinder where the pressure is regulated by two needle valves - one for intake and one for the exhaust. The pressure is measured by an open end manometer. The working fluid is Dow-Corning 200-Silicon Oil - the specific gravity at room temperature, 0.960.

Photographs of the model and the experimental set-up are shown in Figs. 36 and 37.

Comparison of Theory and Experiment

A comparison of the theoretical and experimental results

for both phases of the test are shown in Figs. 32 to 34. The large discrepancy between the theory and experiments of the longeron axial stress may possibly be attributed to the inducement of cross strains into the longeron due to the complete attachment of the outer skin. A tabulation of the maximum error in the theoretical analysis based on the experimental results over the range of pressure investigated is shown below.

DISCREPANCY OF THEORETICAL AND EXPERIMENTAL RESULTS

	Phase I Floating Frames		Phase II Frames Attached
	F.N.C.-M.S.	P.M.S.	P.M.S.
σ_F	-	-	-15%
σ_L	-16%	-47%	-53%
$\sigma_{L_{MAX}}$	-15%	-8%	-9%
σ_x	-26%	-14%	-10%
σ_θ	-11%	-14%	-10%

The Tabulated Results of the Experimental Investigation are Shown Below

Phase I
Floating Frames

P, PSI	σ_F, PSI	σ_L, PSI	$\sigma_{L_{MAX}}$, PSI	σ_x, PSI	σ_θ, PSI
0	-	0	0	0	0
0.266	-	37	121	81	159
0.532	-	67	235	159	332
0.798	-	111	375	238	507
1.064	-	151	515	320	689
1.330	-	188	648	405	872
1.596	-	230	800	489	1057
1.862	-	274	949	568	1240

Phase II
Frames Attached

0	0	0	0	0	0
0.266	18	53	104	79	157
0.532	38	101	211	154	321
0.798	56	152	338	232	487
1.064	80	192	455	305	653
1.330	106	237	583	383	819
1.596	129	285	714	456	984
1.862	156	331	840	529	1145

VIII. CONCLUSIONS

Not until certain tests are performed can the validity of the solutions presented in this paper be established. These tests are presented along with the derivations of the solutions and are easily performed. Care must be taken by the stress analyst to prove the validity of the solution he is utilizing before drawing any conclusions on the indicated stress distribution of the system.

Probably the most limiting geometrical restriction on most of the solutions is the requirement that the membrane assumption be valid (see Fig. 21 and Fig. 35). Fortunately, a large class of current fuselage designs fall within the region of the validity of this restriction (see Fig. 21). Virtually no solutions are available for structural geometries within the curved plate regime (see Fig. 35), except for the highly limited case when the floating frames can be considered sufficiently close together so that longeron bending can be neglected. Unfortunately, some skin thickness and panel width combinations, typical of current aircraft, must be treated as plates and, therefore, cannot be solved by known methods except for the limited case previously mentioned. Several shell solutions have been obtained by Flügge[2], but few designs satisfy the requirements for the validity of the shell solutions.

There is a possibility that some of the restrictions on the validity of the perturbation membrane solution and the membrane solutions for floating frames when the frames are not close together can be relaxed. This is indicated by both the experimental program where the conditions for the validity of these solutions were not

exactly satisfied (see Part VII) and the sample analysis (Part VI) where the two solutions agreed favorably even though these conditions were not satisfied. Present experimental data are insufficient to relax these restrictions at this time.

The idea of the feasibility of the plastic test model proved itself and the author feels that the answers to the problem of the stress distribution in vast structural combinations and loadings can be obtained economically, rapidly, and accurately by this important but little used method.

IX. REFERENCES

1. Howland, W. L., and Beed, C. F.: Test of Pressurized Cabin Structures. Journal of Aeronautical Sciences, Volume 8, No. 1, Nov. 1940, pp. 17-23.

2. Flügge, W.: Stress Problems in Pressurized Cabins. NACA Technical Note 2612, Feb. 1952.

3. Timoshenko, S.: Theory of Plates and Shells. McGraw-Hill Book Co., Inc., 1940., pp. 433-441.

4. Timoshenko, S.: Theory of Elasticity. McGraw-Hill Book Co., Inc., 1953.

5. Wang, Chi-Teh: Applied Elasticity. McGraw-Hill Book Co., Inc., 1953.

6. Steinbacher, F. R., and Lo, Hsu: Determination of Bending Moments in Pressure-Loaded Rings of Arbitrary Shape when Deflections are Considered. NACA Technical Note 1692, Sept. 1948.

7. Love, A. E. H.: A Treatise on the Mathematical Theory of Elasticity. Cambridge University Press, 1927, pp. 515-552.

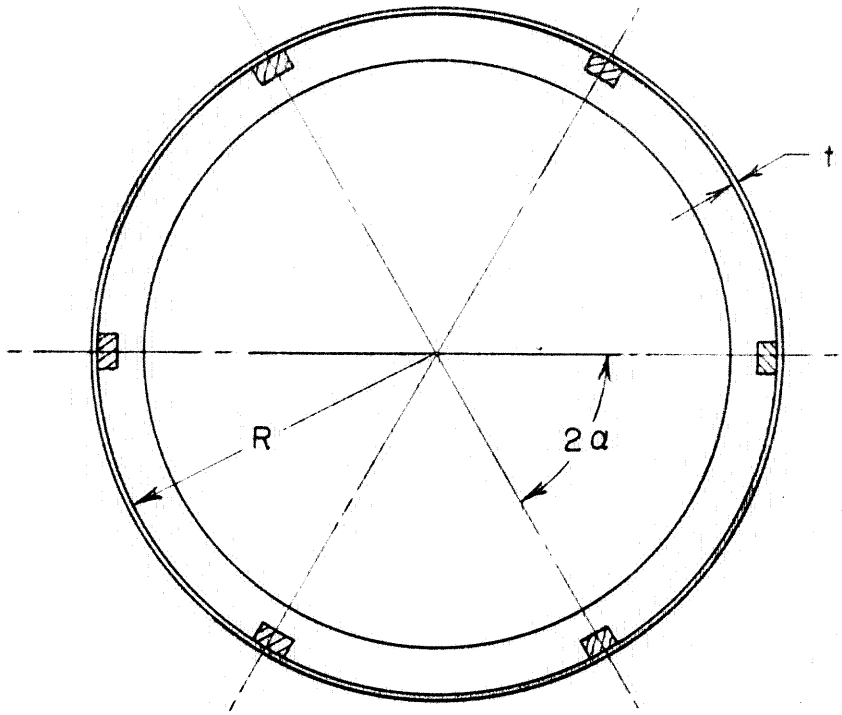

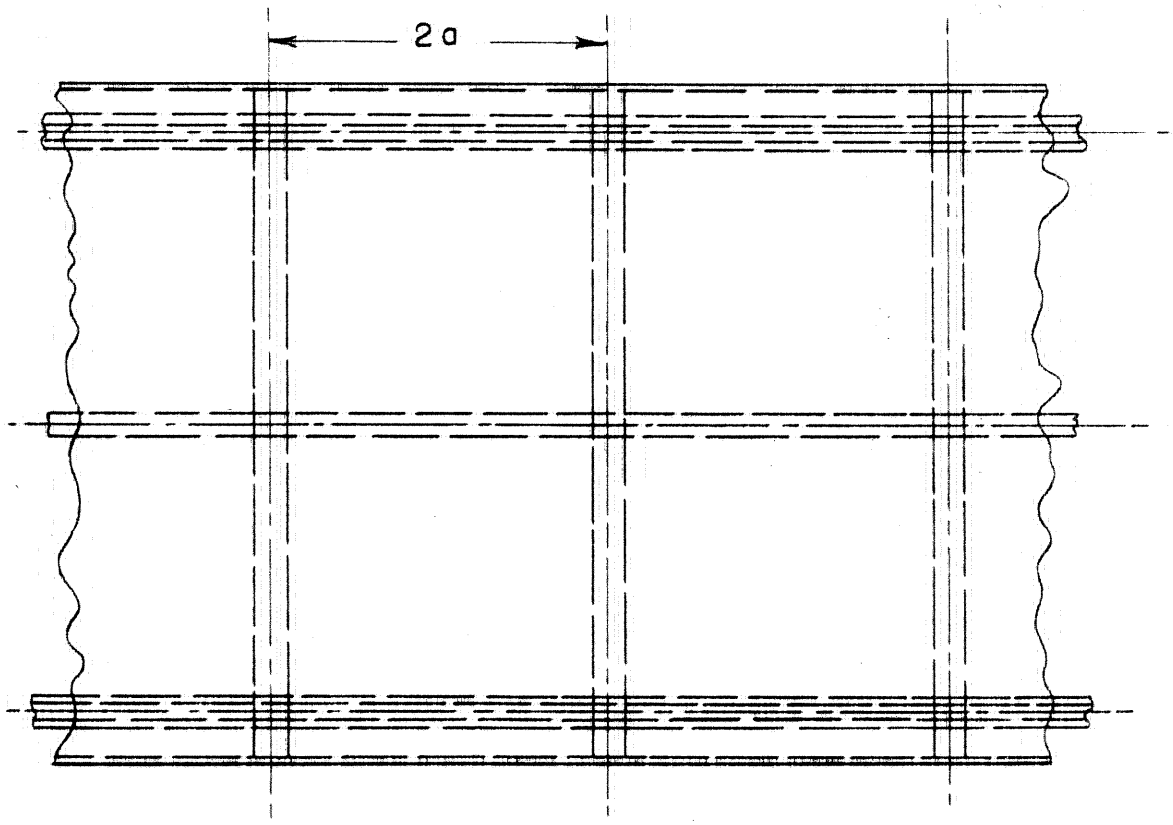

GEOMETRY OF THE IDEALIZED PRESSURIZED FUSELAGE

FIG. 1

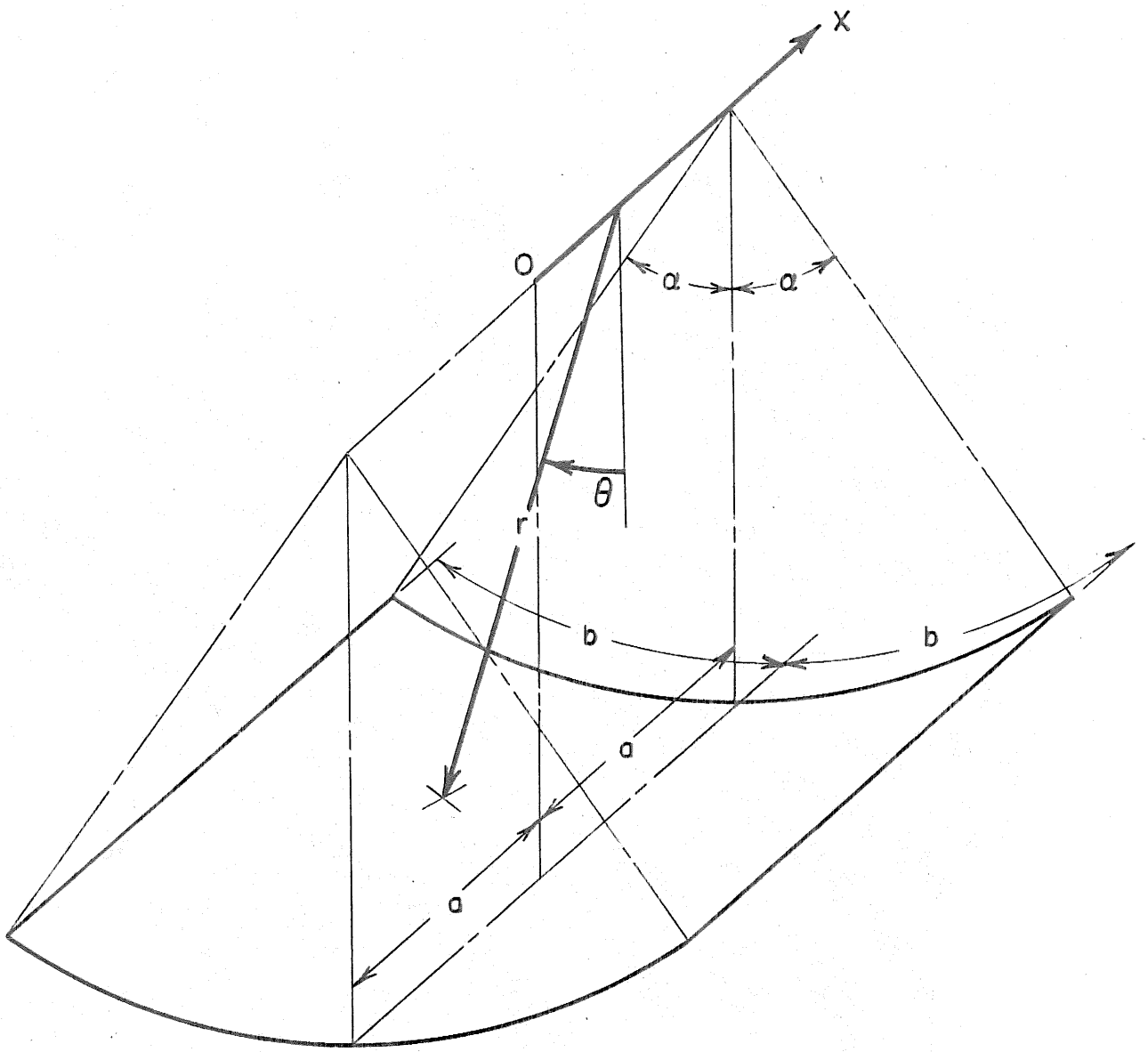

PANEL CYLINDRICAL COORDINATE SYSTEM

FIG. 2

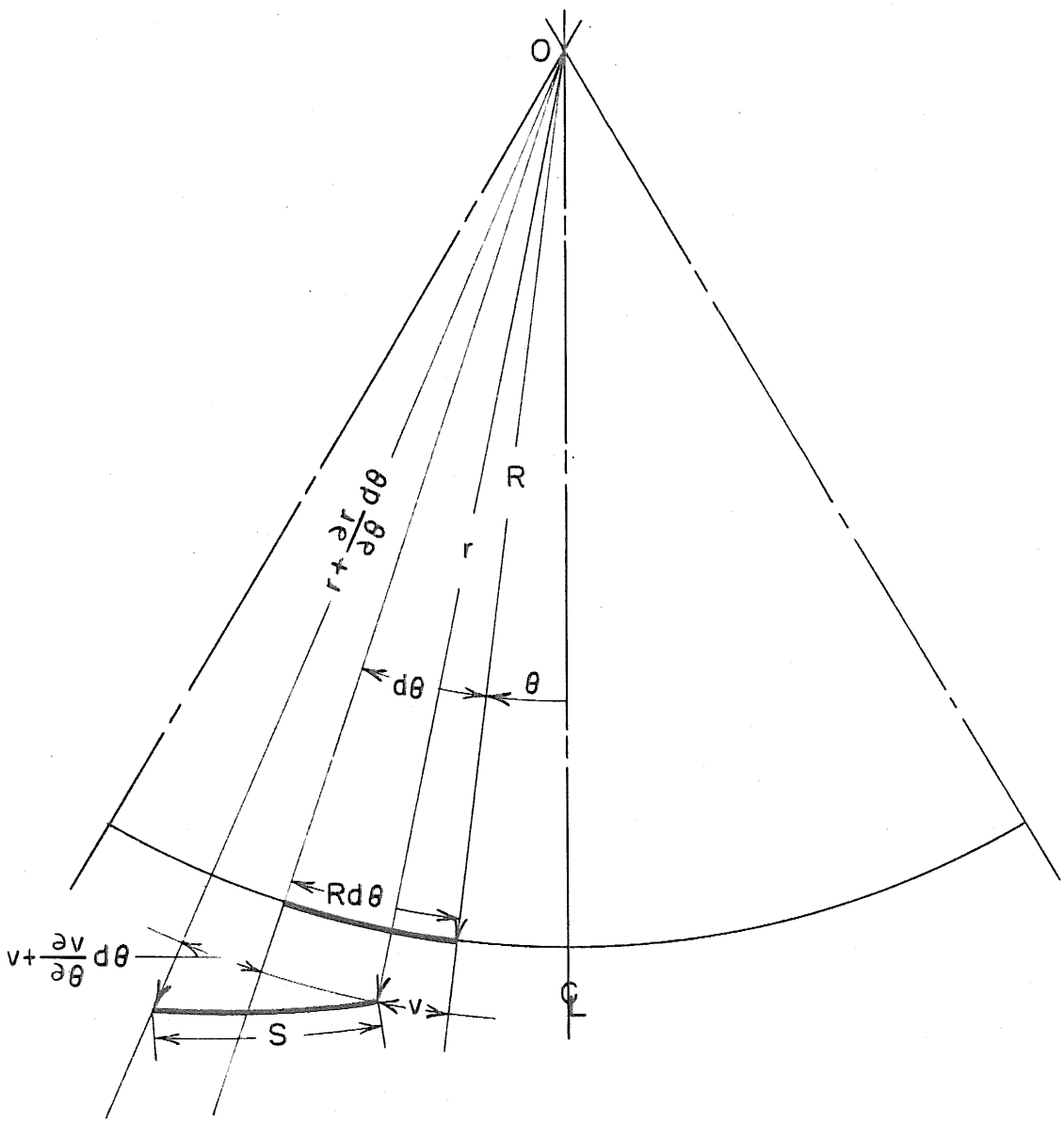

PANEL ELEMENT
BEFORE AND AFTER LOADING

FIG. 3

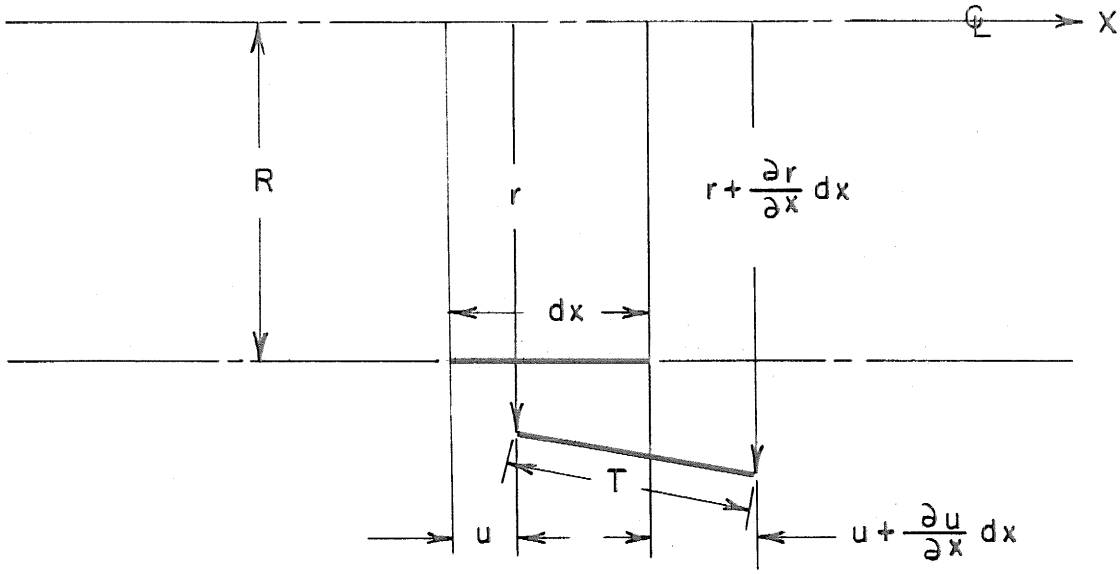

PANEL ELEMENT BEFORE AND AFTER LOADING

FIG. 4

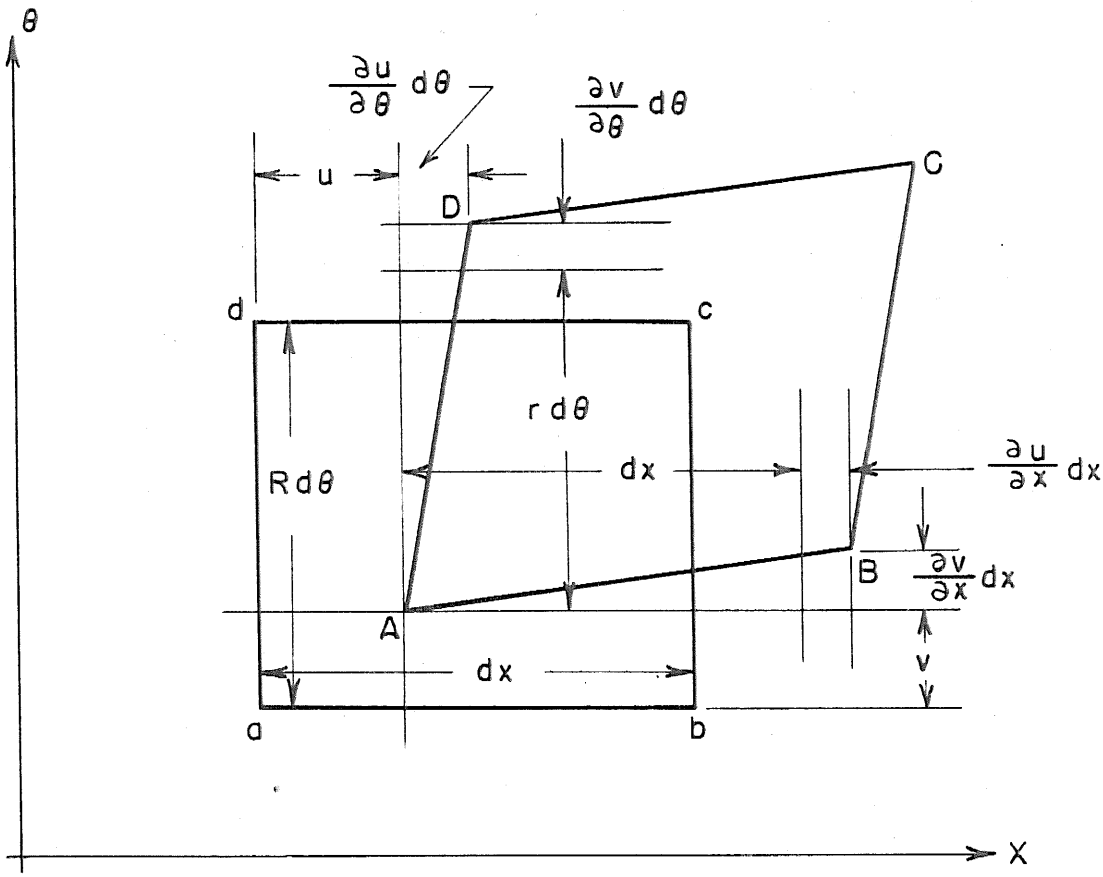

PANEL ELEMENT BEFORE AND AFTER LOADING

FIG. 5

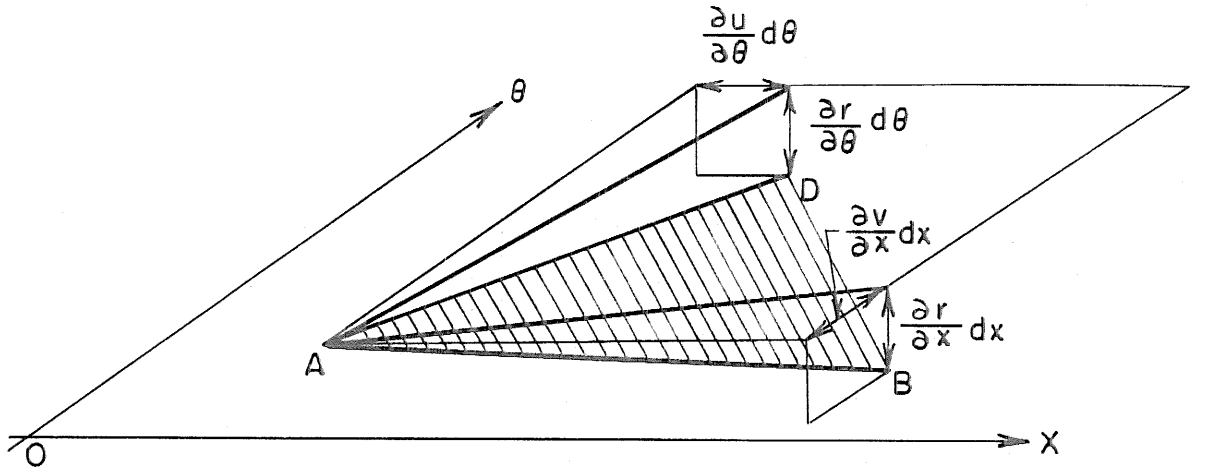

CONTRIBUTION TO THE PANEL SHEAR STRAIN DUE TO RADIAL DEFLECTION

FIG. 6

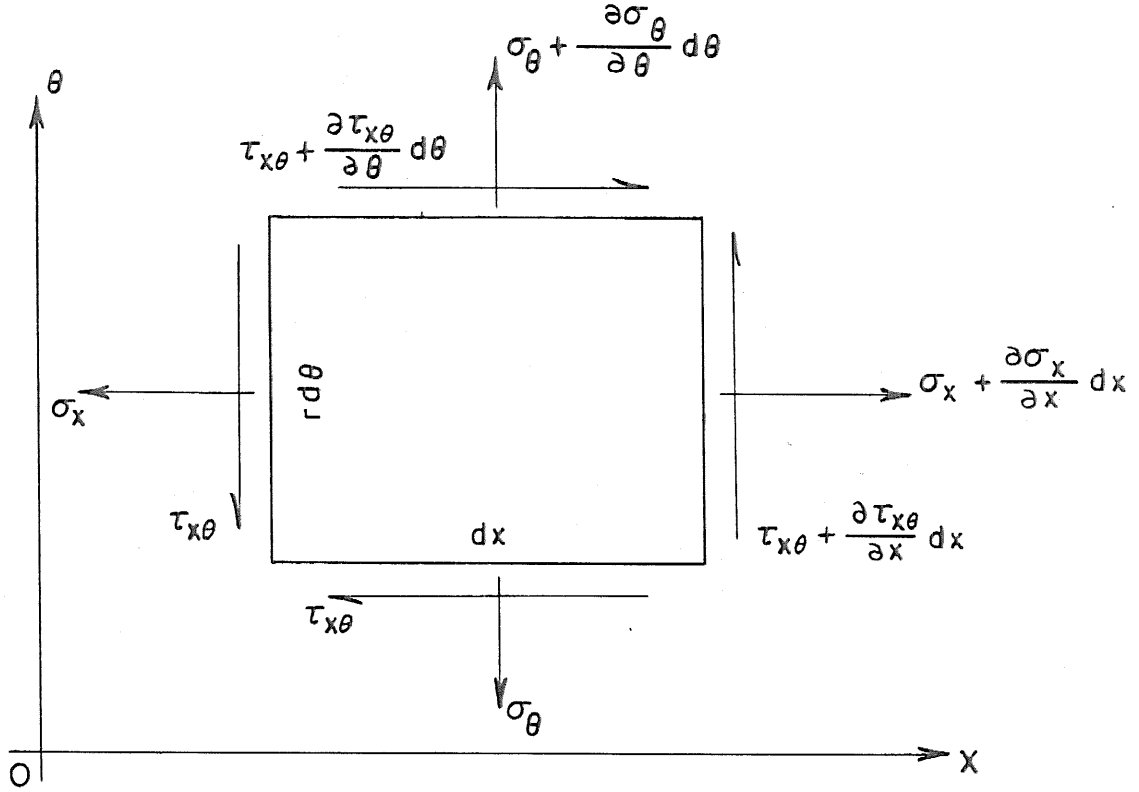

PANEL ELEMENT WITH MIDDLE SURFACE STRESSES ACTING

FIG. 7

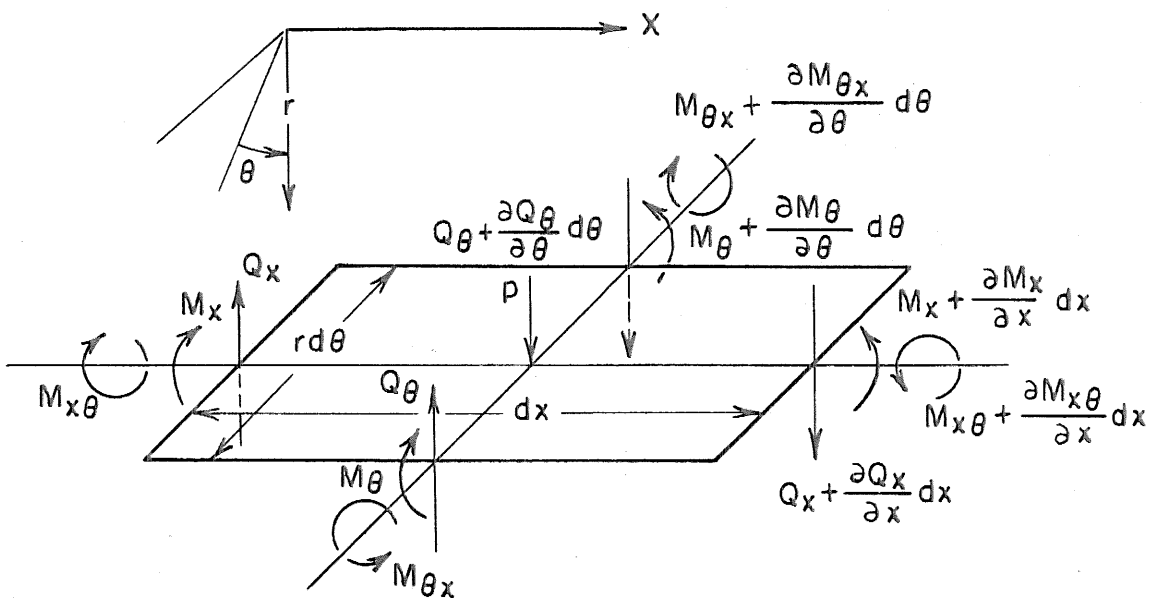

PANEL ELEMENT WITH LATERAL FORCES AND BENDING MOMENTS ACTING

FIG. 8

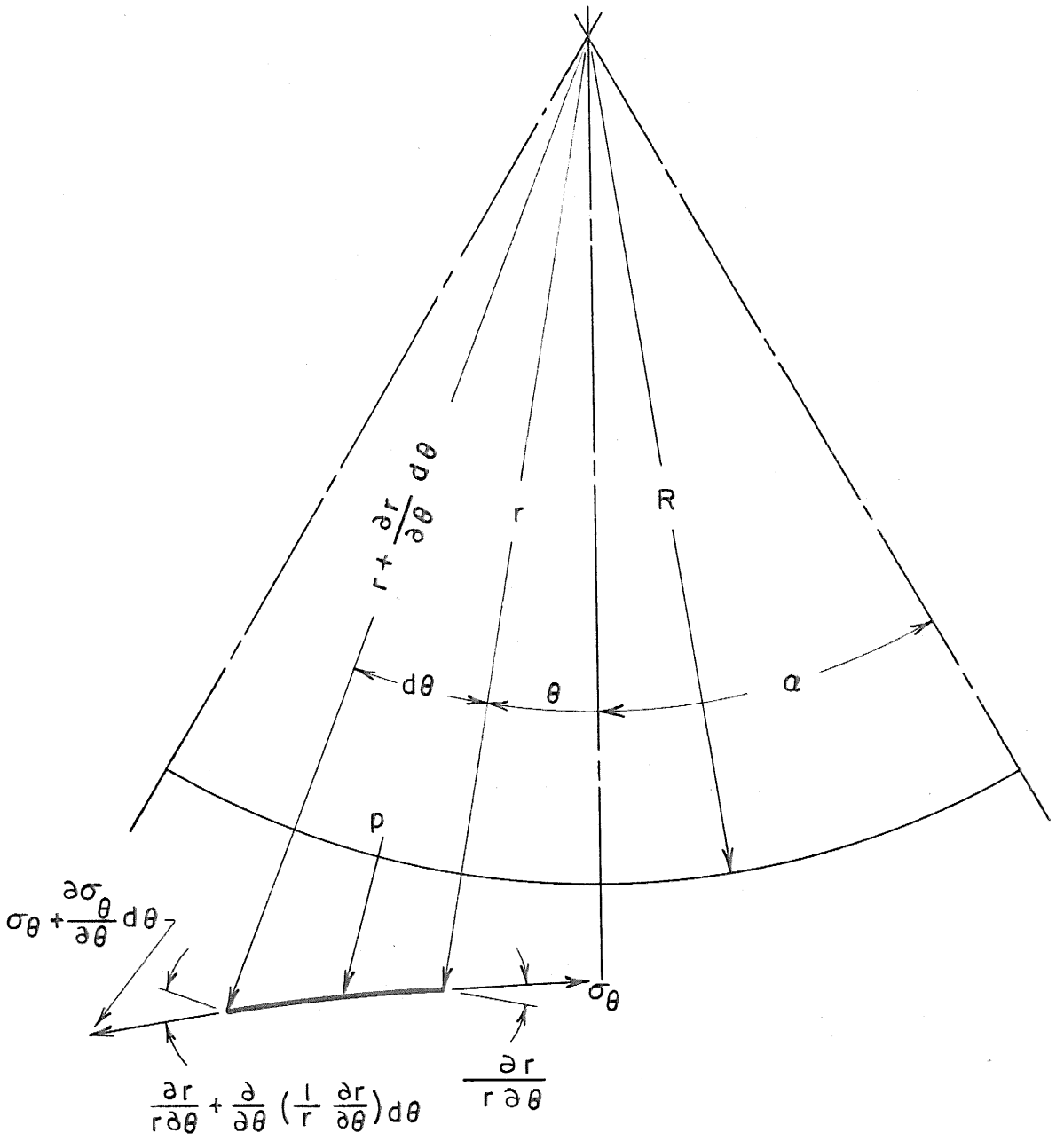

PANEL ELEMENT WITH CIRCUMFERENTIAL MIDDLE SURFACE STRESSES ACTING

FIG. 9

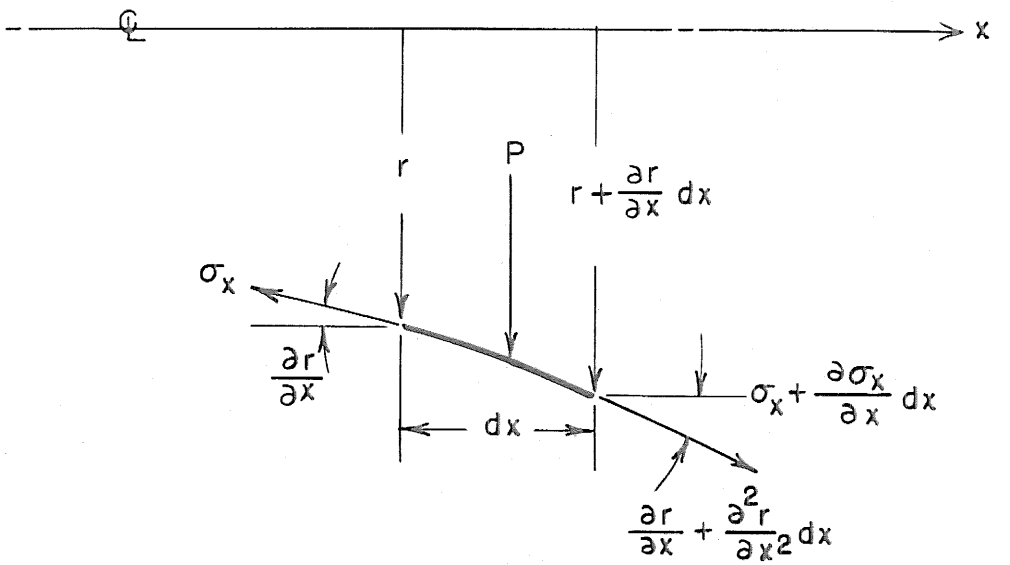

PANEL ELEMENT WITH LONGITUDINAL MIDDLE SURFACE STRESSES ACTING

FIG. 10

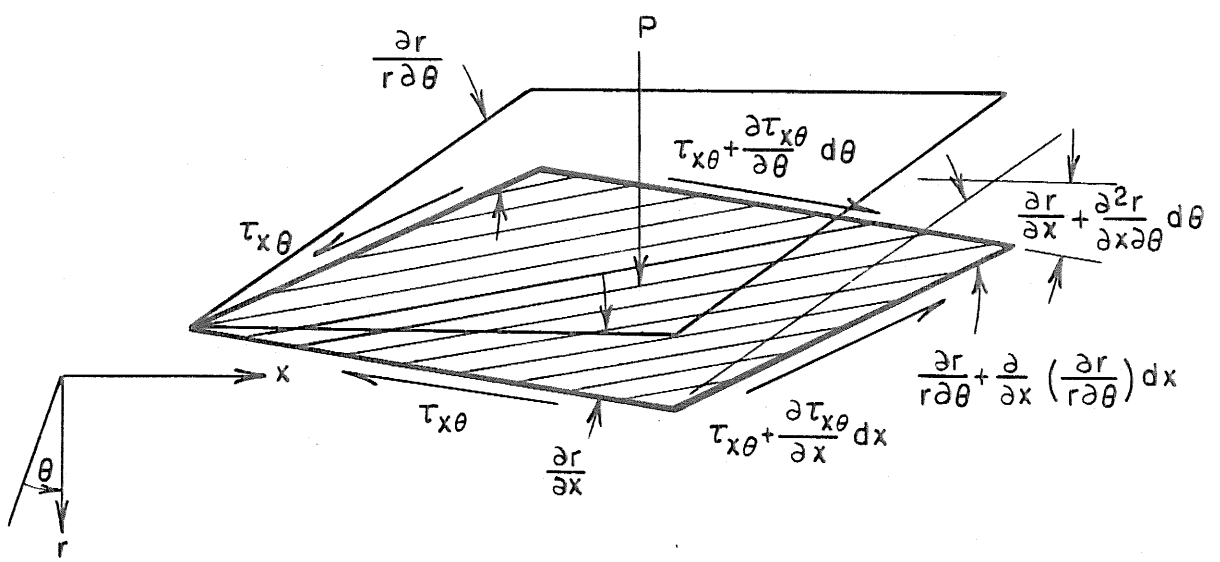

PANEL ELEMENT WITH MIDDLE SURFACE SHEARING STRESSES ACTING

FIG. 11

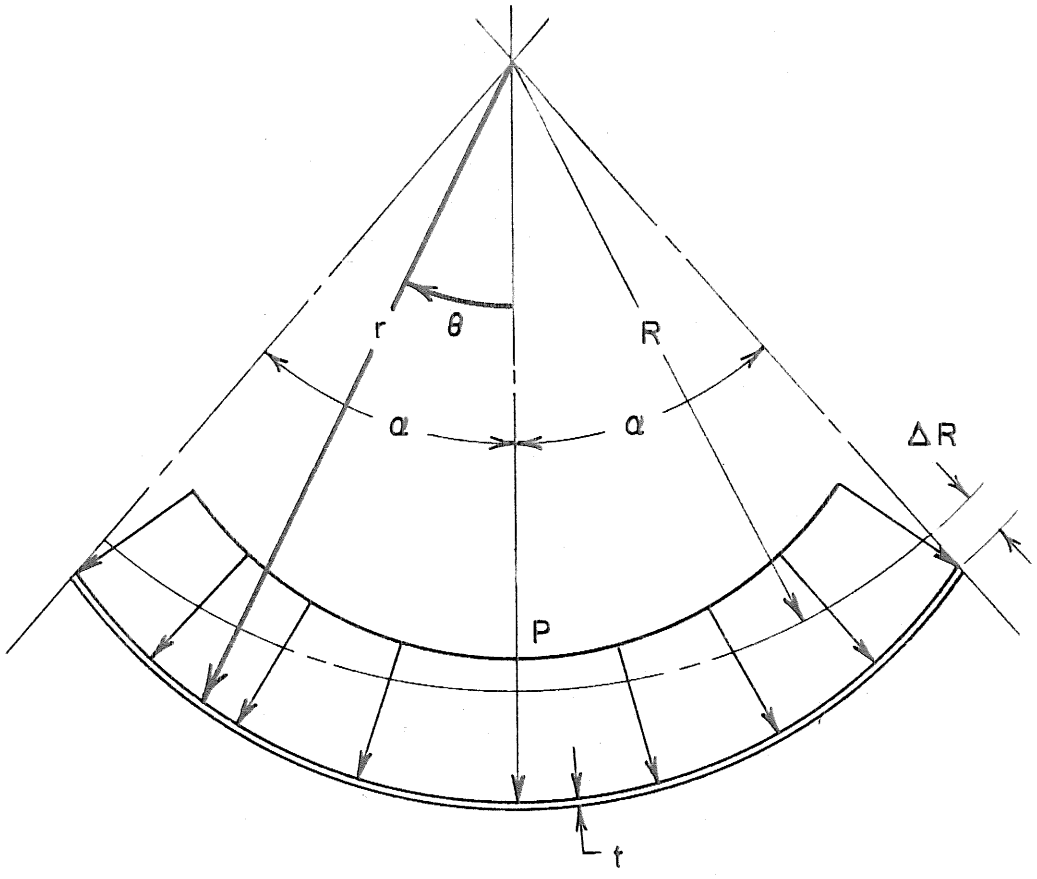

FIG. 12a

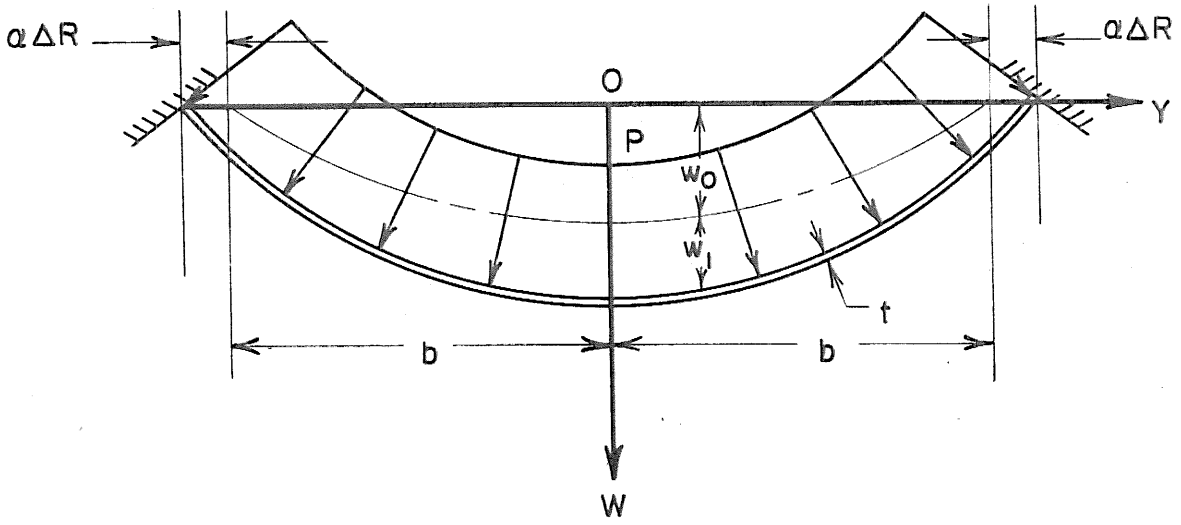

COORDINATE TRANSFORMATION-FRAMES CLOSE TOGETHER-FLOATING FRAMES

FIG. 12b

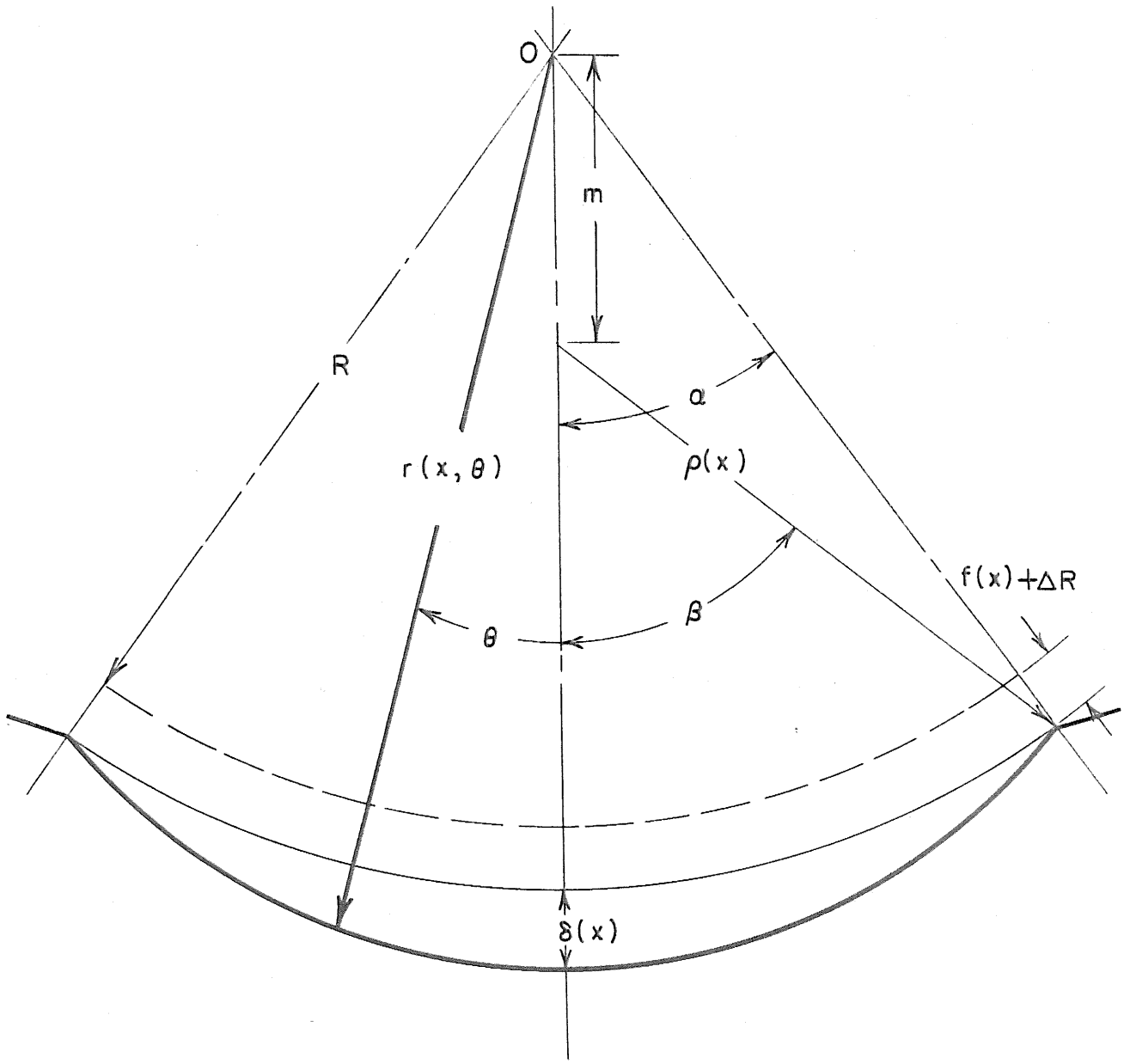

DEFLECTED PANEL GEOMETRY AT A TYPICAL X STATION — FRAMES NOT CLOSE TOGETHER — FLOATING FRAMES — MEMBRANE SOLUTION

FIG. 13

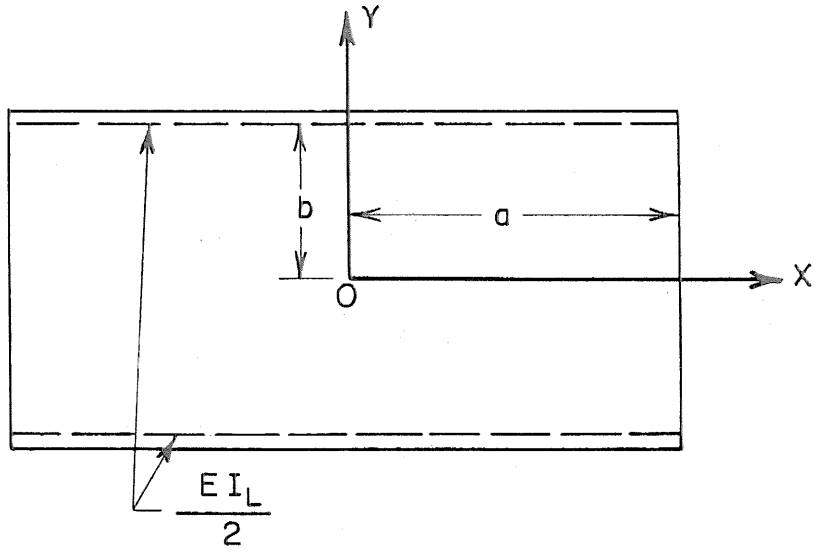

PERTURBATION MEMBRANE SOLUTION-INITIALLY FLAT RECTANGULAR MEMBRANE WITH REDUCED LATERAL LOADING

FIG. 14

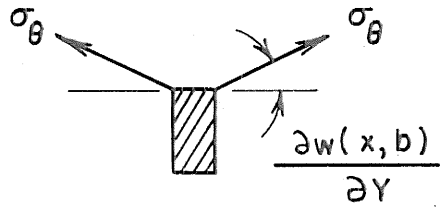

FIG. 15 a

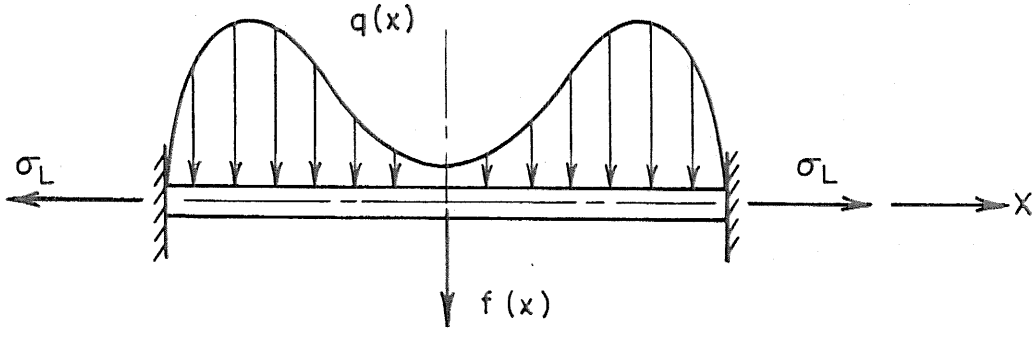

LONGERON LOADING AS A RESULT OF MEMBRANE PANEL DEFLECTION-FRAMES ATTACHED TO SKIN

FIG. 15 b

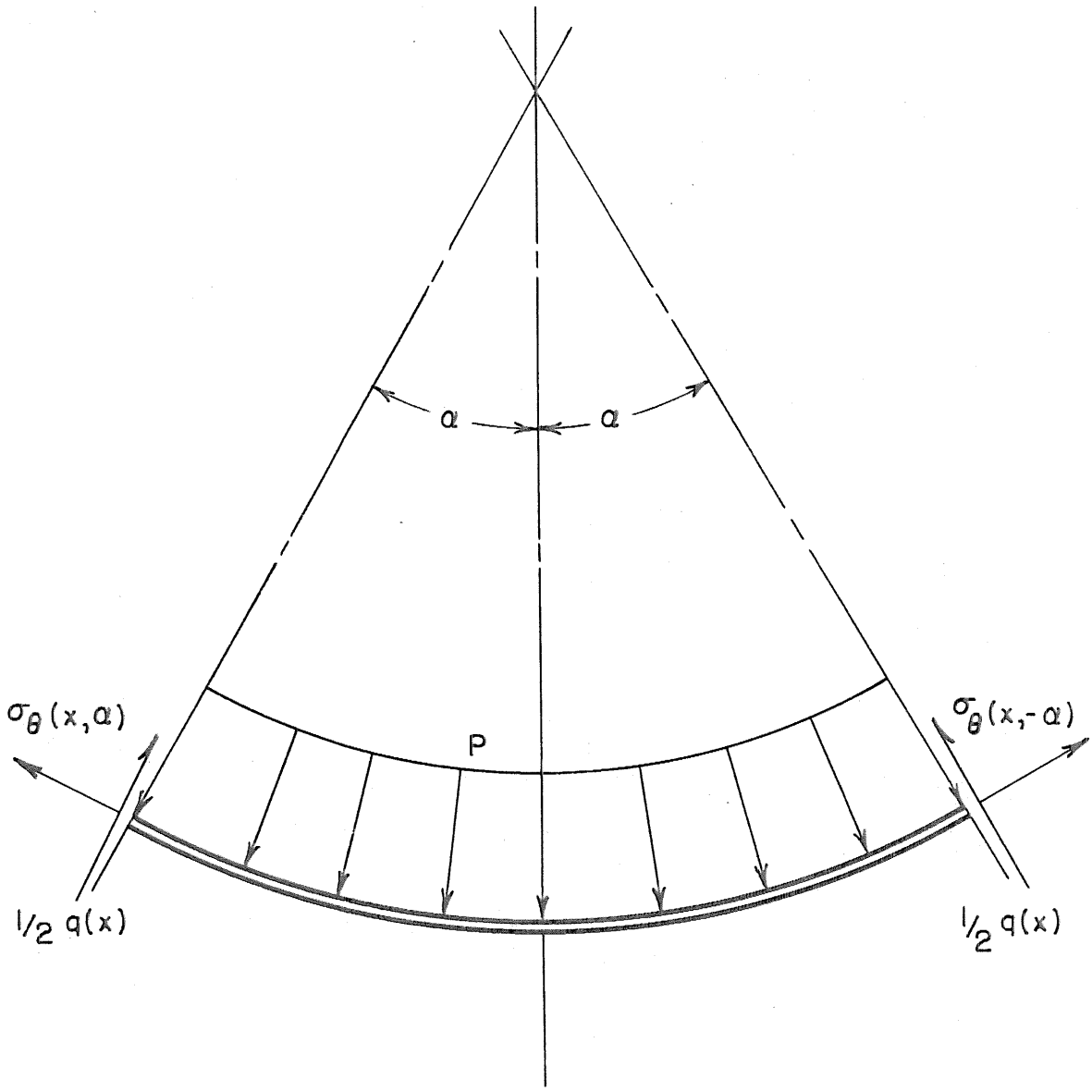

PANEL INFINITESIMAL STRIP WITH ACTING FORCES

FIG. 16

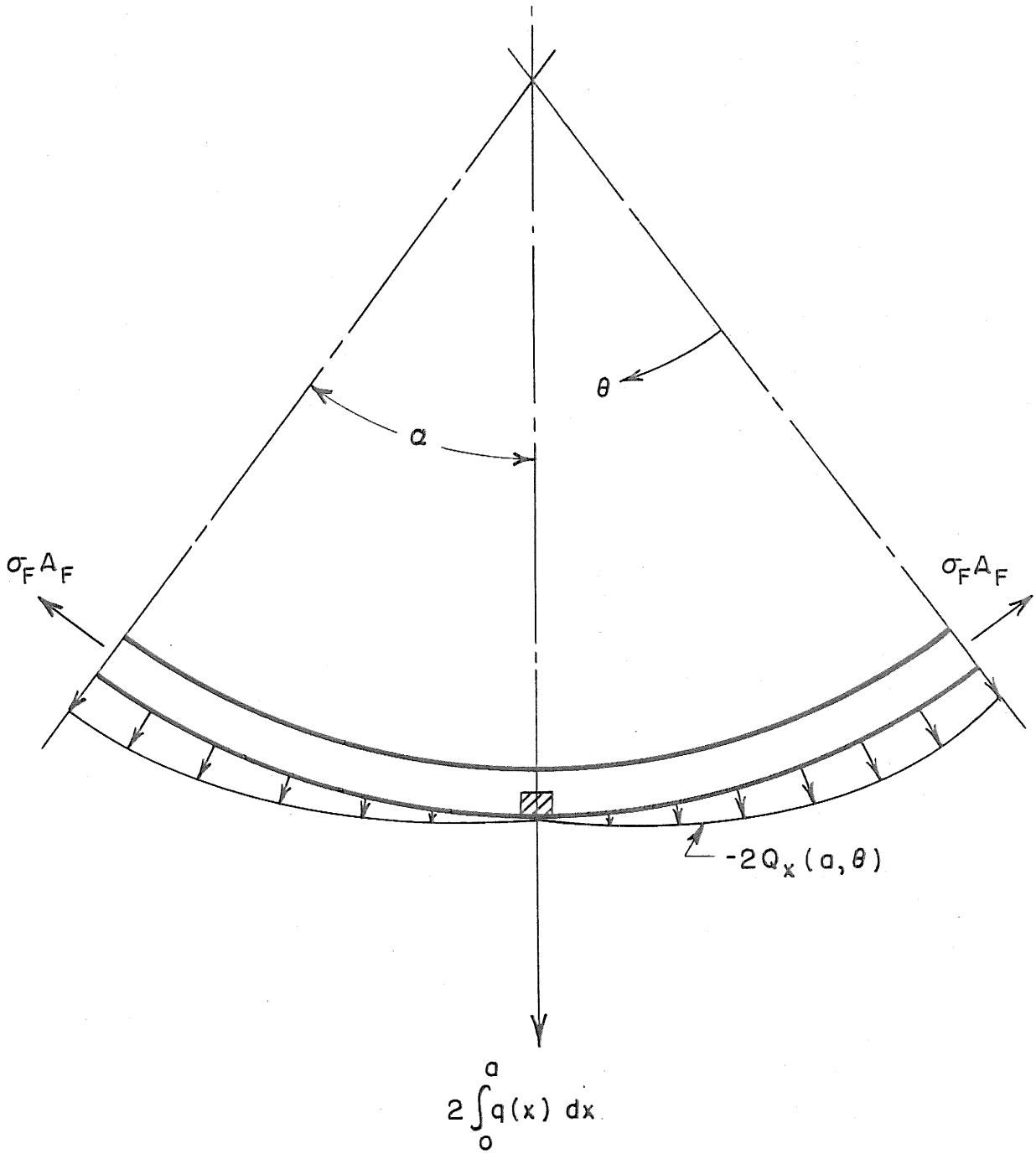

FRAME FREE BODY DIAGRAM

FIG. 17

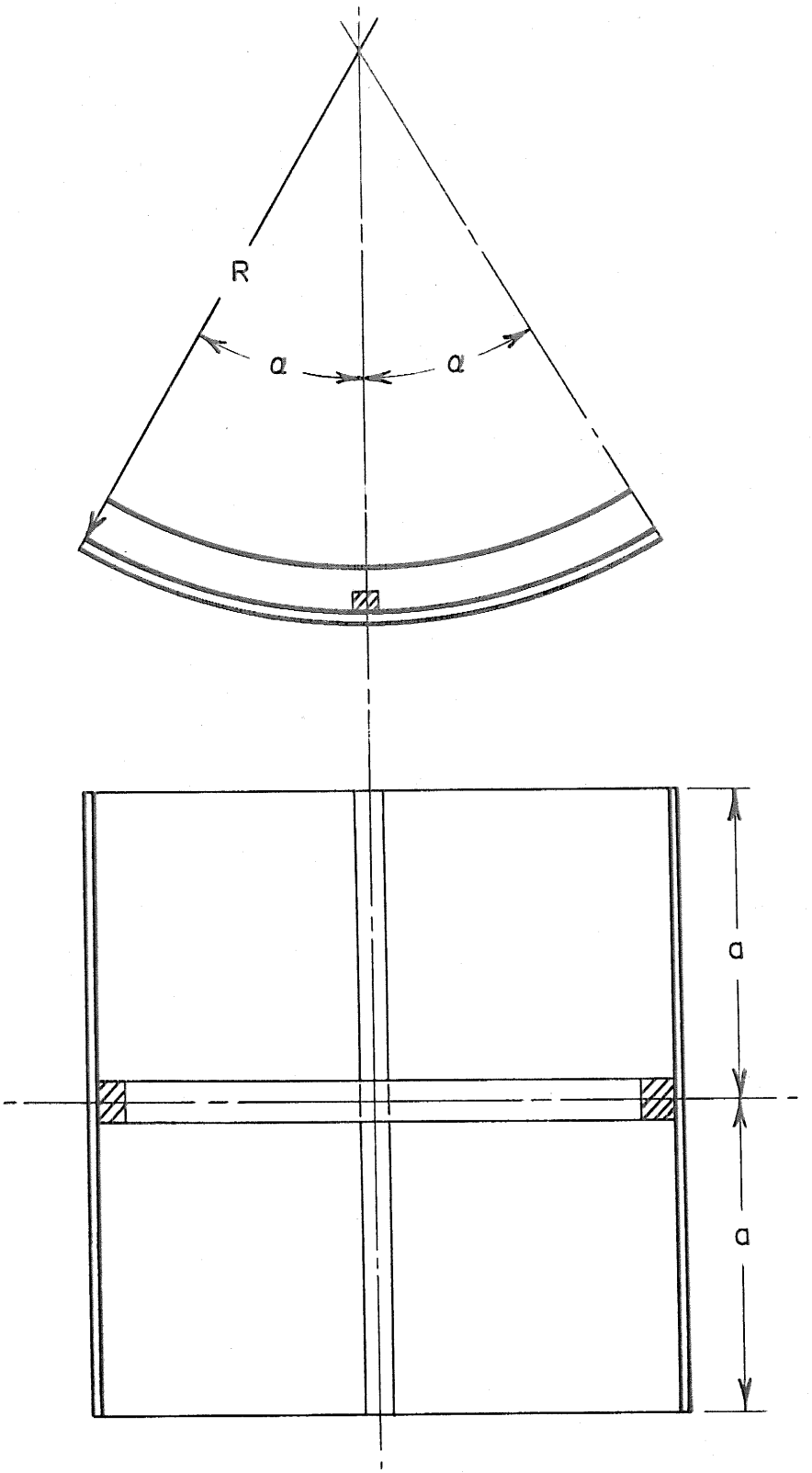

SECTION OF PANEL, LONGERON AND FRAME WHERE STRAIN ENERGY IS SUMMED

FIG. 18

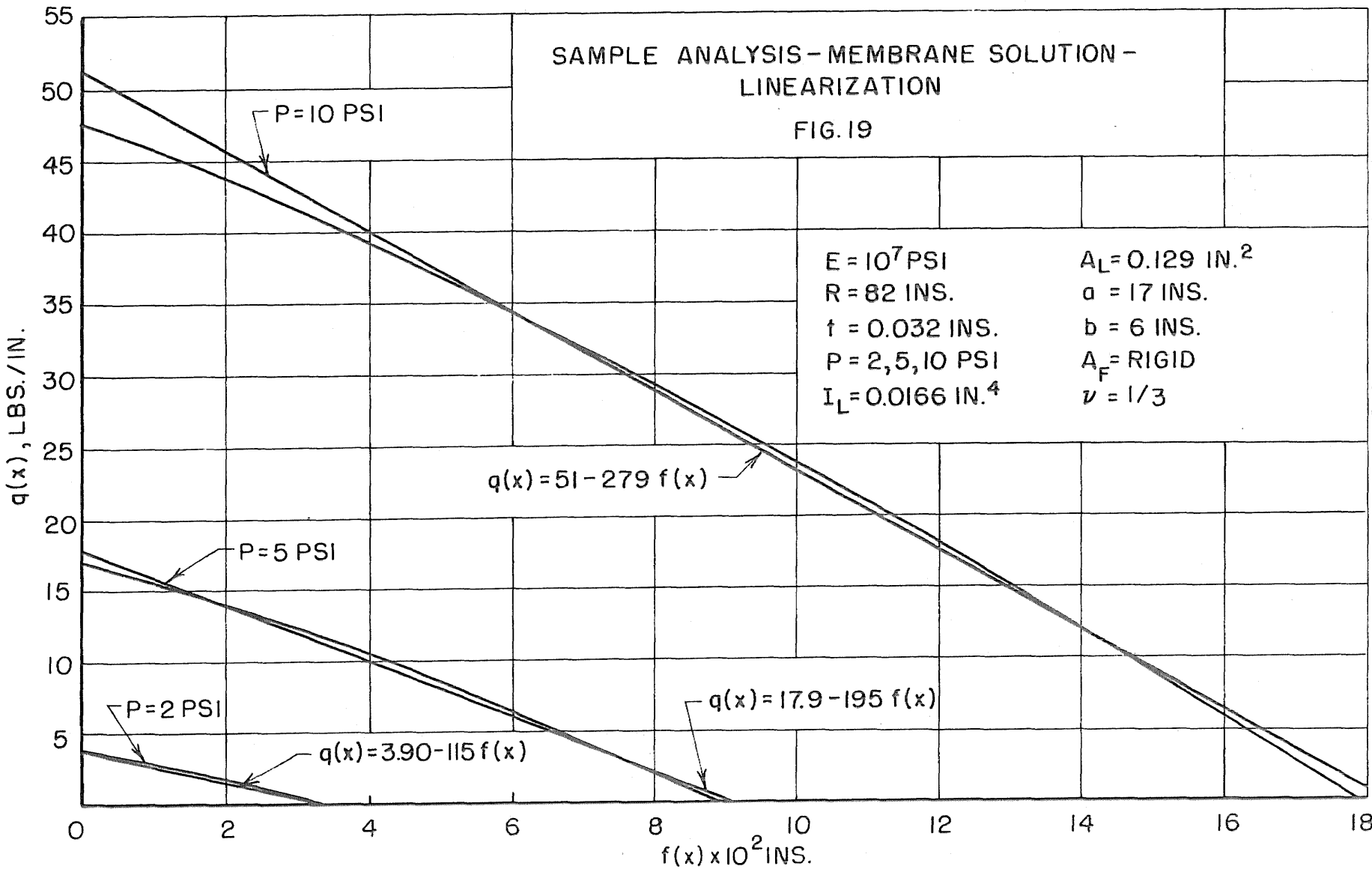
SAMPLE ANALYSIS - MEMBRANE SOLUTION - LINEARIZATION
FIG. 19
E = 10^7 PSI
R = 82 INS.
t = 0.032 INS.
P = 2,5,10 PSI
I_L = 0.0166 IN.^4
A_L = 0.129 IN.^2
a = 17 INS.
b = 6 INS.
A_F = RIGID
ν = 1/3
P = 10 PSI
q(x) = 51 - 279 f(x)
P = 5 PSI
q(x) = 17.9 - 195 f(x)
P = 2 PSI
q(x) = 3.90 - 115 f(x)
q(x), LBS./IN.
f(x) x 10^2 INS.
0
2
4
6
8
10
12
14
16
18
5
10
15
20
25
30
35
40
45
50
55

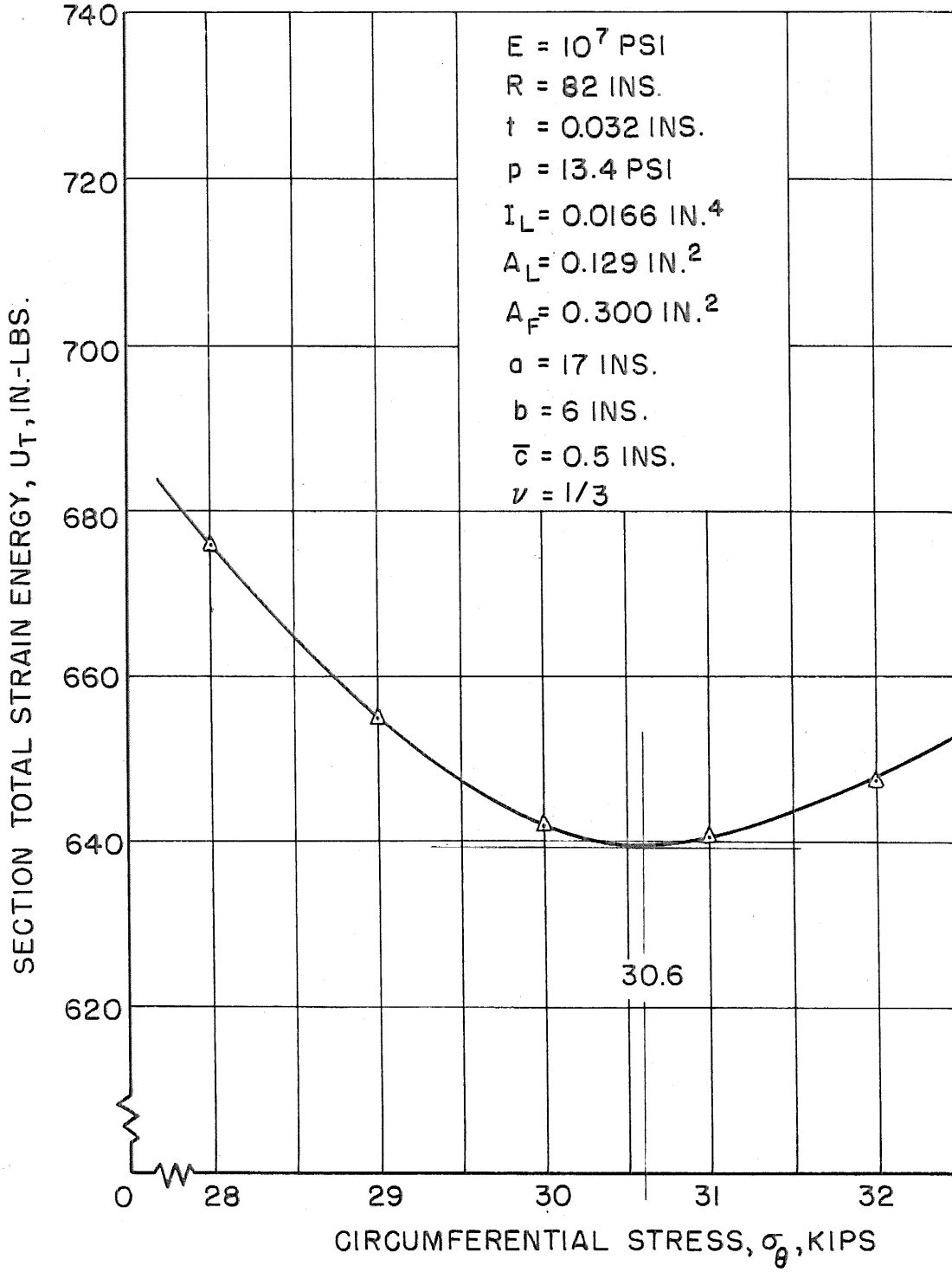

SAMPLE ANALYSIS - PERTURBATION MEMBRANE SOLUTION — DETERMINATION OF CIRCUMFERENTIAL STRESS

FIG. 20

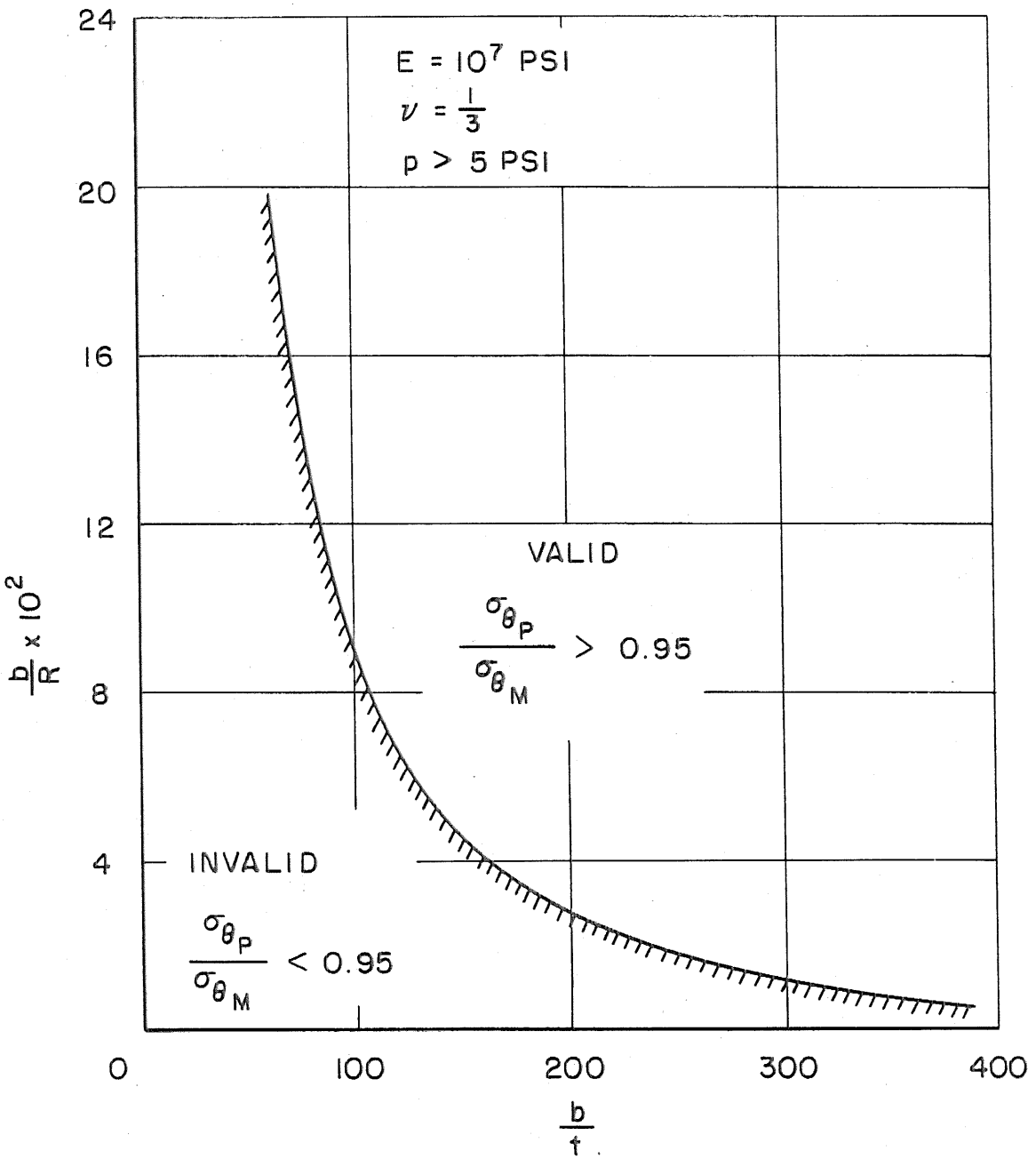

LIMITATIONS OF THE MEMBRANE ASSUMPTION

FIG. 21

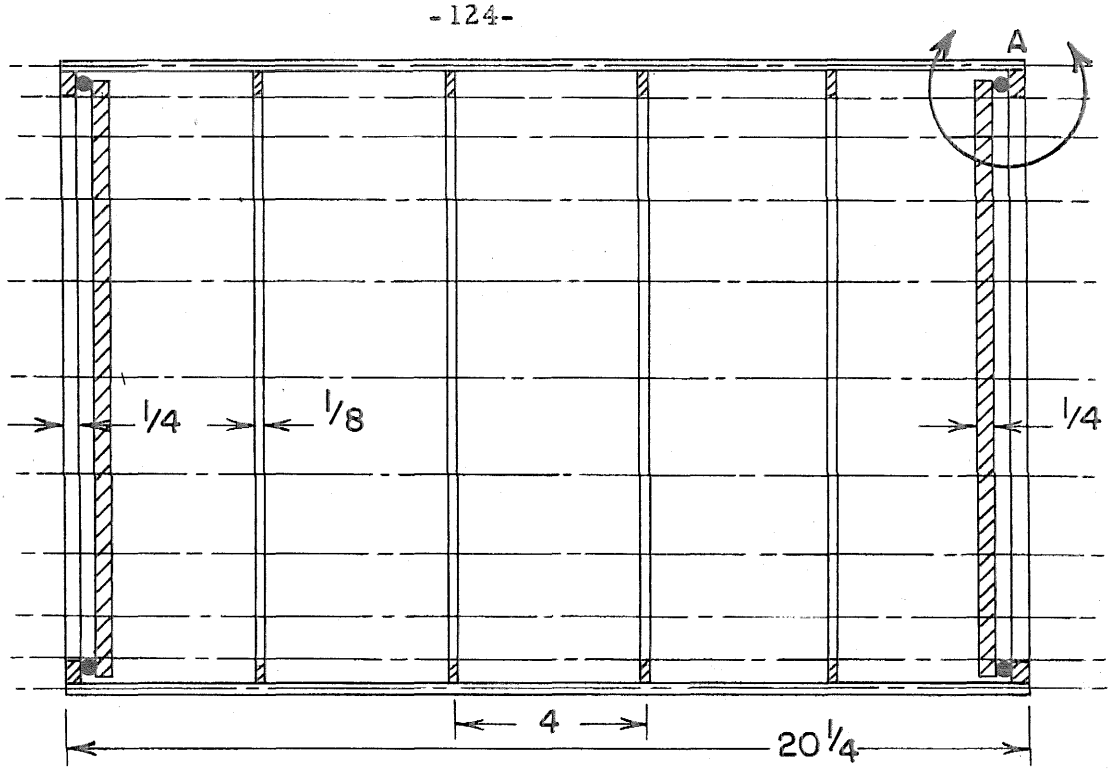

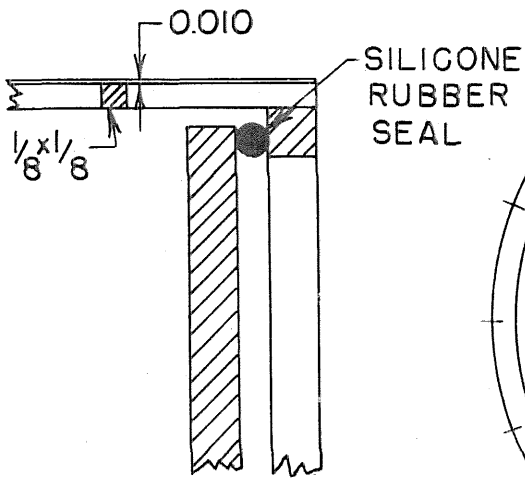

DETAIL A
END BULKHEAD

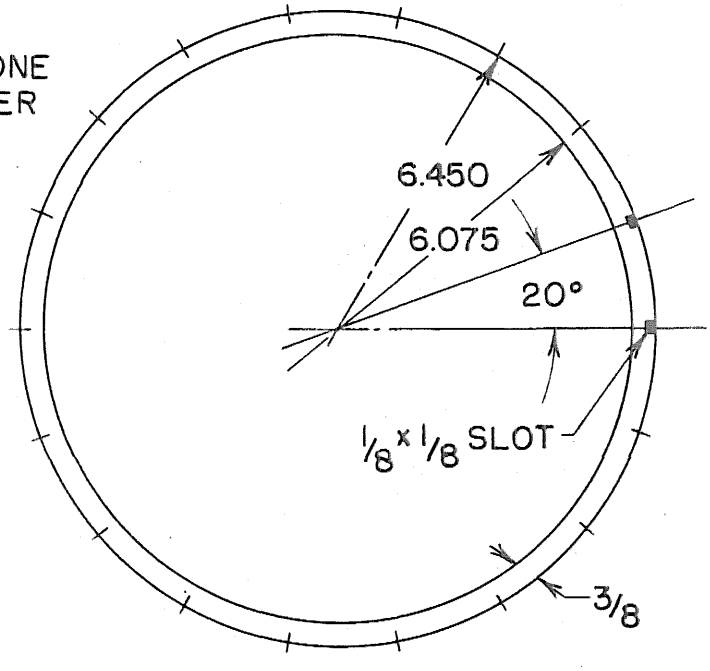

FRAME

PRESSURIZED MODEL FUSELAGE DETAIL

FIG. 22

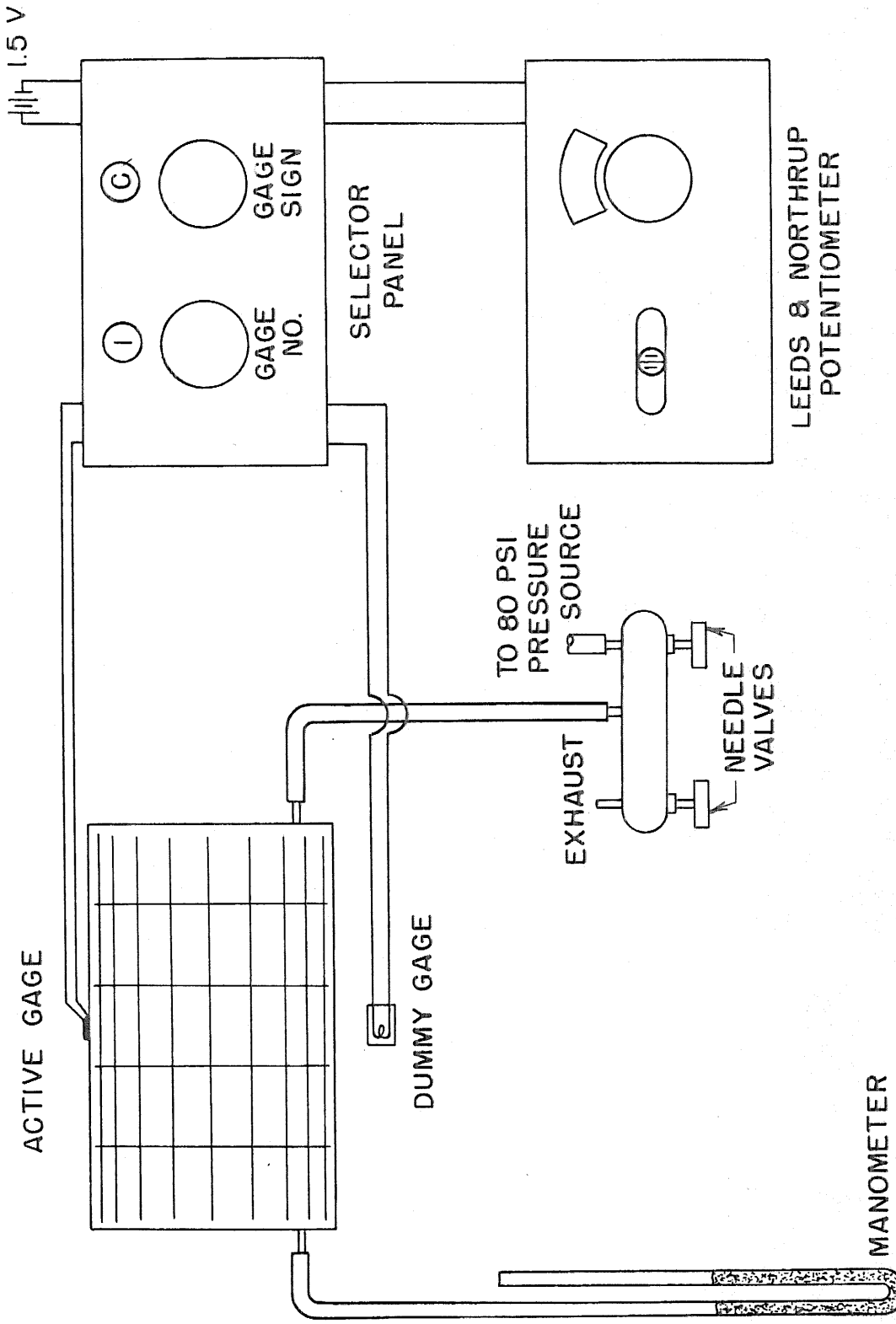

SCHEMATIC OF EXPERIMENTAL SET UP

FIG. 23

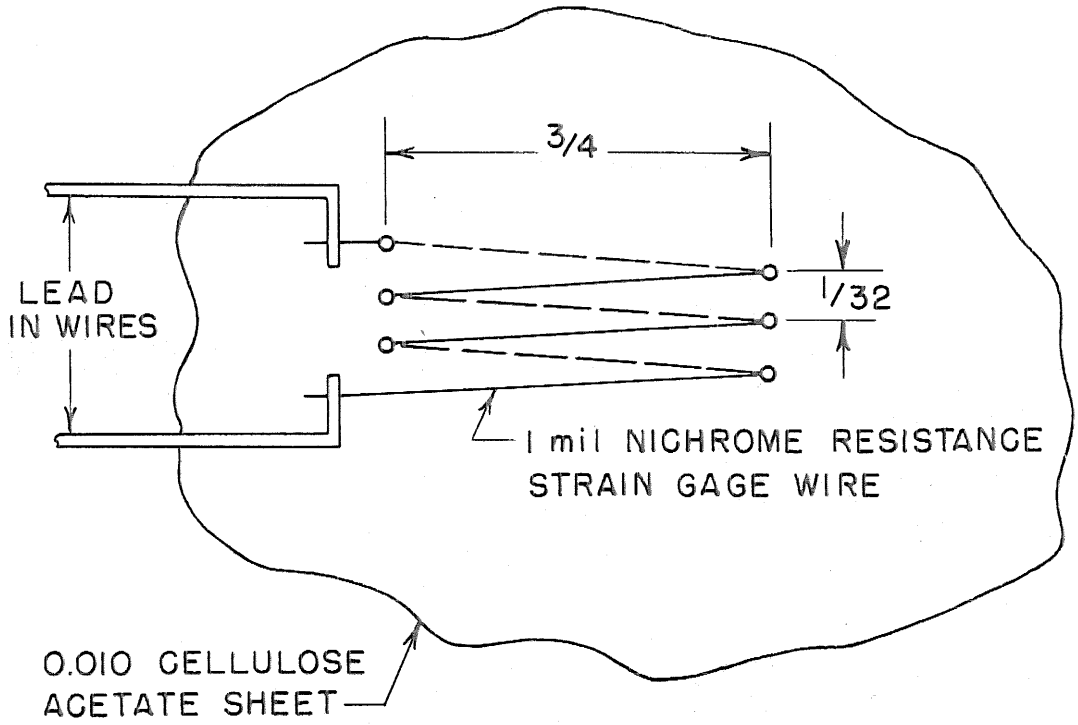

INTEGRAL WOUND RESISTANCE
STRAIN GAGE

FIG. 24

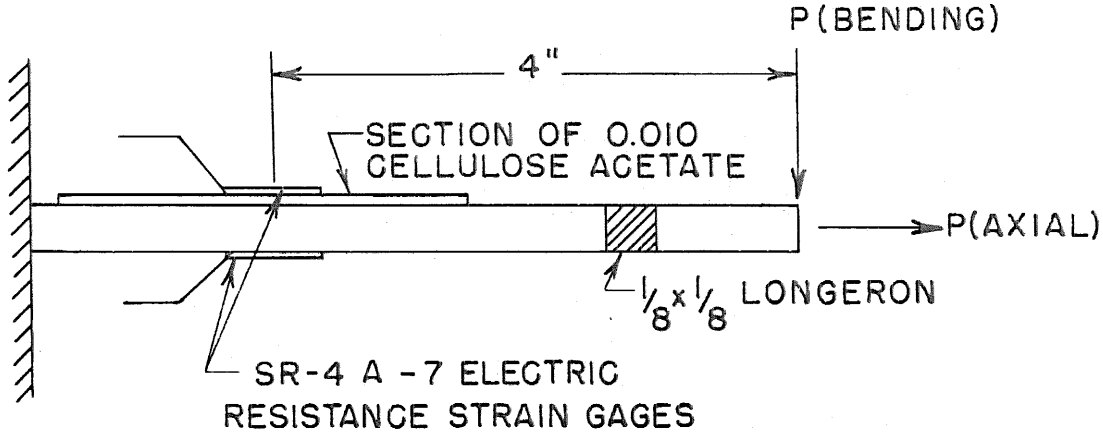

LONGERON A-7 STRAIN GAGE CALIBRATION
BENDING AND AXIAL STRESS

FIG. 25

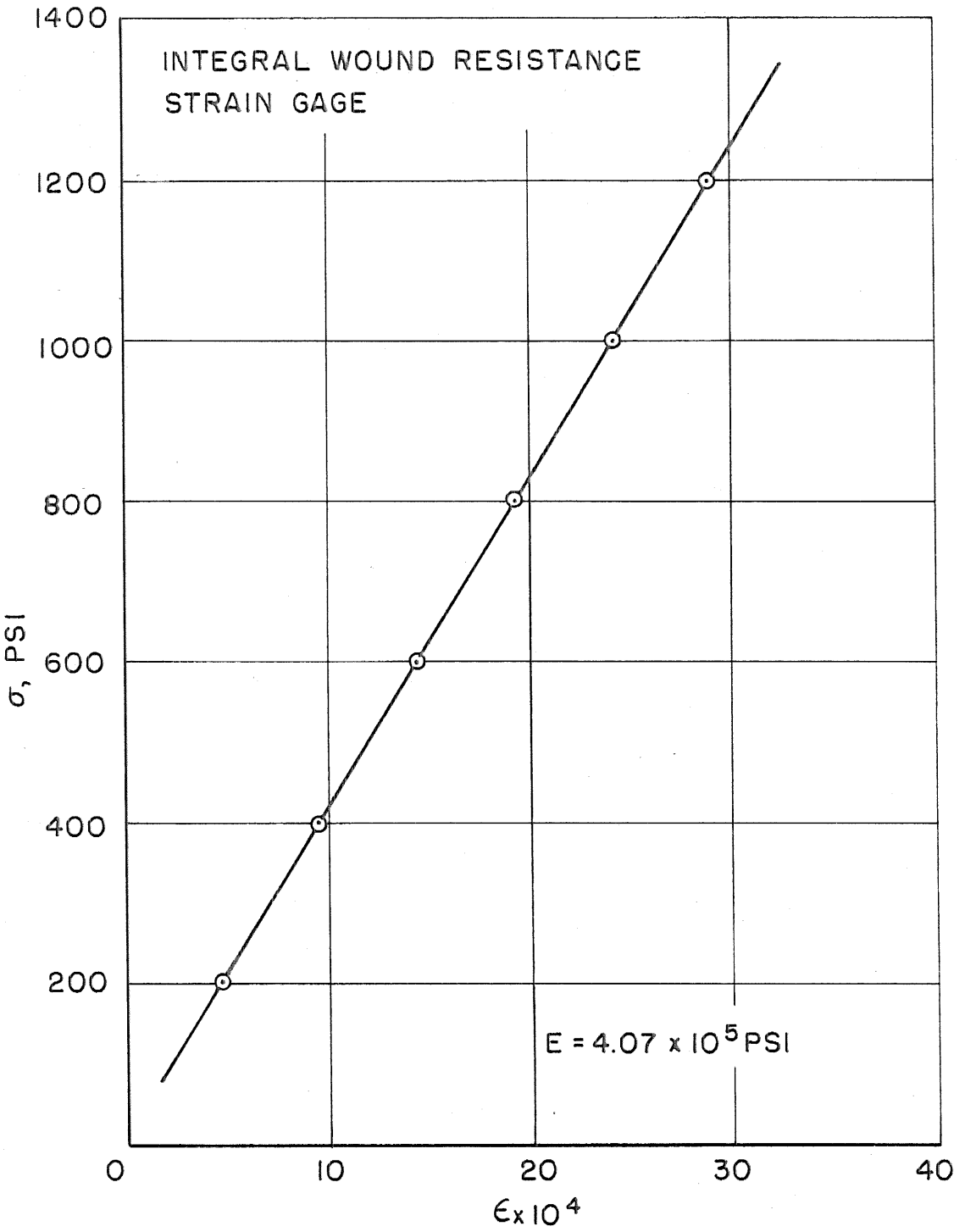

0.010 SHEET CELLULOSE ACETATE - MODULUS OF ELASTICITY TEST

FIG. 26

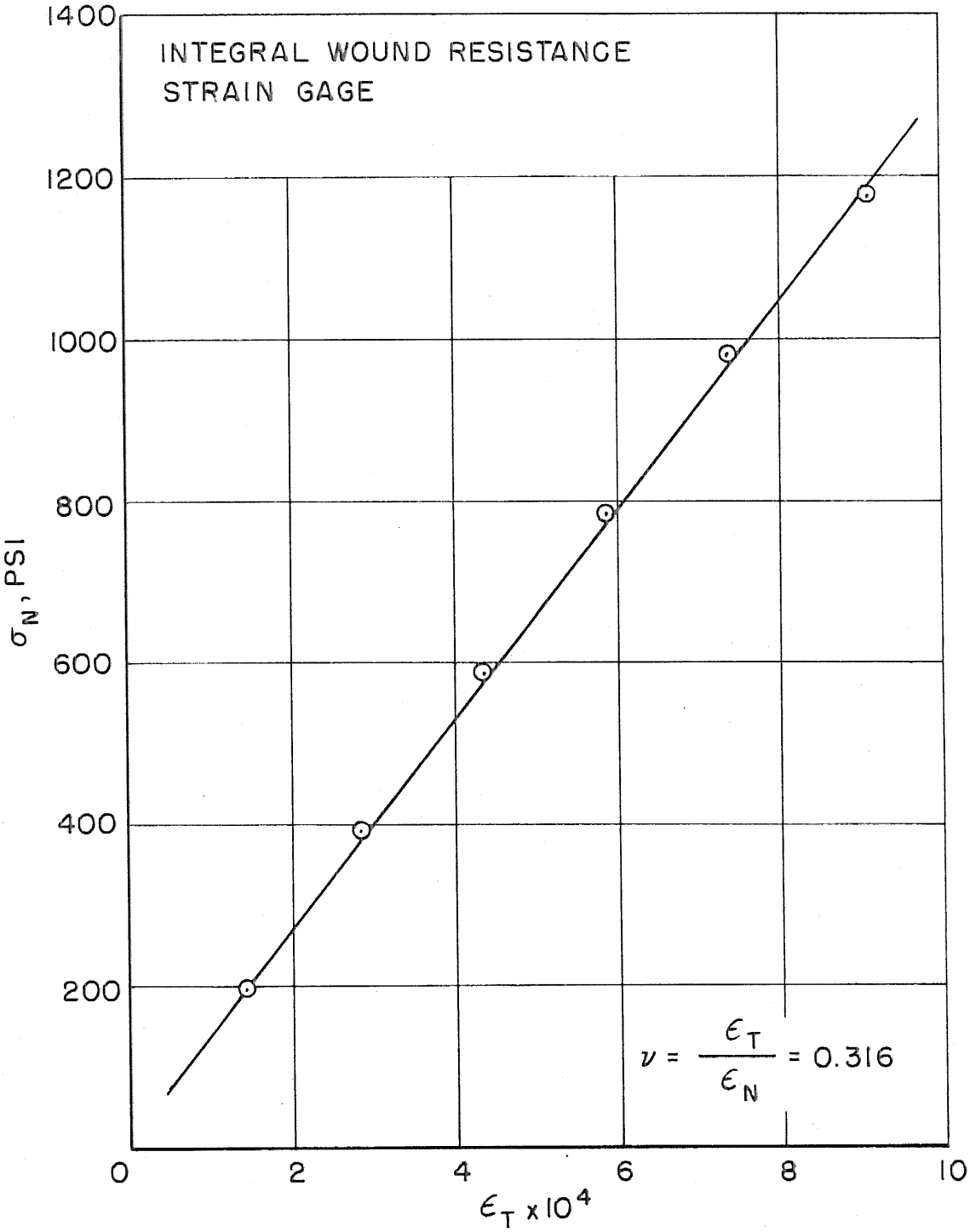

0.010 SHEET CELLULOSE ACETATE - POISSON'S RATIO TEST

FIG. 27

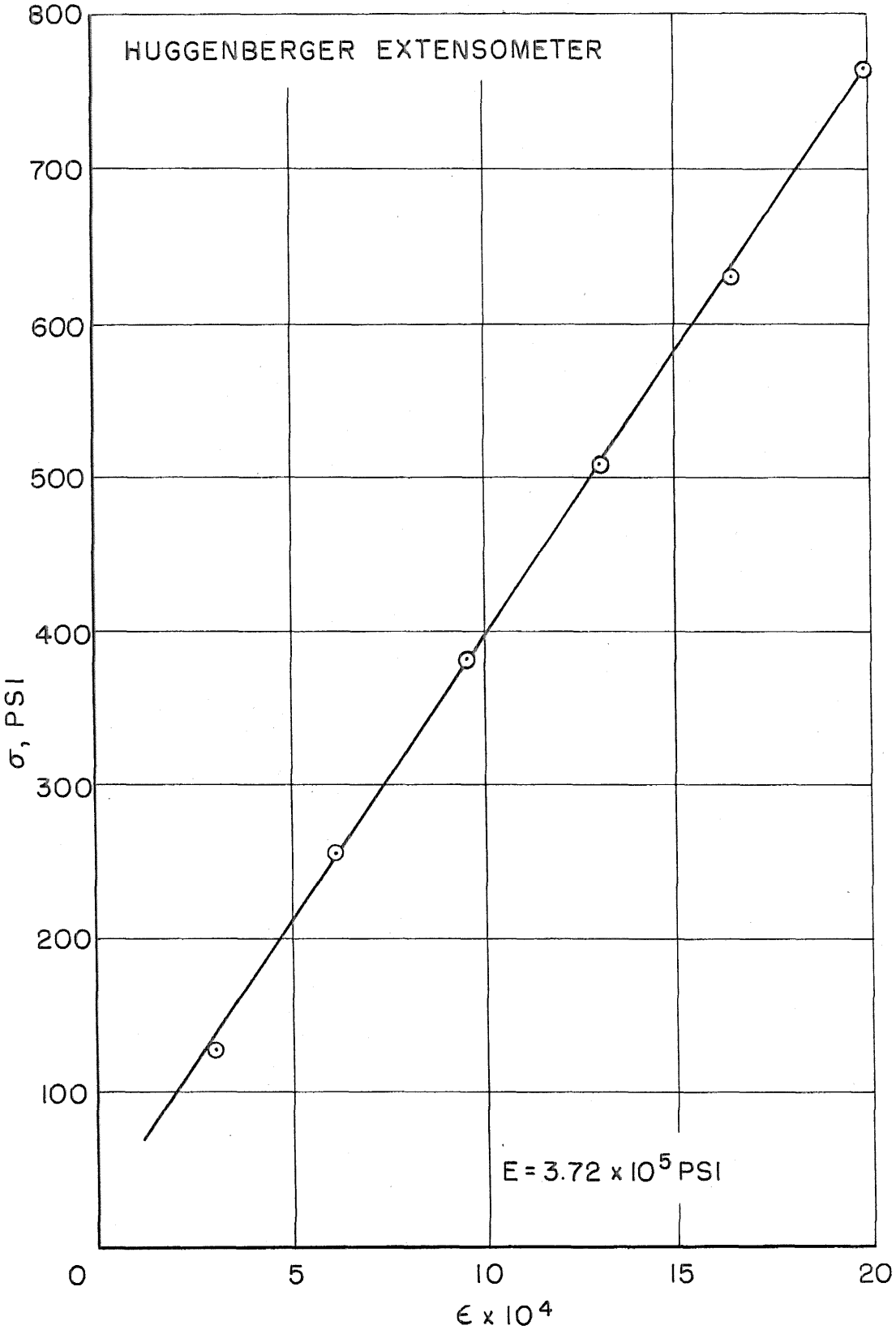

LUCITE LONGERON AND FRAME MODULUS OF ELASTICITY TEST

FIG. 28

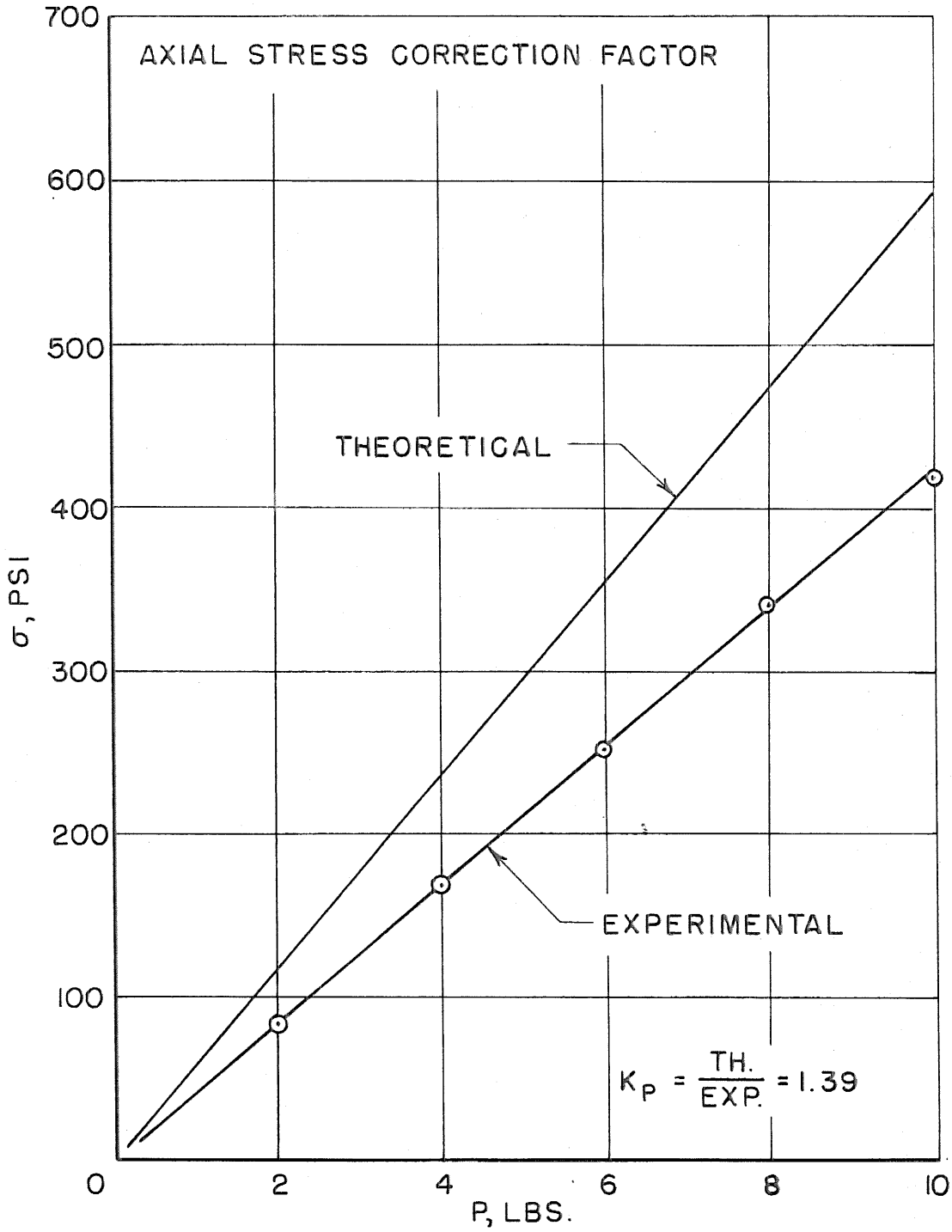

LONGERON A-7 STRAIN GAGE
CALIBRATION TEST

FIG. 29

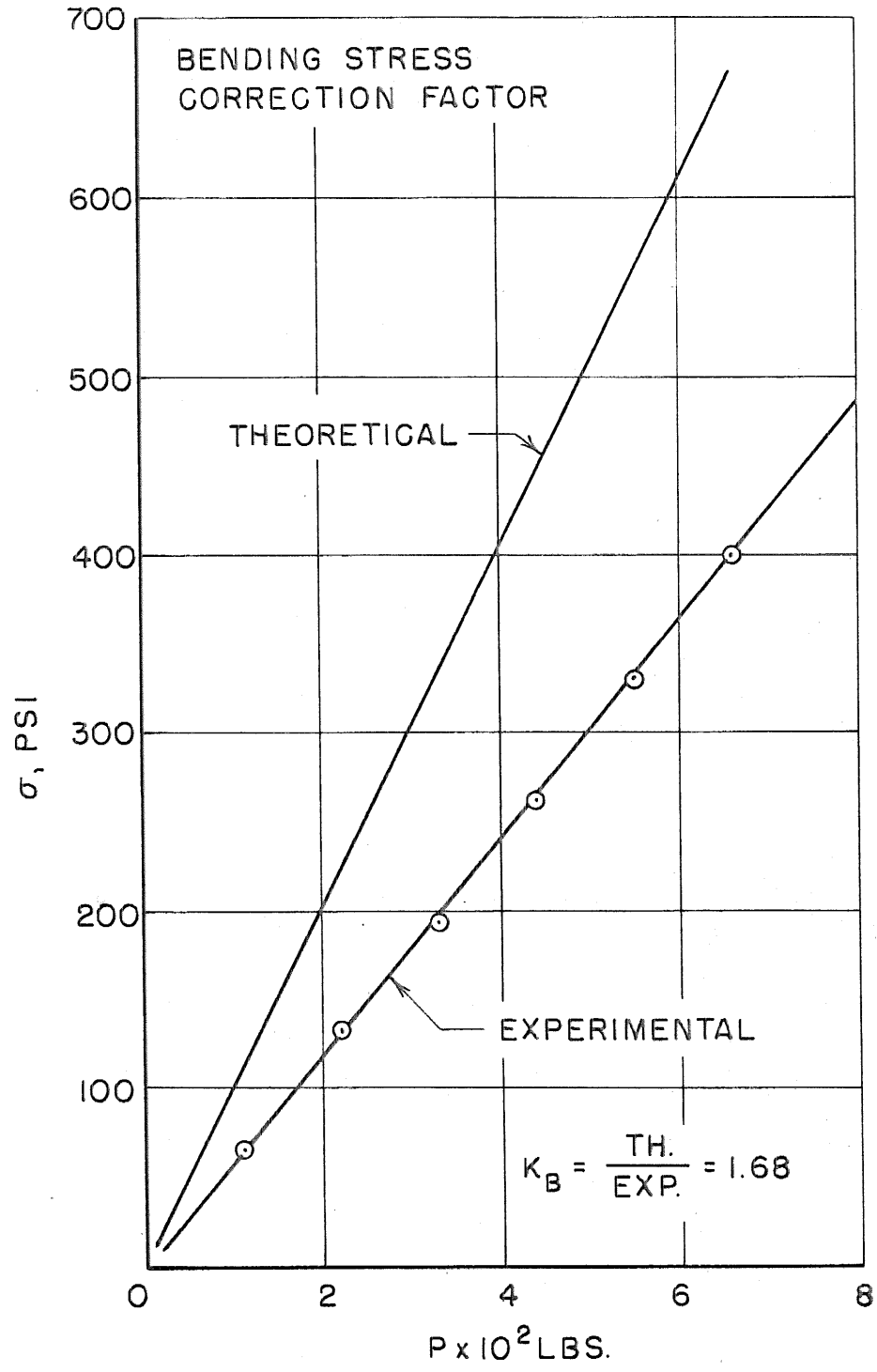

LONGERON A-7 STRAIN GAGE
CALIBRATION TEST

FIG. 30

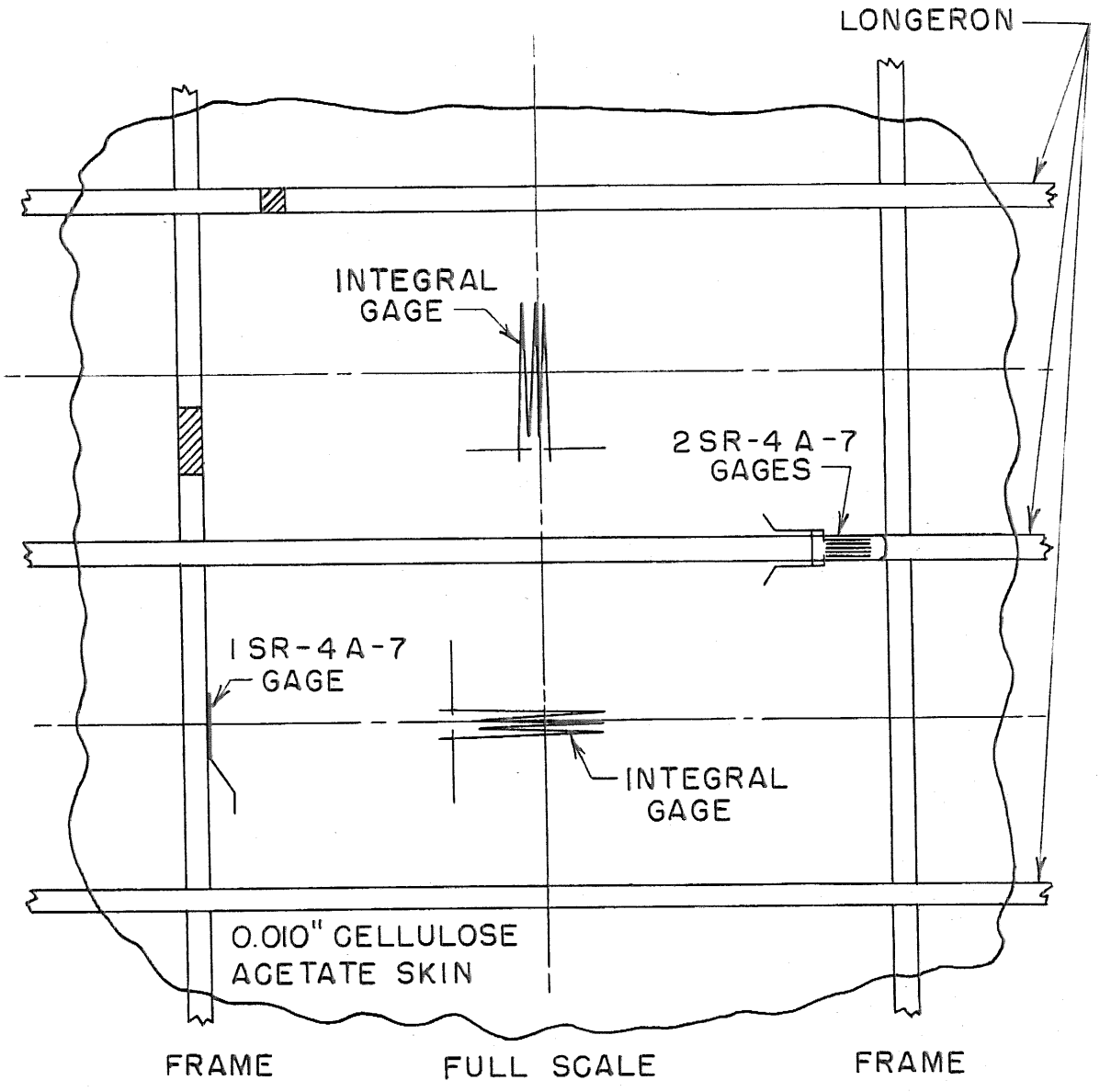

LOCATION OF ELECTRICAL RESISTANCE STRAIN GAGE INSTRUMENTATION

FIG. 31

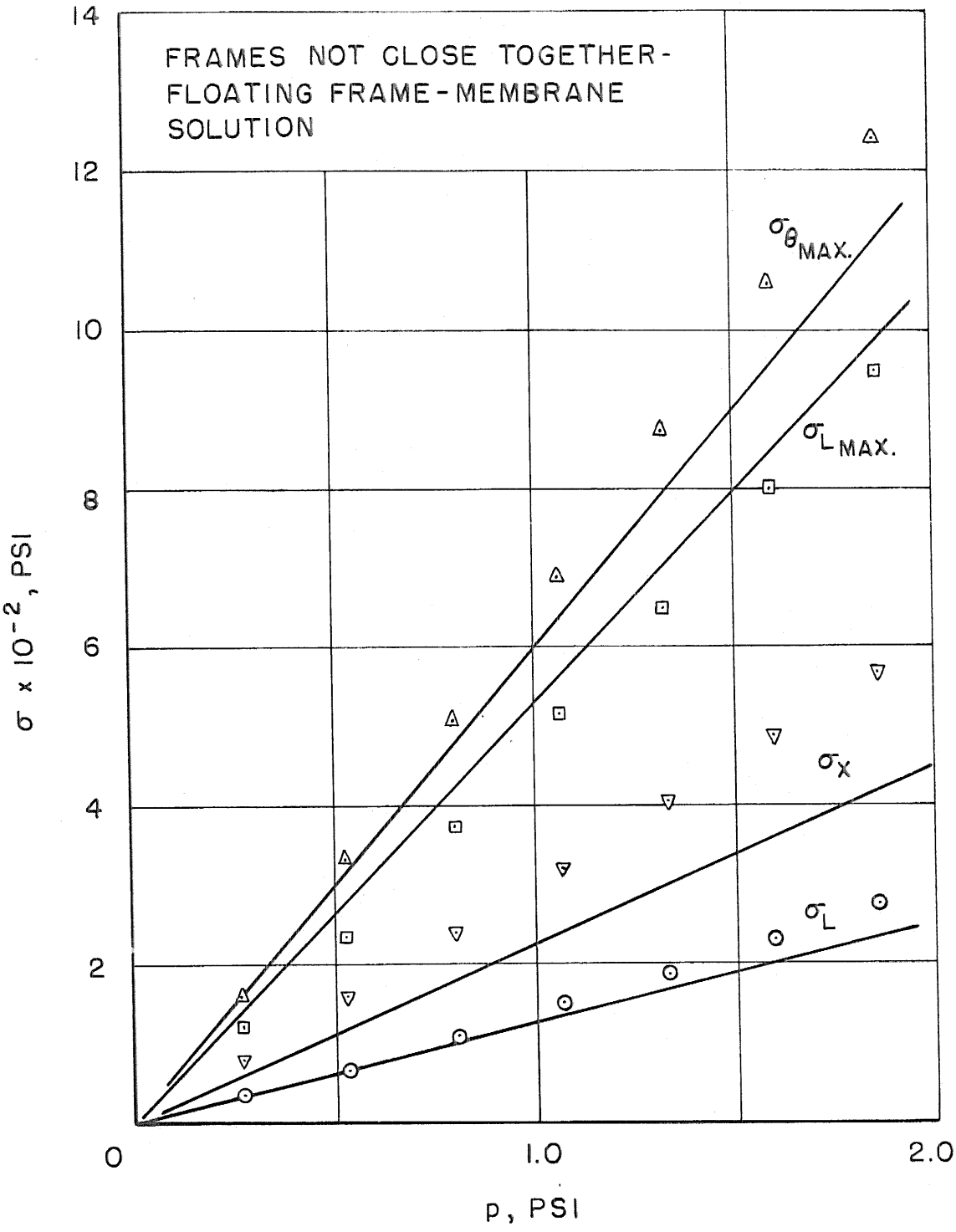

COMPARISON OF THEORETICAL AND EXPERIMENTAL RESULTS

FIG. 32

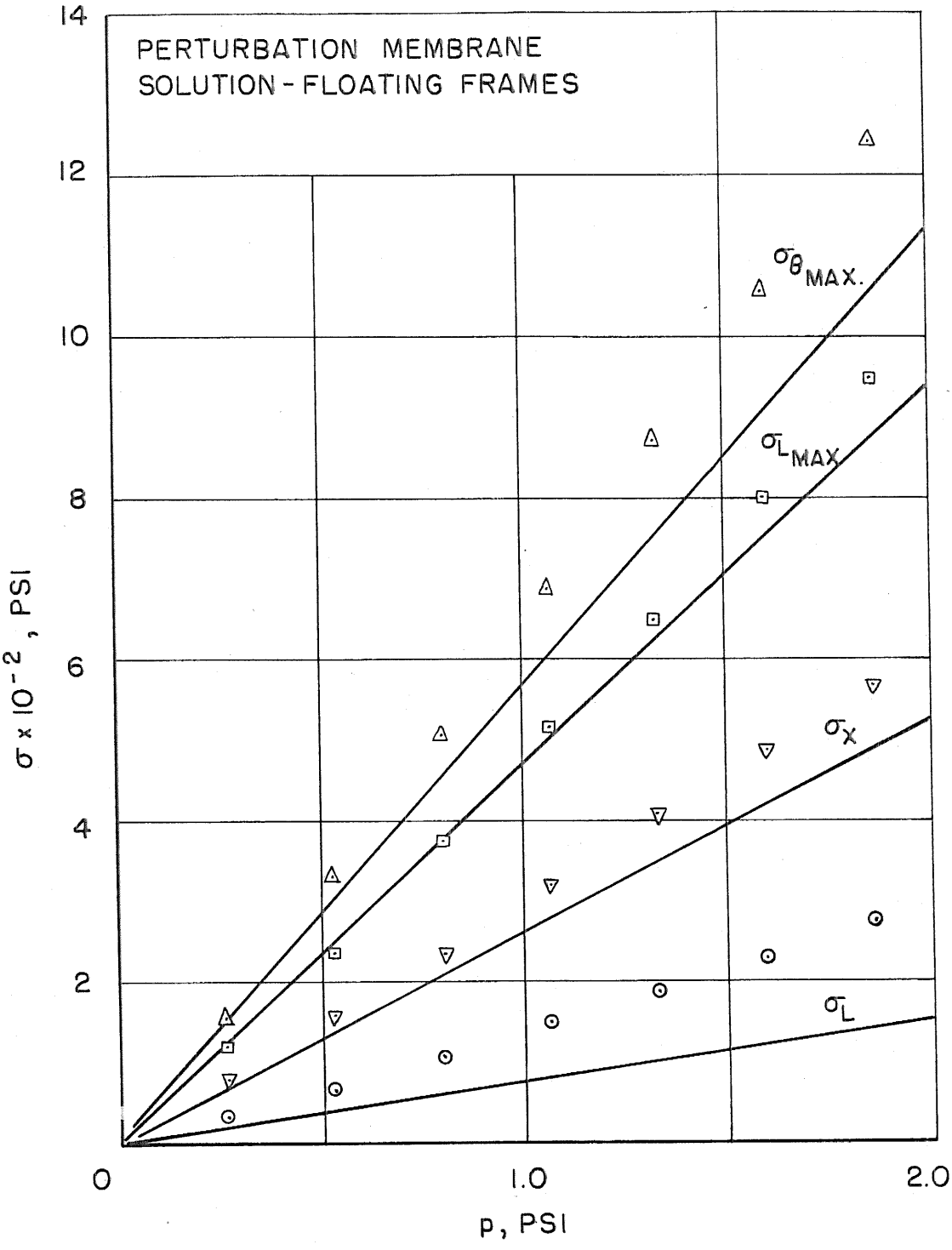

COMPARISON OF THEORETICAL AND EXPERIMENTAL RESULTS

FIG. 33

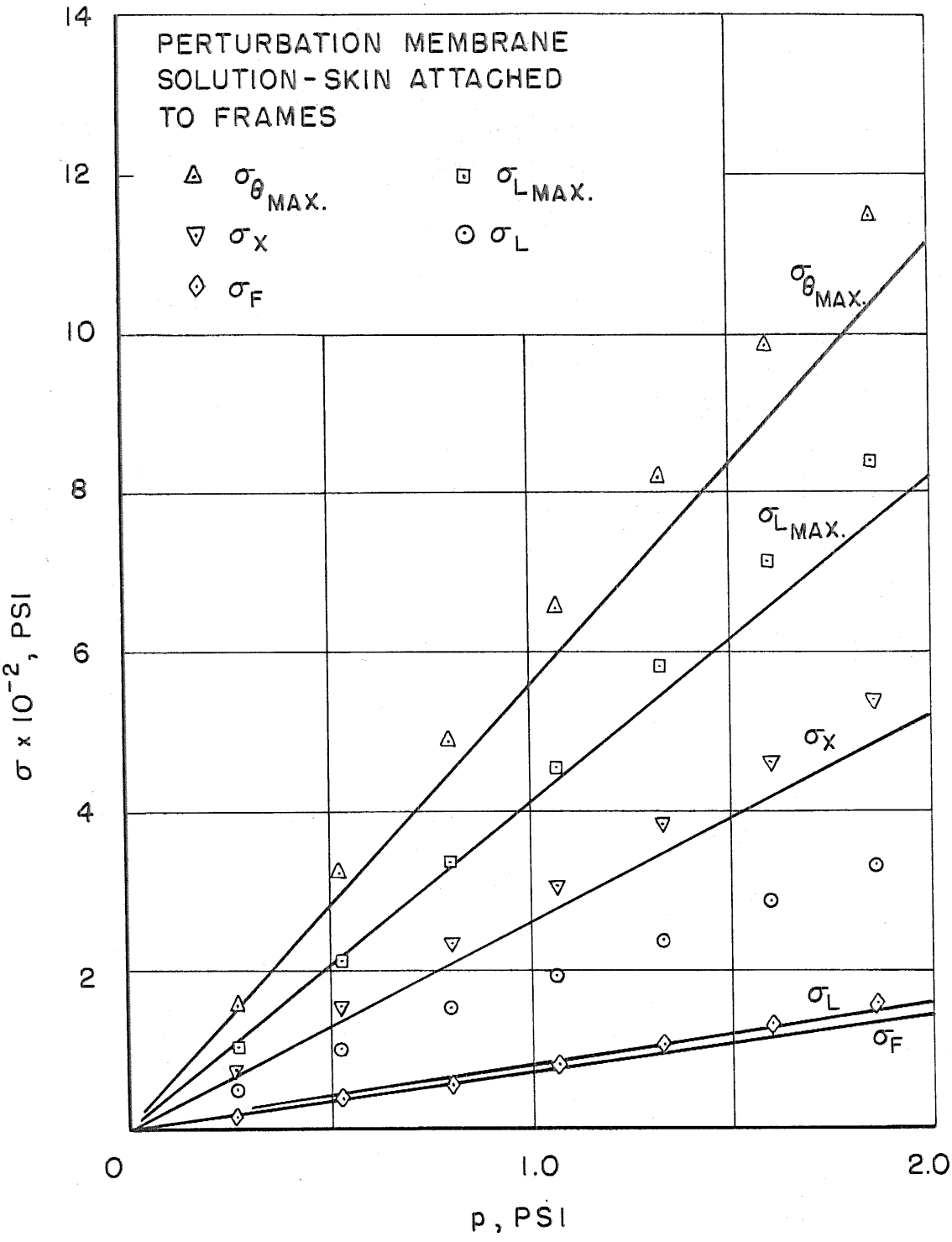

COMPARISON OF THEORETICAL AND EXPERIMENTAL RESULTS

FIG. 34

	FLOATING FRAMES			FRAMES ATTACHED		
	MEMBRANE	PLATE	SHELL	MEMBRANE	PLATE	SHELL
CONTINUOUS LONGERONS	F.C.M.S. F.N.C.-M.S. P.M.S.	F.C.P.S.	F.C.S.S. (FLÜGGE)	P.M.S.		F.C.S.S. (FLÜGGE) F.N.C.S.S. (FLÜGGE)
PINNED LONGERONS	F.C.M.S. F.N.C.-M.S. P.M.S.	F.C.P.S.	F.C.S.S. (FLÜGGE)	P.M.S.		F.C.S.S. (FLÜGGE)

SURVEY OF GEOMETRIES
WHERE SOLUTIONS ARE APPLICABLE

FIG. 35

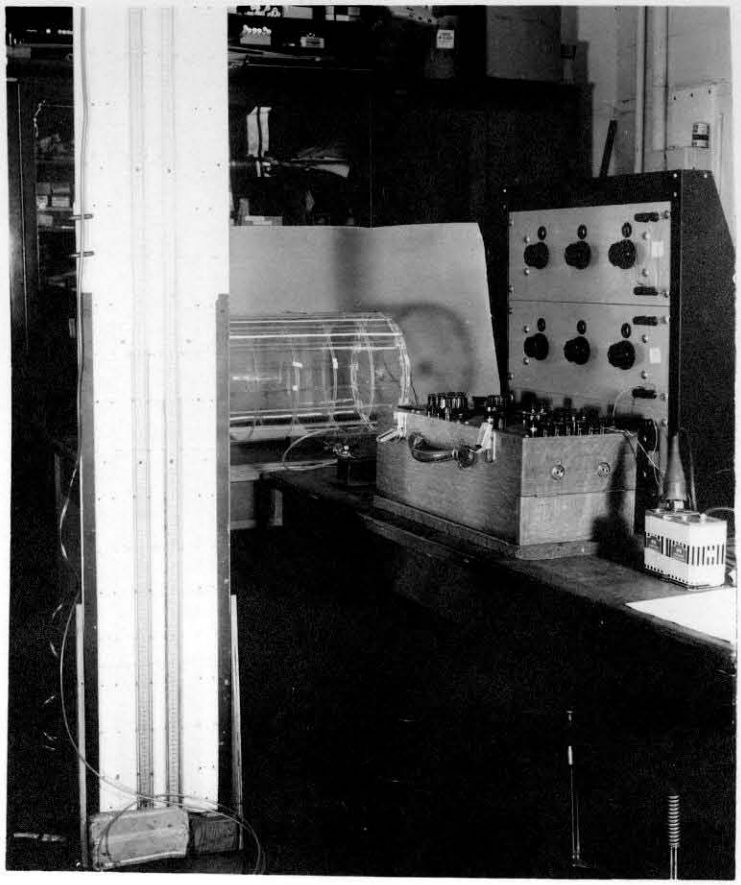

Fig. 36. An overall view of the experimental setup

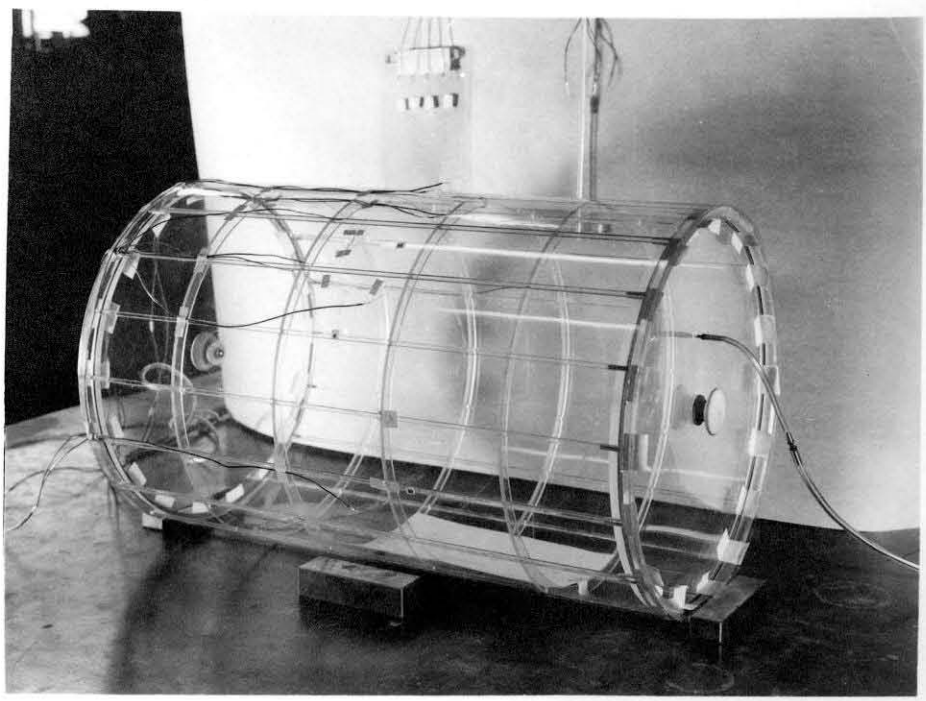

Fig. 37. A detail view of the test model